

edge

**AEC RESEARCH AND DEVELOPMENT REPORT**

CENTRAL RESEARCH LIBRARY  
DOCUMENT COLLECTION

ORNL-1843  
Special

21a

MARTIN MARIETTA ENERGY SYSTEMS LIBRARIES



3 4456 0349812 3

**EFFECTIVE NEUTRON REMOVAL CROSS  
SECTIONS FOR SHIELDING**

G. T. Chapman  
C. L. Störns



OAK RIDGE NATIONAL LABORATORY  
CENTRAL RESEARCH LIBRARY  
DOCUMENT COLLECTION

**LIBRARY LOAN COPY**

DO NOT TRANSFER TO ANOTHER PERSON

If you wish someone else to see this  
document, send in name with document  
and the library will arrange a loan.

UCN-7969  
13 3-671

**OAK RIDGE NATIONAL LABORATORY**  
OPERATED BY

**UNION CARBIDE NUCLEAR COMPANY**

A Division of Union Carbide and Carbon Corporation



POST OFFICE BOX P • OAK RIDGE, TENNESSEE

[REDACTED]

[REDACTED]

[REDACTED]

ORNL-1843

**DECLASSIFIED**

CLASSIFICATION CHANGED TO:

This document consists of 154 pages.

BY AUTHORITY OF:

T-10-1148

Copy 21 of 59, Series A.

BY:

P. Menon 8-26-57

Contract No. W-7405-Eng-26

Applied Nuclear Physics Division  
Lid Tank Shielding Facility

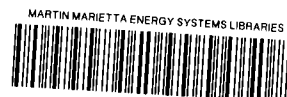
EFFECTIVE NEUTRON REMOVAL CROSS  
SECTIONS FOR SHIELDING

G. T. Chapman, ORNL, and C. L. Storrs, GE-ANP

AUG 31 1955

[REDACTED]

OAK RIDGE NATIONAL LABORATORY  
Operated by  
UNION CARBIDE NUCLEAR COMPANY  
A Division of Union Carbide and Carbon Corporation  
Post Office Box P  
Oak Ridge, Tennessee



3 4456 0349812 3

1944

1944

1944

1944

INTERNAL DISTRIBUTION

- |                       |                                      |
|-----------------------|--------------------------------------|
| 1. S. Auslander       | 13. R. B. Murray                     |
| 2. P. P. Blizard      | 14. R. W. Peelle                     |
| 3. A. Charpie         | 15. R. H. Ritchie                    |
| 4. D. Callihan        | 16. A. Simon                         |
| 5. T. Chapman         | 17. M. F. Valerino                   |
| 6. E. Clifford        | 18. J. Van Hoomissen                 |
| 7. J. B. Dee          | 19. A. M. Weinberg                   |
| 8. A. Fraas           | 20. C. D. Zerby                      |
| 9. W. Jordan          | 21. Central Research Library         |
| 10. F. B. Keller      | 22. Laboratory Records, ORNL R.C.    |
| 11. F. C. Maienschein | 23-26. Laboratory Records Department |
| 12. F. H. Murray      |                                      |

EXTERNAL DISTRIBUTION

- 27. H. A. B. he, P.O. Box 451, Ithaca, N.Y.
- 28. F. A. Cleveland, Lockheed Aircraft Corporation
- 29. C. F. deahl, Pratt & Whitney Aircraft Division
- 30. W. R. Faulkner, Office of Naval Research, Washington, D.C.
- 31. M. Fox, Brookhaven National Laboratory
- 32. H. Goldstein, Nuclear Development Associates
- 33. Marshall Grosshans, Argonne National Laboratory
- 34. V. V. Holmes, Douglas Aircraft Corp., Santa Monica Division
- 35-36. J. R. Hood, Wright Air Development Center
- 37. C. R. Horner, AEC, Washington
- 38. Herman Kahn, RAND Corporation
- 39. R. M. Little, Comair, Fort Worth
- 40-41. F. W. Mezger, General Electric Company (ANPD)
- 42. R. Minogue, Bureau of Ships, Washington
- 43. T. R. Mitchell, General Electric Company (ANPD)
- 44. T. F. Nagey, Glenn L. Martin Company
- 45-46. Ralph Allen, AEC, Washington
- 47. H. Reese, Curtiss-Wright Corporation
- 48. H. M. Roth, AEC, Oak Ridge
- 49. B. F. Ruffner, Boeing Airplane Company
- 50. H. E. Stone, Knolls Atomic Power Laboratory
- 51. C. L. Storrs, General Electric Company (ANPD)
- 52. J. J. Taylor, Westinghouse Electric Corporation
- 53. A. F. Thompson, AEC, Washington
- 54. E. S. Wilson, Wright Air Development Center (WCLPU-2)
- 55. R. Zirkind, Bureau of Aeronautics
- 56. E. L. Czapek, Electric Boat Division, General Dynamics Corp.
- 57-59. Technical Information Service, Oak Ridge

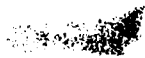
10/10/10

10

10/10/10

TABLE OF CONTENTS

Acknowledgements . . . . .	v
Abstract . . . . .	1
Introduction . . . . .	2
I. Description of Lid Tank Shielding Facility . . . . .	4
II. Procedure and Results of Removal Cross-Section Measurements at the LTSF. . . . .	6
III. Procedure for Removal Cross-Section Calculations from LTSF Data. . . . .	11
IV. Sample Calculation of a Removal Cross Section. . . . .	18
V. Summary of Removal Cross Sections and Discussion . . . . .	21
App. A. Radiation Intensities beyond Various Materials: Experimental Data. . . . .	28
App. B. Values of the Source Geometric Correction Factor F . . .	127





## ACKNOWLEDGMENTS

The work presented in this paper represents the combined efforts of many persons over a period of three years. The authors wish to express their gratitude to E. P. Blizard and C. E. Clifford for their advice and valuable assistance and to all the former and present members of the LTSF staff who have been associated with this program, particularly, T. V. Blosser, J. D. Flynn, Jr., J. M. Miller, D. K. Trubey, and F. N. Watson who in many cases obtained the original data and presented it in other publications. Finally, the authors wish to recognize their indebtedness to L. S. Abbott, G. M. Estabrook, R. Rickman, E. McBee, and C. Bounds for their assistance in preparing the paper for publication.



100

100



## ABSTRACT

The effective removal cross section concept as applied in shield calculations is discussed and a method of determining the numerical value of this cross section from LTSF experimental data is presented. Radiation intensity measurements in water beyond some 20 elements and compounds and the corresponding removal cross section values are reported. These values are useful in determining the relative shielding effectiveness of the various materials, but can be used with complete assurance for shielding calculations only when the geometry under consideration closely resembles that employed at the LTSF. Specifically there must be many relaxation lengths of hydrogenous shield following the material.

A graphical comparison of the effective removal cross sections and the total cross sections at a high neutron energy (8 Mev) is also made and should be applicable to shield calculations. In addition, calculations are presented of correction factors for various values of the water thickness, sample thickness, and attenuation lengths in order to facilitate the calculation of the removal cross section from future measurements.

## INTRODUCTION

In a predominantly hydrogen shield it is possible to represent the effect of the other elements in the shield on the fast-neutron attenuation by a simple exponential, just as if the only effect were one of absorption. The cross section that best fits the experimental data is called the "effective removal cross section."<sup>1,2</sup> Clearly this is not a well-defined concept, since the effectiveness of the element varies with its position in the shield. For the present purposes, the removal cross section is understood to be the equivalent absorption cross section that fits the attenuation of a slab of material located near the source as measured by a detector separated from the source by a large thickness of water. Since, in order to obtain an effect large enough to measure, it is necessary to use a fairly thick slab, the interpretation of experimental information in terms of this removal cross section is not both precise and simple, though it may be either.

The selection and evaluation of materials for shielding mobile reactors have been prime objectives of the program at the ORNL Lid Tank Shielding Facility.<sup>3</sup> Insofar as neutron shielding is concerned, the codification of the neutron data which have been obtained during the last two and one-half years has depended heavily on the concept of the removal cross section. In this report a compilation of all the LTSF neutron measurements beyond various

<sup>1</sup> R. D. Albert and T. A. Welton, WAPD-15 (Nov. 30, 1950)(Classified).

<sup>2</sup> E. P. Blizard and T. A. Welton, Reactor Sci. Tech. 1, No. 3, p. 15 (Dec., 1951); TID-73 (Classified).

<sup>3</sup> E. P. Blizard, CF-51-10-70, Part II Revised, p. 75 (Mar. 7, 1952) (Classified).

single materials in water is presented. A corresponding parameter for gamma-ray shielding, taking into account secondary gamma production, has not yet been derived; nevertheless, numerous gamma-ray measurements beyond the materials are also given.

## I. DESCRIPTION OF THE LID TANK SHIELDING FACILITY

The LTSF consists of a large water tank adjacent to an opening in the concrete shield of the Standard Graphite Reactor (X-10 Pile) as shown in Fig. 1. A converter plate of uranium covers the opening between the water tank and the reactor shield. This plate absorbs most of the incident thermal neutrons emerging from the reactor and the resulting fissions in turn produce the known uranium spectrum of neutrons as well as gamma rays of various energies. Shielding samples are inserted in the tank and the transmitted radiation is measured behind the shield.

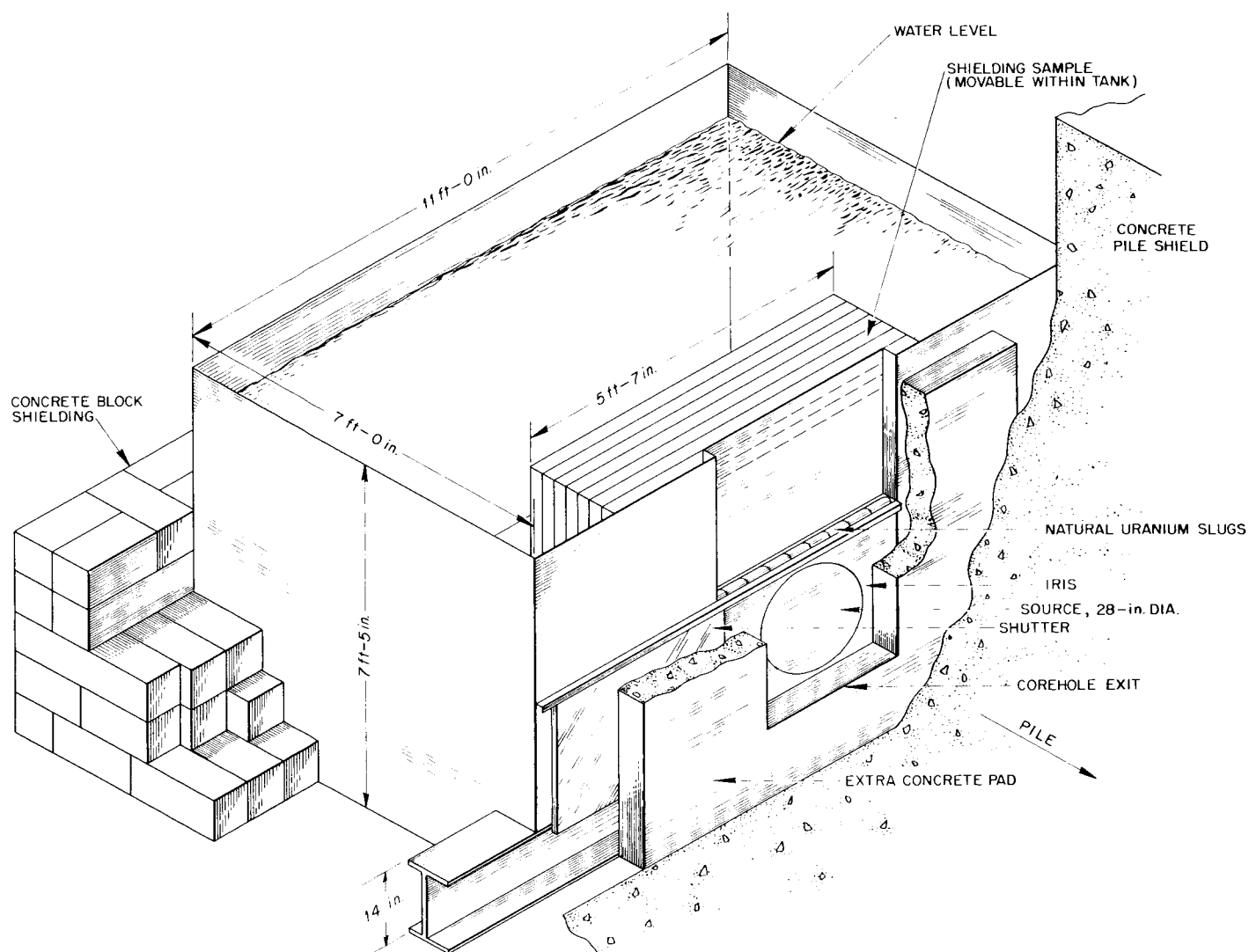


Fig.1. ORNL Lid Tank Shielding Facility.

## II. PROCEDURE AND RESULTS OF REMOVAL CROSS-SECTION MEASUREMENTS AT THE LTSF

In each of the 22 experiments reported here a large sample of the material being studied was placed in the water adjacent to the source plate. The samples had approximately plane parallel surfaces sufficient in area to amply cover the source. Measurements of the fast-neutron dose rate, gamma-ray dose rate, and thermal-neutron flux were made in the water behind the samples along the source axis, using the usual LTSF instruments and techniques.<sup>4</sup>

It was sometimes necessary to prevent the material from getting wet or mixing with water, in which case the sample was encased in a stainless steel container. The steel was treated as if it were iron in correcting the data. In one experiment, the lithium measurement, the sample was submerged in a tank of oil which was then placed in the LTSF. The pertinent information for all the experiments is given in Table 1. In some cases this includes a value for the density of the material times its thickness,  $\rho t$ , determined by measuring the area and weights of the sample.

Plots and tabulations of all the neutron and gamma-ray measurements beyond the various materials are given in Appendix A.

<sup>4</sup> For a description of the instruments and an estimate of experimental error see F. H. Abernathy et al., ORNL-1616, p. 8 ff (Oct. 5, 1954) (██████████).

Table 1

Summation of Experimental Arrangements for the LTSF  
Removal Cross-Section Experiments

( $\rho$  = density;  $t$  = thickness)

Material	Experimental Form	$\rho$ (g/cm <sup>3</sup> )	$t$ (cm)	$\rho t$ (g/cm <sup>2</sup> )	Container Composition and Total Wall Thickness	LTSF Exp. No.	Publication(s) <sup>a</sup>
Aluminum (Al)	Solid slabs against source plate	2.70	15.88		None	23	ORNL-1477; ED ORNL-1630 ORNL-1649 ORNL-1820
Beryllium (Be)	a. Pellets in container against source plate	1.23	28.5		Iron, 0.6 cm	31	ORNL-1477; ED ORNL-1515 ORNL-1609 ORNL-1630 ORNL-1649 ORNL-1820
	b. Solid slabs in con- tainer against source plate	1.84	9.43		Iron, 0.64 cm	49	ORNL-1609; ED ORNL-1630 ORNL-1820
Bismuth (Bi)	Solid slabs against source plate <sup>b</sup>	9.80	14.8	145	None	60	ORNL-1649 ORNL-1820
Boric Oxide (B <sub>2</sub> O <sub>3</sub> )	Powdered B <sub>2</sub> O <sub>3</sub> in container against source plate			39.0 $\pm$ 1%	Iron, 0.64 cm	61	ORNL-1715 ORNL-1820
Boron Carbide (B <sub>4</sub> C)	a. Solid slab against source plate <sup>c</sup>	1.82	51.5 $\pm$ 0.6		Iron, 1.27 cm	33	ORNL-1630 ORNL-1649 ORNL-1820



Table 1 (continued)

Material	Experimental Form	$\rho$ (g/cm <sup>3</sup> )	t (cm)	$\rho t$ (g/cm <sup>2</sup> )	Container Composition and Total Wall Thickness	LTSF Exp. No.	Publication(s) <sup>a</sup>
Boron carbide (B <sub>4</sub> C)	b. Twelve 1-in.-thick B <sub>4</sub> C slabs against source plate <sup>d</sup>	1.81±0.02	29.7		Aluminum, 3.49 cm, and iron, 0.63 cm	42	ORNL-1630 ORNL-1649 ORNL-1820
Carbon (C)	Solid AGHT graphite against source plate <sup>e</sup>	1.62±0.03	32.6		Iron, 0.6 cm	34	ORNL-1477; ED ORNL-1556 ORNL-1630 ORNL-1649 ORNL-1715 ORNL-1820
Copper (Cu)	Solid slabs against source plate	8.90	15.24		None	41	ORNL-1515 ORNL-1630 ORNL-1649 ORNL-1820
Fluorothene (C <sub>2</sub> F <sub>3</sub> Cl)	Solid slabs against source plate	2.19	15.2±1.0		None	53	ORNL-1609; ED ORNL-1649 ORNL-1820
Heavy water (D <sub>2</sub> O)	Liquid D <sub>2</sub> O in con- tainer against source plate	1.1	66.0		Iron, 0.95 cm	40	
Iron (Fe)	Eleven 2.22-cm-thick slabs separated by 3.05-cm-thick layers of water; first slab 0.9 cm from source	7.8±0.1	24.4		None	35	CF-52-12-34; ED ORNL-1477; ED ORNL-1515 ORNL-1630 ORNL-1649 ORNL-1820

Table 1 (continued)

Material	Experimental Form	$\rho$ (g/cm <sup>3</sup> )	t (cm)	$\rho t$ (g/cm <sup>2</sup> )	Container Composition and Total Wall Thickness	LTSF Exp. No.	Publication(s) <sup>a</sup>
Lead (Pb)	Solid slabs against source plate	11.3	14.2	160	None	57	ORNL-1630 ORNL-1820
Lithium (Li)	Solid lithium in con- tainer against source plate <sup>f</sup>	0.53	27.23		Iron, 1.91 cm	65	CF-54-11-3; ED ORNL-1816; ED ORNL-1820; ED
Lithium Fluoride (LiF)	Powdered LiF in con- tainer against source plate	0.7±0.07	37.5		Iron, 0.6 cm	32	ORNL-1477; ED ORNL-1820
Nickel (Ni)	Solid slabs against source plate	8.83	15.25		None	47	ORNL-1556 ORNL-1630 ORNL-1649 ORNL-1820
Oil (CH <sub>2</sub> )	Liquid in container against source plate	0.876	37.5		Iron, 0.6 cm	39	ORNL-1556 ORNL-1820
Paraffin (C <sub>30</sub> H <sub>62</sub> )	Solid slab against source plate	0.952	19.8		None	43	ORNL-1556; ED ORNL-1820
Perfluoro- heptane (C <sub>7</sub> F <sub>16</sub> )	Liquid in container against source plate	1.72	a. 66.4 b. 37.5		Iron, 0.95 cm Iron, 0.63 cm	54 55	ORNL-1609; ED ORNL-1649 ORNL-1820 ORNL-1649 ORNL-1715 ORNL-1820

Table 1 (continued)

Material	Experimental Form	$\rho$ (g/cm <sup>3</sup> )	t (cm)	$\rho t$ (g/cm <sup>2</sup> )	Container Composition and Total Wall Thickness	LTSF Exp. No.	Publication(s) <sup>a</sup>
Tungsten (W)	Powdered tungsten embedded in unichrome plastic; slabs against source plate <sup>g</sup>	18.8	4.13	77.8	None	30	ORNL-1477; ED ORNL-1630 ORNL-1649 ORNL-1715 ORNL-1820
Uranium (U)	Solid slab 30 cm from source plate <sup>h</sup>	18.8	7.62		None	51	CF-53-9-96; ED ORNL-1630; ED ORNL-1820

- a This column includes only those references which report a presently accepted removal cross section value and/or the details of the experiment. "ED" following a report number indicates that the experimental details are presented.
- b Measurements were repeated during Exp. 65 with the slabs in oil. The results were the same (see CF-54-11-3 and ORNL-1816).
- c Absolute water content of B<sub>4</sub>C not known.
- d Uncertainty in t = +10% to -5%.
- e It was necessary to fill a small air void in the iron tank by inserting a thin water-filled aluminum tank (0.6 cm total wall thickness) behind the graphite in the iron tank.
- f Data run with sample submerged in oil rather than water.
- g Tungsten-plastic slabs circular in shape, 61 cm in diameter.
- h Uranium slab had 3/16-in. thick plexibor (boron-impregnated Plexiglas) on each side and was displaced 30 cm from the source to eliminate fission neutrons from sample.

### III. PROCEDURE FOR REMOVAL CROSS-SECTION CALCULATIONS FROM LTSF DATA<sup>5</sup>

Removal cross sections are calculated from two sets of LTSF neutron measurements: (1) those taken in plain water along the source centerline, and (2) those taken in the water behind the slab of material for which the removal cross section is to be determined. In the calculation below the subscripts 1 and 2 will be used to identify measurements in these two situations, it being understood that the data to be used will in both cases be that with relatively large ( $\approx 120$  cm) thicknesses of water. Other notations include:

$D_1(z)$  and  $D_2(z' + t)$  = doses as measured without and with the sample

inserted, respectively,

$a$  = radius of the circular source (cm),

$\rho$  = distance from the source centerline to the  
element of source area,

$G(R)$  = attenuation kernel, i.e., the dose at distance  
 $R$  from unit source, here taken to be the strength  
of 1 cm<sup>2</sup> of the Lid Tank source; the validity of  
the kernel concept has been discussed elsewhere,<sup>3</sup>

$R_w$  = ray length in water,

$R_x$  = ray length through the sample,

$R$  = total ray length,

$\lambda$  = relaxation length in water (cm),

<sup>5</sup> This procedure is largely quoted from a memorandum by E. P. Blizard, "Procedure for Obtaining Effective Removal Cross Sections from Lid Tank Data," CF-54-6-164 (June 22, 1954) (Declassified, 1955).

$z$  = distance from the source to the detector (cm),  
 $z'$  = distance from the sample to the detector, i.e.,  
 water thickness (cm),  
 $t$  = thickness of the sample,  
 $\Sigma$  = macroscopic removal cross section.

The dose at a distance  $z$  with plain water is

$$D_1(z) = 2\pi \int_{\rho=0}^a G(R) \rho \, d\rho \quad (1)$$

Now since

$$\rho^2 + z^2 = R^2$$

and

$$2\rho \, d\rho = 2R \, dR$$

then

$$D_1(z) = 2\pi \int_z^{\sqrt{z^2+a^2}} G(R) R \, dR \quad (2)$$

If the attenuation kernel is approximated in the region of interest by a simple exponential, then

$$G_1(R) = \frac{g_1(R)}{4\pi R^2} \approx \frac{g_1(z) e^{-(R-z)/\lambda}}{4\pi R^2} \quad (3)$$

where  $\lambda$  is as yet undetermined, but is assumed to be only slowly varying with  $R$  (or  $z$ ). Substitution of Eq. (3) in Eq. (2) gives

$$D_1(z) = \frac{1}{2} g(z) e^{z/\lambda} \int_z^{\sqrt{z^2+a^2}} \frac{e^{-R/\lambda}}{R} \, dR$$

$$= \frac{1}{2} g(z) e^{z/\lambda} \int_{z/\lambda}^{\sqrt{z^2 + a^2}/\lambda} \frac{e^{-x}}{x} dx \quad (4)$$

The exponential integral is

$$E_1(x) = \int_x^\infty \frac{e^{-p}}{p} dp \quad (5)$$

so

$$D_1(z) = \frac{1}{2} g(z) e^{z/\lambda} \left[ E_1(\sqrt{z^2 + a^2}/\lambda) - E_1(z/\lambda) \right] \quad (6)$$

For the case in which a slab of material to be tested has been inserted (see Fig. 2),

$$D_2(z' + t) = 2\pi \int_{z'+t}^{\sqrt{(z'+t)^2 + a^2}} G_2(R) R dR \quad (7)$$

The attenuation kernel in this case is taken to be

$$G_2(R) = \frac{g_1(R_w) g_x(R_x)}{4\pi R^2}$$

where

$$g_x(R_x) = e^{-\Sigma R_x}$$

and the macroscopic effective removal cross section is  $\Sigma$ .

Equation (7) now becomes

$$D_2(z' + t) = \frac{1}{2} \int_{z'+t}^{\sqrt{(z'+t)^2 + a^2}} \frac{g_1(R_w) g_x(R_x)}{R} dR \quad (8)$$

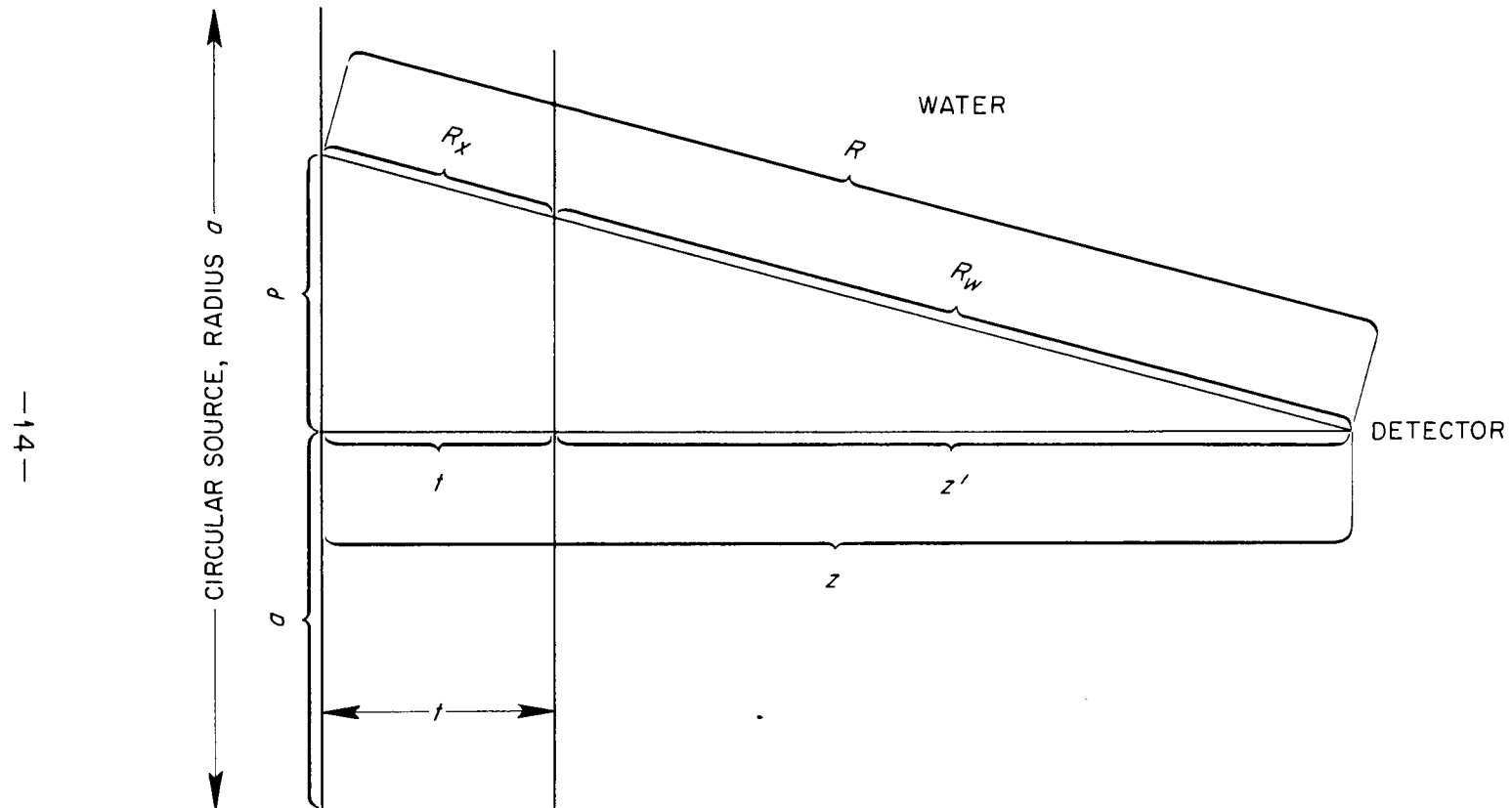


Fig. 2. Geometry for Removal Cross Section Calculation from LTSF Measurements.

If, analogous to Eq. (3),

$$g_1(R_w) = g(z') e^{-(R_w - z')/\lambda} \quad (9)$$

and since

$$\frac{R_x}{t} = \frac{R_w}{z}$$

$$R = R_w + R_x = R_w \left(1 + \frac{t}{z'}\right)$$

then

$$D_2(z' + t) = \frac{g(z') e^{z'/\lambda}}{2} \int_{z'}^{z' \sqrt{1 + \frac{a^2}{(z' + t)^2}}} \frac{e^{-\left[\frac{t}{z'} + \frac{1}{\lambda}\right] R_w}}{R_w} dR_w \quad (10)$$

or

$$D_2(z' + t) = \frac{g(z') e^{z'/\lambda}}{2} \int_{\frac{z'}{\lambda} + \frac{t}{\lambda}}^{\left(\frac{z'}{\lambda} + \frac{t}{\lambda}\right) \sqrt{1 + \left(\frac{a}{z' + t}\right)^2}} \frac{e^{-x}}{x} dx \quad (11)$$

In addition to their magnitudes, the slopes of  $D_1$  and  $D_2$  are also observables.

The water thicknesses are now chosen to be the same in both cases, so that  $z' = z$ . In taking the derivatives of  $D_1$  and  $D_2$ , it is to be noted that  $g(z) e^{z/\lambda}$  is constant in  $z$  in the region of  $z$ . Then

$$\frac{dD_1(z)}{dz} \left( = - \frac{D_1(z)}{\lambda_1} \right) = \frac{g(z) e^{z/\lambda}}{2} \left\{ \frac{z e^{-\frac{z}{\lambda} \left(1 + \frac{a^2}{z^2}\right)^{1/2}}}{z^2 + a^2} - \frac{e^{-z/\lambda}}{z} \right\} \quad (12)$$



$$\frac{dD_2(z+t)}{dz} \left( = - \frac{D_2(z+t)}{\lambda_2} \right) = \frac{g(z)e^{z/\lambda}}{2} \left\{ \left[ \frac{1}{z + \lambda \Sigma t} - \frac{a^2}{(z+t)^3 + a^2(z+t)} \right] e^{-\left(\frac{z}{\lambda} + \Sigma t\right) \sqrt{1 + \left(\frac{a}{z+t}\right)^2}} - \frac{e^{-\left(\frac{z}{\lambda} + \Sigma t\right)}}{z + \lambda \Sigma t} \right\} \quad (13)$$

Equations (12) and (13) can be used to eliminate the unknown  $g(z)$  and determine the desired quantity  $\Sigma$ . The value of  $\lambda$  does not enter the calculations in an important way, as will become apparent later. It is therefore permissible to use a mean value,  $(\lambda_1 + \lambda_2)/2$ .

In order to reduce the labor of computation, it is appropriate to introduce some algebraic approximations at this point.<sup>6</sup> If  $a^2$  is appreciably less than  $z^2$  or  $(z+t)^2$ , then this permits simplification with little sacrifice of accuracy. Thus if, say,  $a = z/4$ , then

$$\sqrt{1 + \left(\frac{a}{z}\right)^2} = 1 + \frac{1}{32} - \frac{1}{2048} + \dots$$

and clearly, even in the exponent, the third term is negligible. Thus the following approximation is permissible:

$$\sqrt{1 + \left(\frac{a}{z}\right)^2} \approx 1 + \frac{1}{2} \left(\frac{a}{z}\right)^2$$

Equation (12) becomes

$$D_1(z) = \frac{\lambda_1 g(z) e^{z/\lambda}}{2} \left[ \frac{e^{-z/\lambda}}{z} - \frac{e^{-z/\lambda} e^{-(z/2\lambda)(a/z)^2}}{z} + \frac{a^2}{z^2} \frac{e^{-z/\lambda} e^{-(z/2\lambda)(a/z)^2}}{z} \right] \\ \approx \frac{\lambda_1 g(z) a^2}{4\lambda z^2} \left( 1 - \frac{a^2}{4\lambda z} \right) \quad (14)$$

<sup>6</sup> Other approximations have also been made, cf. R. Aronson, CF-54-5-63 (May 12, 1954)(Classified); this memorandum was written by Aronson, NDA, to E. P. Blizard, ORNL, and probably is not available for general distribution.

Equation (13) becomes

$$D_2(z+t) = \frac{\lambda_2 g(z) e^{-\Sigma t}}{2} \left[ \frac{a^2}{(z+t)^3 + a^2(z+t)} + \frac{a^2}{2\lambda(z+t)^2} - \frac{a^4(z + \lambda \Sigma t)}{2\lambda(z+t)^5 + 2\lambda a^2(z+t)^3} - \frac{a^4(z + \lambda \Sigma t)}{8\lambda^2(z+t)^4} \right]$$

Combining terms and keeping the largest, and approximating  $\lambda \Sigma$  by unity in the smaller term in the brackets,

$$D_2(z+t) = \frac{\lambda_2 g(z) e^{-\Sigma t} a^2}{4\lambda(z+t)^2} \left[ 1 - \frac{a^2}{4\lambda(z+t)} \right] \quad (15)$$

$$\begin{aligned} \frac{D_1(z)}{D_2(z+t)} &= \frac{\lambda_1}{\lambda_2} \frac{(z+t)^2}{z^2} \left[ \frac{1 - \frac{a^2}{4\lambda z}}{1 - \frac{a^2}{4\lambda(z+t)}} \right] e^{\Sigma t} \\ &= \frac{\lambda_1}{\lambda_2} \left( \frac{z+t}{z} \right)^2 \left( 1 - \frac{a^2 t}{4\lambda z(z+t) - a^2 z} \right) e^{\Sigma t} \end{aligned} \quad (16)$$

This approximate formula has been used exclusively in analyzing LTSF results. The algebraic approximations introduce only a few percent error in the geometries used for computations, which is not significant in view of the experimental errors involved.

#### IV. SAMPLE CALCULATION OF A REMOVAL CROSS SECTION

As an example of the method in which LTSF data is used with the preceding calculational procedure, consider the experiment in which the effective removal cross section for nickel was determined (Exp. 47). The thermal-neutron flux measurements are presented in Fig. A-15 and Table A-39 (Appendix A). In this experiment a total thickness of 15.2 cm of nickel was placed against the source, and the measurements were then made in the water behind the nickel slabs. The distance  $z' + t$  was chosen to be 150 cm since the data curve was parallel to the previously determined water data curve in this region and  $\lambda$  is slowly varying in this region. Since the water thicknesses for the measurements with and without the sample in place were the same, i.e., since  $z = z'$ , the distance  $z$  was determined from  $z' + t$  to be 134.8 cm and the following values were calculated at these points:

$$D_1(z) = D_{H_2O}(134.8 \text{ cm}) = 5.30 \times 10^{-1} \text{ neutrons/cm}^2/\text{sec},$$

$$D_2(z + t) = D_{Ni}(150 \text{ cm}) = 3.65 \times 10^{-2} \text{ neutrons/cm}^2/\text{sec},$$

$$\lambda_1 = \lambda_{H_2O}(134.8 \text{ cm}) = 8.9 \text{ cm},$$

$$\lambda_2 = \lambda_{Ni}(150 \text{ cm}) = 9.4 \text{ cm}.$$

As previously pointed out, the source radius ( $a$ ) is 35.56 cm and  $\lambda$  may be approximated as the average of  $\lambda_1$  and  $\lambda_2$ . These numbers can be applied in Eq. (16):

$$\frac{D_1(z)}{D_2(z + t)} = \frac{\lambda_1}{\lambda_2} \left[ \frac{z + t}{z} \right]^2 \left[ 1 - \frac{a^2 t}{4\lambda z(z + t) - a^2 z} \right] e^{\Sigma t}$$

so that

$$\frac{5.30 \times 10^{-1}}{3.65 \times 10^{-2}} = \frac{8.9}{9.4} \left[ \frac{150}{134.8} \right]^2 \left[ 1 - \frac{(35.56)^2(15.2)}{(4)(9.2)(134.8)(150) - (35.56)^2(134.8)} \right] e^{\Sigma_t}$$

or

$$14.52 = (0.95)(1.24)(0.966) e^{\Sigma_t}$$

$$e^{\Sigma_t} = 12.8$$

$$\Sigma_t = 2.55$$

The microscopic removal cross section is determined from this as follows:

$$\Sigma = \frac{\rho N}{A} \sigma_R$$

where

$$\rho = \text{density (g/cc)} = 8.83 \text{ g/cc},$$

$$N = \text{Avogadro's number} = 0.6023 \times 10^{24},$$

$$A = \text{atomic weight} = 58.7,$$

$$\sigma_R = \text{microscopic removal cross section (barns)}.$$

Thus

$$\sigma_R = \frac{A(\Sigma_t)}{\rho N t} = \frac{(58.7)(2.55)}{(8.83)(0.6023)(15.2)}$$

$$\sigma_R = 1.85 \text{ barns}$$

For cases in which there is more than one material present such as is the case when the sample is encased in a metal container,<sup>7</sup> the procedure is the same except that the factor  $\Sigma_t$  is taken to be the total of all materials present; i.e.,

<sup>7</sup> See, for example, G. T. Chapman et al., "Measurement of an Effective Neutron Removal Cross Section of Lithium at the Lid Tank Shielding Facility," ORNL-CF-54-11-3 (Nov. 2, 1954) (Classified); "Physics Division Quarterly Progress Report for Period Ending December 20, 1952," ORNL-1477, p. 9 ( ).

$$\sum t = \sum_c t_c + \sum_M t_M$$

where the subscript c refers to the material of the container and M refers to the sample.

## V. SUMMARY OF REMOVAL CROSS SECTIONS AND DISCUSSION

The removal cross sections which have been computed from the data in Appendix A are presented in Tables 2 and 3. These values were derived from the thermal-neutron measurements made behind samples followed by a thickness of water chosen large enough so that the neutron spectra were essentially the same, but small enough to insure accurate data (usually a distance of 150 cm from the source was chosen). Since it was necessary to use a set of comparable data for plain water in each calculation, a measurement of the thermal-neutron flux in plain water was repeated at nearly the same time that a measurement behind a sample was made, thus reducing the errors due to gradual changes in the sensitivity of the detectors. The effect of the containers in which some of the materials were held was taken into account by using the appropriate removal cross sections to compute correction terms. The errors quoted in Tables 2 and 3 almost always reflect an assumed uncertainty of  $\pm 10\%$  in the flux measurements,<sup>4</sup> although in a few instances the errors in density or thickness dominate.

The experimental effort to date has been directed toward surveying a large number of materials. To carry out this objective, the program has consisted of a standard experiment followed by a standard computation. The resulting removal cross section values are useful in comparing materials and in predicting doses in configurations closely resembling the standard experimental configuration. It remains to be shown that the removal cross sections thus determined can be used in shielding calculations where the geometry is markedly different.

Table 2

## Removal and Total (at 8 Mev) Cross Sections for Various Elements

(A = atomic weight; N = Avogadro's number;  $\sigma_R$  = microscopic removal cross section;  $\sigma_T$  = microscopic total cross section;  $\Sigma_R$  = macroscopic removal cross section;  $\Sigma_T$  = macroscopic total cross section;  $\rho$  = density;  $\Sigma/\rho$  = mass attenuation coefficient)

Element	A	$\frac{N}{A} = \frac{0.6023 \times 10^{-24}}{A}$	$\sigma_R$ (barns)	$\frac{\Sigma_R}{\rho} = \frac{N}{A} \sigma_R$ (cm <sup>2</sup> g <sup>-1</sup> )	$\sigma_T$ at 8 Mev (barns)	$\frac{\Sigma_T}{\rho}$ at 8 Mev (cm <sup>2</sup> g <sup>-1</sup> )
Hydrogen <sup>a</sup>	1.008	$5.98 \times 10^{-1}$	$1.00 \pm 0.05$	$(5.98 \pm 0.3) \times 10^{-1}$	1.10	$6.58 \times 10^{-1}$
Lithium	6.94	$8.70 \times 10^{-2}$	$1.01 \pm 0.04$	$(8.79 \pm 0.35) \times 10^{-2}$	1.80	$1.57 \times 10^{-1}$
Beryllium	9.01	$6.70 \times 10^{-2}$	$1.07 \pm 0.06$	$(7.17 \pm 0.43) \times 10^{-2}$	1.70	$1.14 \times 10^{-1}$
Boron <sup>a</sup>	10.82	$5.57 \times 10^{-2}$	$0.97 \pm 0.10$	$(5.40 \pm 0.54) \times 10^{-2}$	1.50	$8.36 \times 10^{-2}$
Carbon	12.01	$5.02 \times 10^{-2}$	$0.81 \pm 0.05$	$(4.07 \pm 0.24) \times 10^{-2}$	1.60	$8.03 \times 10^{-2}$
Oxygen <sup>a</sup>	16.06	$3.76 \times 10^{-2}$	$0.99 \pm 0.10$	$(3.72 \pm 0.37) \times 10^{-2}$	1.20	$4.51 \times 10^{-2}$
Fluorine <sup>a</sup>	19.00	$3.17 \times 10^{-2}$	$1.29 \pm 0.06$	$(4.09 \pm 0.20) \times 10^{-2}$	1.60	$5.07 \times 10^{-2}$
Aluminum	26.98	$2.23 \times 10^{-2}$	$1.31 \pm 0.05$	$(2.92 \pm 0.12) \times 10^{-2}$	1.80	$4.01 \times 10^{-2}$
Chlorine <sup>a</sup>	35.46	$1.70 \times 10^{-2}$	$1.2 \pm 0.8$	$(2.0 \pm 1.4) \times 10^{-2}$	2.40	$4.08 \times 10^{-2}$
Iron	55.85	$1.08 \times 10^{-2}$	$1.98 \pm 0.08$	$(2.14 \pm 0.09) \times 10^{-2}$	3.20	$3.46 \times 10^{-2}$
Nickel	58.69	$1.03 \times 10^{-2}$	$1.89 \pm 0.10$	$(1.90 \pm 0.10) \times 10^{-2}$	3.45	$3.55 \times 10^{-2}$
Copper	63.54	$9.50 \times 10^{-3}$	$2.04 \pm 0.11$	$(1.94 \pm 0.11) \times 10^{-2}$	3.65	$3.47 \times 10^{-2}$
Tungsten	183.92	$3.27 \times 10^{-3}$	$2.51 \pm 0.55$	$(8.21 \pm 1.81) \times 10^{-3}$	4.90	$1.60 \times 10^{-2}$
Lead	207.21	$2.91 \times 10^{-3}$	$3.53 \pm 0.30$	$(1.03 \pm 0.09) \times 10^{-2}$	5.20	$1.51 \times 10^{-2}$
Bismuth	209.00	$2.88 \times 10^{-3}$	$3.49 \pm 0.35$	$(1.01 \pm 0.10) \times 10^{-2}$	5.10	$1.47 \times 10^{-2}$
Uranium	238.07	$2.53 \times 10^{-3}$	$3.6 \pm 0.4$	$(9.1 \pm 1.0) \times 10^{-3}$	6.10	$1.54 \times 10^{-2}$

<sup>a</sup> Derived  $\sigma_R$  values from measurements behind compounds of the elements.

Table 3  
Removal Cross Sections for Various Compounds

Compound	$\sigma_R$ , Microscopic Removal Cross Section (barns)
Boric Oxide, $B_2O_3$	$4.30 \pm 0.41$
Boron Carbide, $B_4C$	$4.3 \pm 0.4^a$ $5.1 \pm 0.4^b$
Fluorothene, $C_2F_3Cl$	$6.66 \pm 0.8$
Heavy Water, $D_2O$	$2.76 \pm 0.11$
Lithium Fluoride, $LiF$	$2.43 \pm 0.34$
Oil, $CH_2$	$2.84 \pm 0.11$
Paraffin, $C_{30}H_{62}$	$80.5 \pm 5.2$
Perfluoroheptane, $C_7F_{16}$	$26.3 \pm 0.8$

a Twelve 1-in.-thick  $B_4C$  slabs against source plate (Exp. 42).

b Solid slab against source plate (Exp. 33).



Enough data have now been obtained to investigate several aspects of this geometry problem. The calculations so far have made use of the best source geometry possible. The geometrical corrections, aside from the inverse distance squared term, consequently have been of the order of 10%, and Eq. (16) has produced sufficiently accurate results. To make use of the data closer to the source, including the fast-neutron data, it will be necessary to perform a more rigorous calculation, perhaps using Eqs. (12) and (13) directly. It would then be possible to describe the dependence of the removal cross section upon the thickness of the specimen and of the water following it, and to compare the results from the fast- and thermal-neutron data.

In order to facilitate such an approach the ratio of Eq. (12) to Eq. (13) was obtained and  $g(z)$  eliminated as follows:

$$\frac{D_1(z)}{D_2(z+t)} = \frac{\frac{\lambda_1}{ze^{z/\lambda}} \left\{ \frac{z^2}{z^2 + a^2} e^{(z/\lambda)} \left[ 1 - \sqrt{1 + (a/z)^2} \right] - 1 \right\}}{\frac{\lambda_2}{(z+t)e^{(z/\lambda) + \Sigma t}} \left\{ \left[ \frac{z+t}{z + \lambda \Sigma t} - \frac{a^2}{(z+t)^2 + a^2} \right] e^{\left( \frac{z + \lambda \Sigma t}{\lambda} \right) \left[ 1 - \sqrt{1 + \left( \frac{a}{z+t} \right)^2} \right]} - \frac{z+t}{z + \lambda \Sigma t} \right\}}$$

$$\frac{D_1(z)}{D_2(z+t)} = \frac{\lambda_1}{\lambda_2} e^{\Sigma t} \frac{\left( \frac{z+t}{z} \right) \left\{ \left( \frac{z^2}{z^2 + a^2} \right) e^{(z/\lambda)} \left[ 1 - \sqrt{1 + (a/z)^2} \right] - 1 \right\}}{\left( \frac{z+t}{z + \lambda \Sigma t} - \frac{a^2}{(z+t)^2 + a^2} \right) e^{\left( \frac{z + \lambda \Sigma t}{\lambda} \right) \left[ 1 - \sqrt{1 + \left( \frac{a}{z+t} \right)^2} \right]} - \frac{z+t}{z + \lambda \Sigma t}}$$

$$\frac{D_1(z)}{D_2(z+t)} = \frac{\lambda_1}{\lambda_2} e^{\Sigma t} \quad (F)$$

where  $F$  is a source geometric correction factor<sup>8</sup> dependent upon the variables  $z$ ,  $t$ , and  $\lambda$ . In Appendix B tabulated and graphical forms of the values of  $F$  for various values of  $\lambda$ ,  $t$ , and  $z + t$  with  $\lambda\Sigma = 0.7, 1.0$ , and  $1.3$  are presented. It is important to note that the variation with  $\lambda\Sigma$  is small, which is a welcome fact since of course  $\Sigma$  is the quantity to be determined.

It has been assumed that removal cross sections are additive, as are total cross sections. However, the experimental justification for this procedure is not yet available, since the present data are not sufficiently accurate to provide a suitable check. The measurements on C,  $C_7F_{16}$ , LiF, and Li and on C,  $B_4C$ ,  $B_2O_3$ , and  $CH_2$  should have provided this information, but unfortunately both chains contain weak links, namely, the measurements of LiF and  $B_4C$ .

There have been several attempts<sup>1,9,10</sup> to correlate the removal cross section with more rigorously defined properties of the atom, particularly the atomic weight and the total cross section. The paucity of the data has limited such generalizations, although for heavy atoms the calculations have met with some success. A plot of removal cross sections which may prove useful to shield calculations is shown in Fig. 3. Here the mass attenuation coefficient (the ratio of the macroscopic removal cross section to the density of the material,  $\Sigma/\rho$ ,  $\text{cm}^2\text{g}^{-1}$ ), a number proportional to the removal cross

---

<sup>8</sup> For a discussion of source geometries see E. P. Blizard, "Introduction to Shield Design," ORNL-CF-51-10-70, Part I Revised (Jan. 30, 1952); Part II Revised (Mar. 7, 1952).

<sup>9</sup> F. H. Murray, "Some Estimates of Removal Cross Sections Based on the Continuum Theory of the Scattering of Neutrons from Nuclei," ORNL-CF-53-12-60 (Dec. 11, 1953) (Declassified, 1955).

<sup>10</sup> H. Goldstein and R. Aronson, Reactor Sci. Tech. 4, No. 4 (Dec., 1954); TID-2015 ( ).

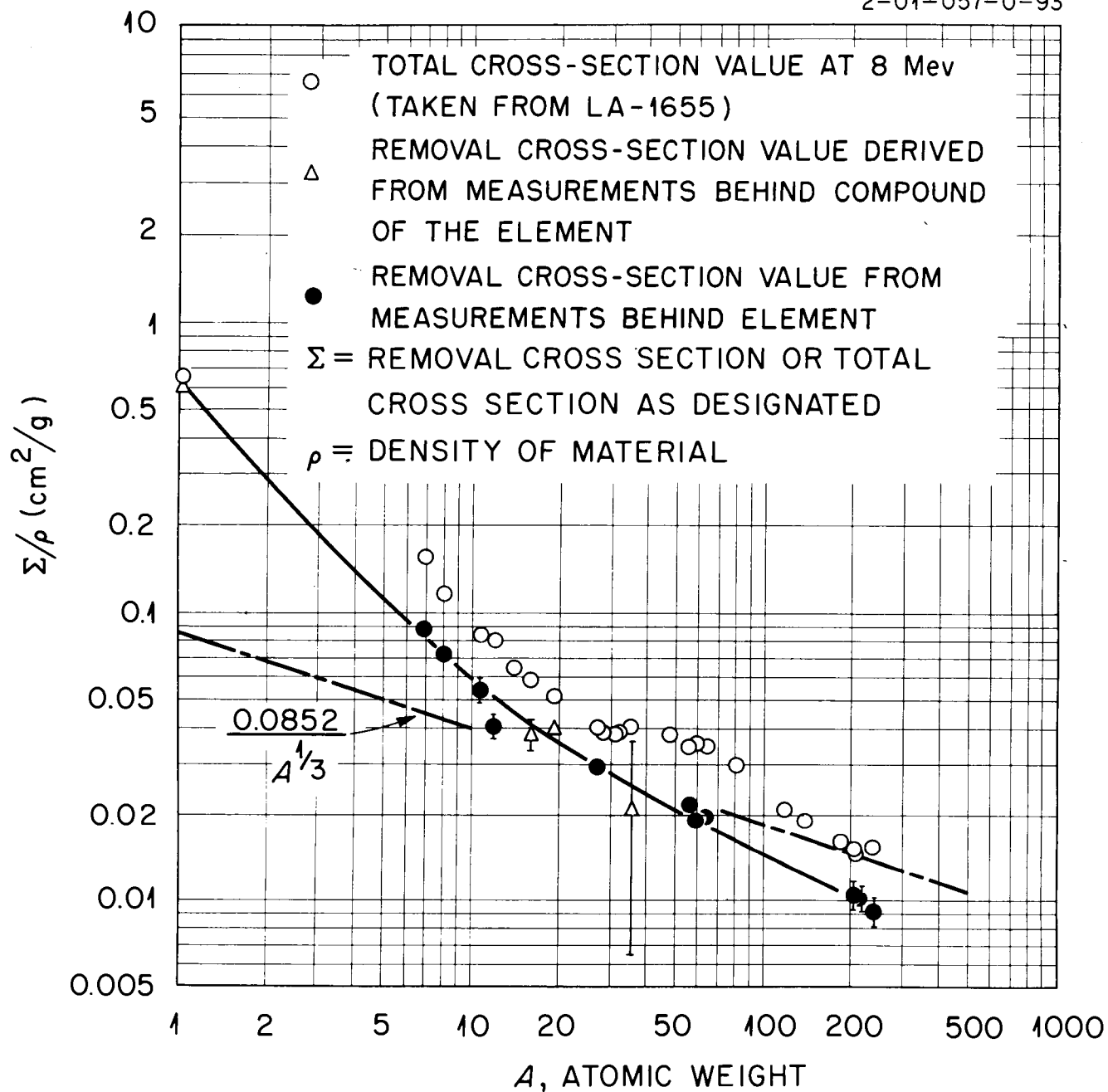


Fig. 3. Neutron Shielding Ability per Unit Weight of a Material as a Function of Atomic Weight.

per nucleon, is plotted against the atomic weight. This data is compared to the total cross section at 8 Mev as obtained by N. G. Nereson et al.<sup>11</sup> at Los Alamos Scientific Laboratory. Total cross sections at 8 Mev for the various elements are also given in Table 2.

---

<sup>11</sup> N. G. Nereson et al., "Survey of Average Neutron Total Cross Sections from 3 to 13 Mev," LA-1655 (April, 1954).

Appendix A

RADIATION INTENSITIES BEYOND VARIOUS MATERIALS: EXPERIMENTAL DATA

The descriptions of the experiments with the various materials at the LTSF were presented in Table 1, p. 7. The thermal-neutron flux, fast-neutron dose rate, and gamma-ray dose rate measurements beyond these materials are plotted and tabulated on the following pages as listed below:

	<u>Fig. No.</u>	<u>Pg. No.</u>	<u>Table No.</u>	<u>Pg. No.</u>
Thermal-neutron flux:				
Aluminum	A-1	31	A-1	86
Beryllium (pellets)	A-2	32	A-4	88
Beryllium (solid)	A-3	33	A-7	90
Bismuth	A-4	34	A-10	92
Boric oxide	A-5	35	A-12	94
Boron carbide	A-6	36	A-14	96
Carbon	A-7	37	A-17	98
Copper	A-8	38	A-20	100
Fluoroethene	A-9	39	A-23	102
Heavy water	A-10	40	A-26	104
Iron	A-11	41	A-29	106
Lead	A-12	42	A-32	108
Lithium	A-13	43	A-34	110
Lithium fluoride	A-14	44	A-36	112
Nickel	A-15	45	A-39	114
Oil	A-16	46	A-42	116
Paraffin	A-17	47	A-45	119
Perfluoroheptane	A-18	48	A-48	121

	<u>Fig. No.</u>	<u>Pg. No.</u>	<u>Table No.</u>	<u>Pg. No.</u>
Tungsten	A-19	49	A-51	123
Uranium	A-20	50	A-54	125
Fast-neutron dose rate:				
Aluminum	A-21	51	A-2	87
Beryllium (pellets)	A-22	52	A-5	89
Beryllium (solid)	A-23	53	A-8	91
Boron carbide	A-24	54	A-15	97
Carbon	A-25	55	A-18	99
Copper	A-26	56	A-21	101
Fluorothene	A-27	57	A-24	103
Heavy water	A-28	58	A-27	105
Iron	A-29	59	A-30	107
Lithium fluoride	A-30	60	A-37	113
Nickel	A-31	61	A-40	115
Oil	A-32	62	A-43	117
Paraffin	A-33	63	A-46	120
Perfluoroheptane	A-34	64	A-49	122
Tungsten	A-35	65	A-52	124
Gamma-ray dose rate:				
Aluminum	A-36	66	A-3	87
Beryllium (pellets)	A-37	67	A-6	89
Beryllium (solid)	A-38	68	A-9	91
Bismuth	A-39	69	A-11	93
Boric oxide	A-40	70	A-13	95
Boron carbide	A-41	71	A-16	97
Carbon	A-42	72	A-19	99

	<u>Fig. No.</u>	<u>Pg. No.</u>	<u>Table No.</u>	<u>Pg. No.</u>
Copper	A-43	73	A-22	101
Fluorothene	A-44	74	A-25	103
Heavy water	A-45	75	A-28	105
Iron	A-46	76	A-31	107
Lead	A-47	77	A-33	109
Lithium	A-48	78	A-35	111
Lithium fluoride	A-49	79	A-38	113
Nickel	A-50	80	A-41	115
Oil	A-51	81	A-44	118
Paraffin	A-52	82	A-47	120
Perfluoroheptane	A-53	83	A-50	122
Tungsten	A-54	84	A-53	124
Uranium	A-55	85	A-55	126

In most cases the type of instrument used for the measurement is indicated on the tables in an abbreviated form. The instruments used<sup>1</sup> and the abbreviated forms are as follows:

Thermal-neutron flux measurements:

1/2-in. fission chamber	1/2 FC
3-in. fission chamber	3 FC
8-in. BF <sub>3</sub> counter	8 BF <sub>3</sub>
12-1/2-in. BF <sub>3</sub> counter (single barrel)	BF <sub>3</sub> (SB)
12-1/2-in. BF <sub>3</sub> counter (double barrel)	BF <sub>3</sub> (DB)

Fast-neutron dose rate measurements:

Hurst-type fast-neutron dosimeter	HD
-----------------------------------	----

Gamma-ray dose rate measurements:

90-cc ion chamber	90 IC
900-cc ion chamber	900 IC
Anthracene scintillation crystal	ASC

<sup>1</sup> These instruments are described in detail by G. T. Chapman in ORNL-1889, "Instrumentation at the ORNL Shielding Facilities" (to be issued).

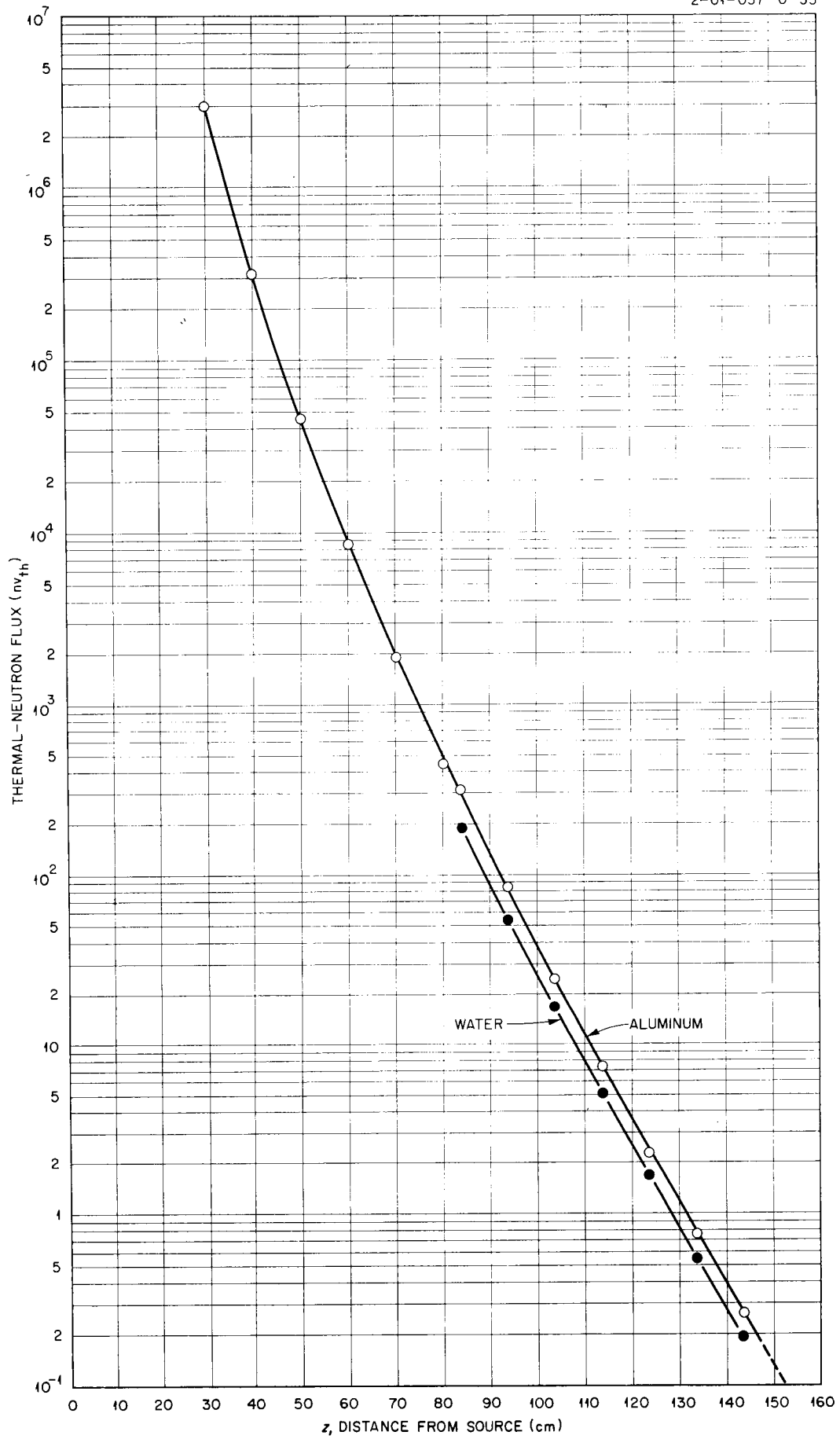


Fig. A-1. Thermal-Neutron Flux Beyond Aluminum



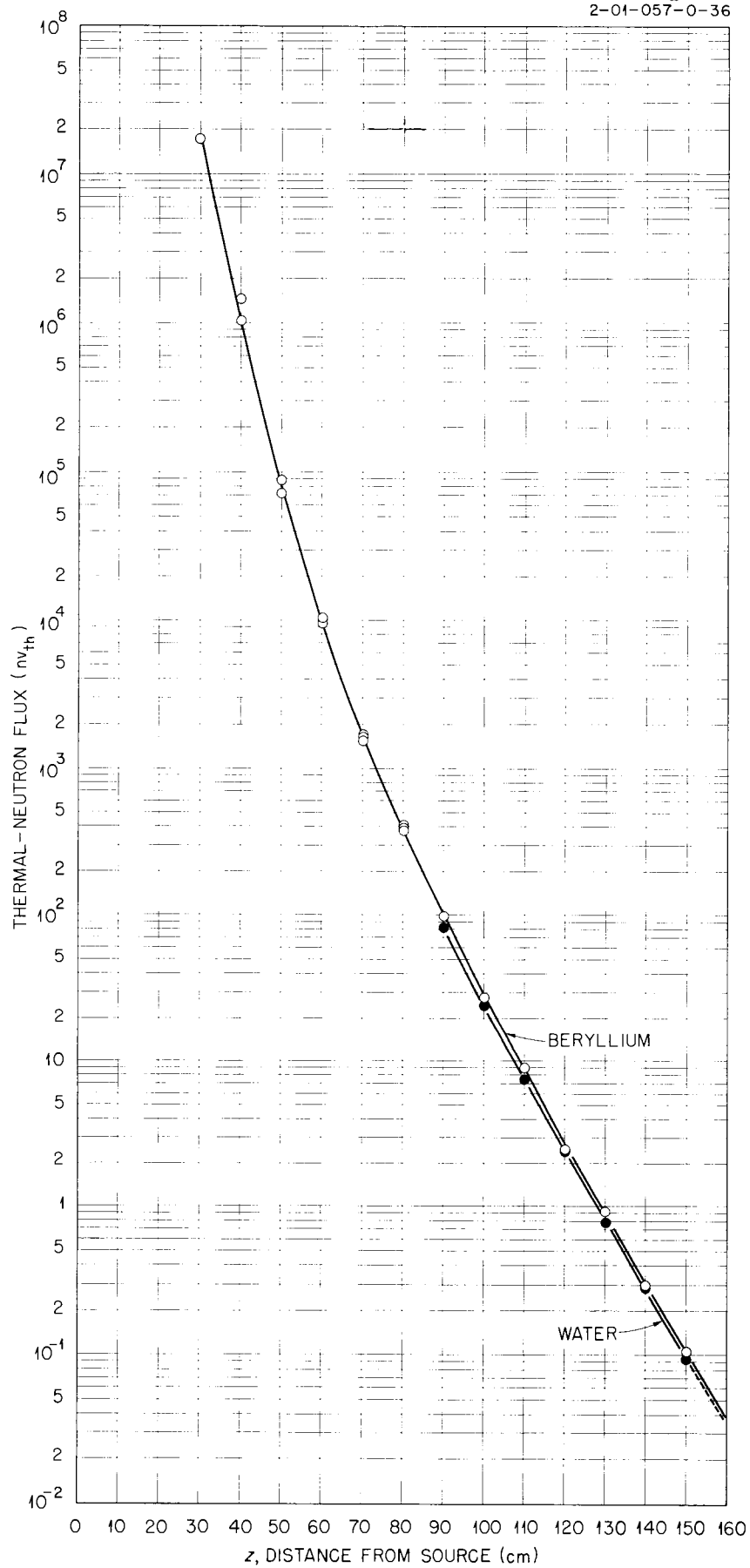


Fig. A-2. Thermal-Neutron Flux Beyond Beryllium Pellets

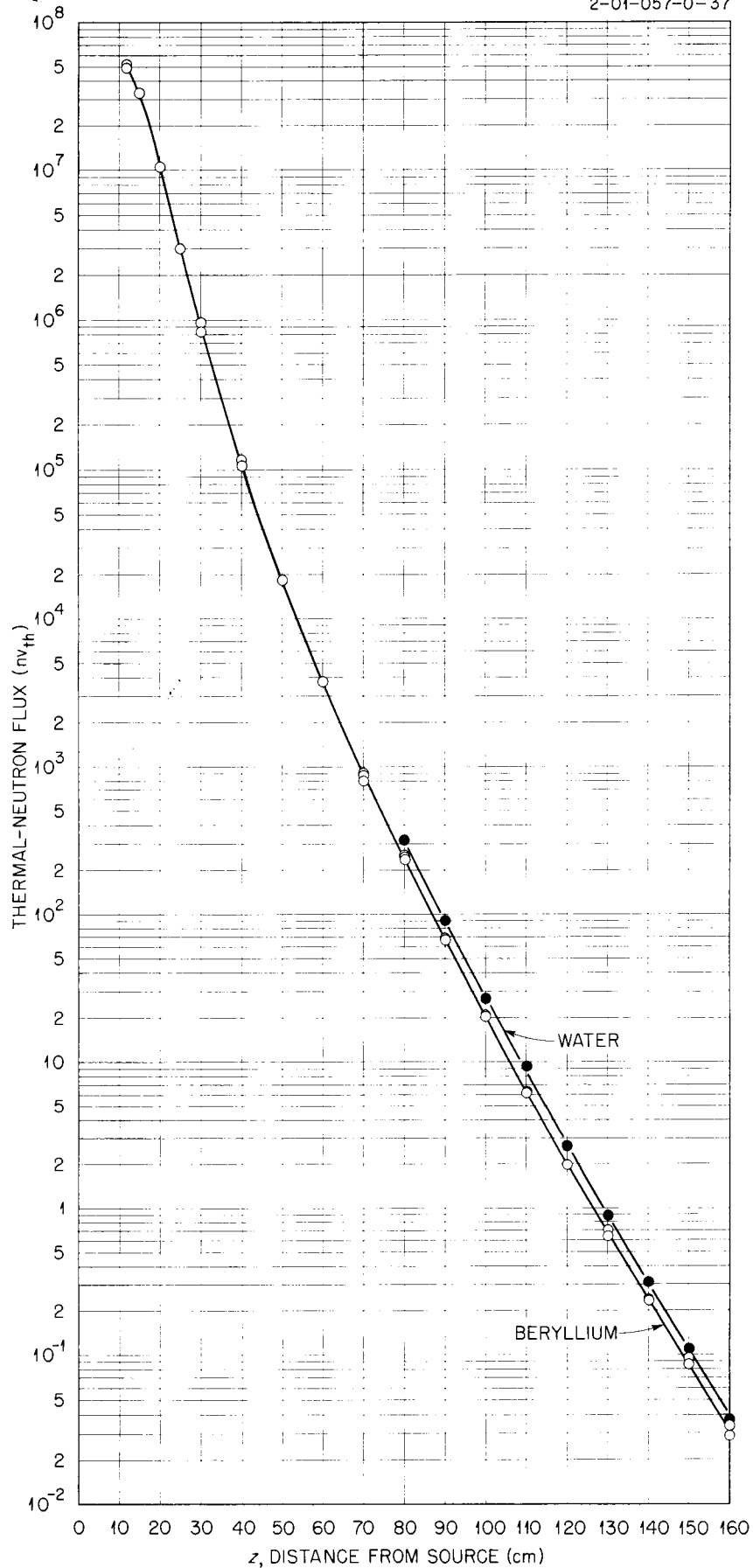


Fig. A-3. Thermal-Neutron Flux Beyond Solid Beryllium

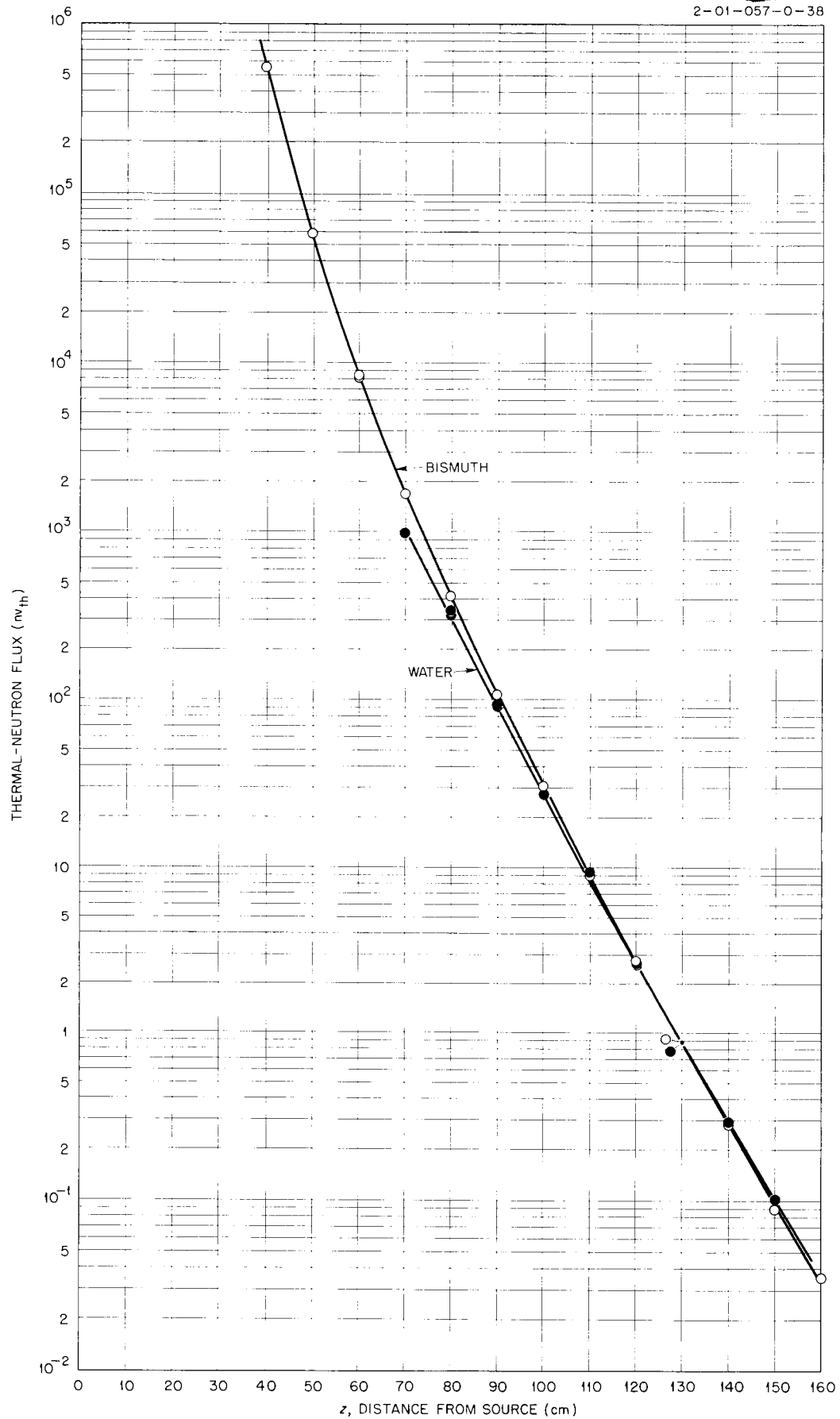
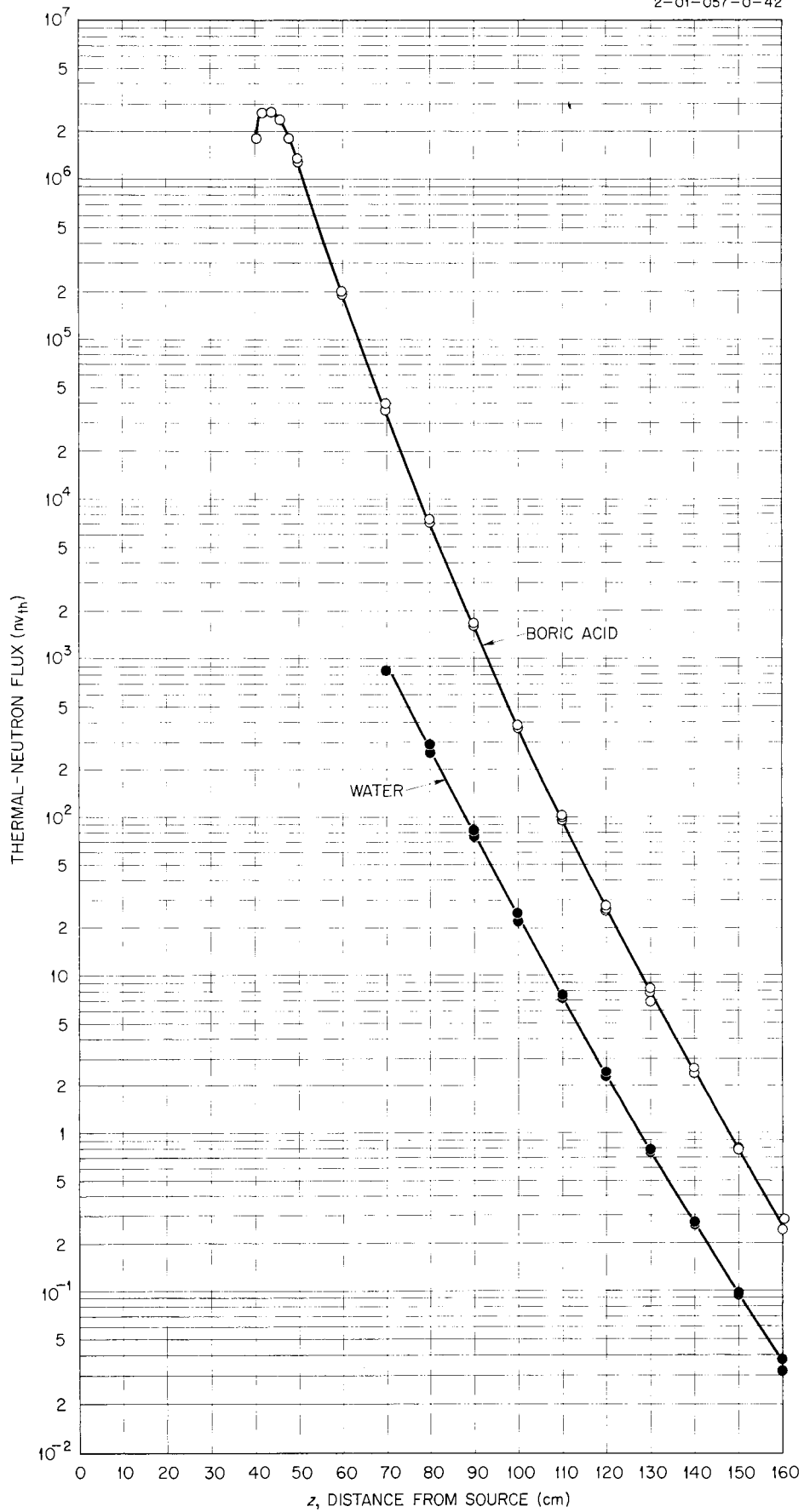
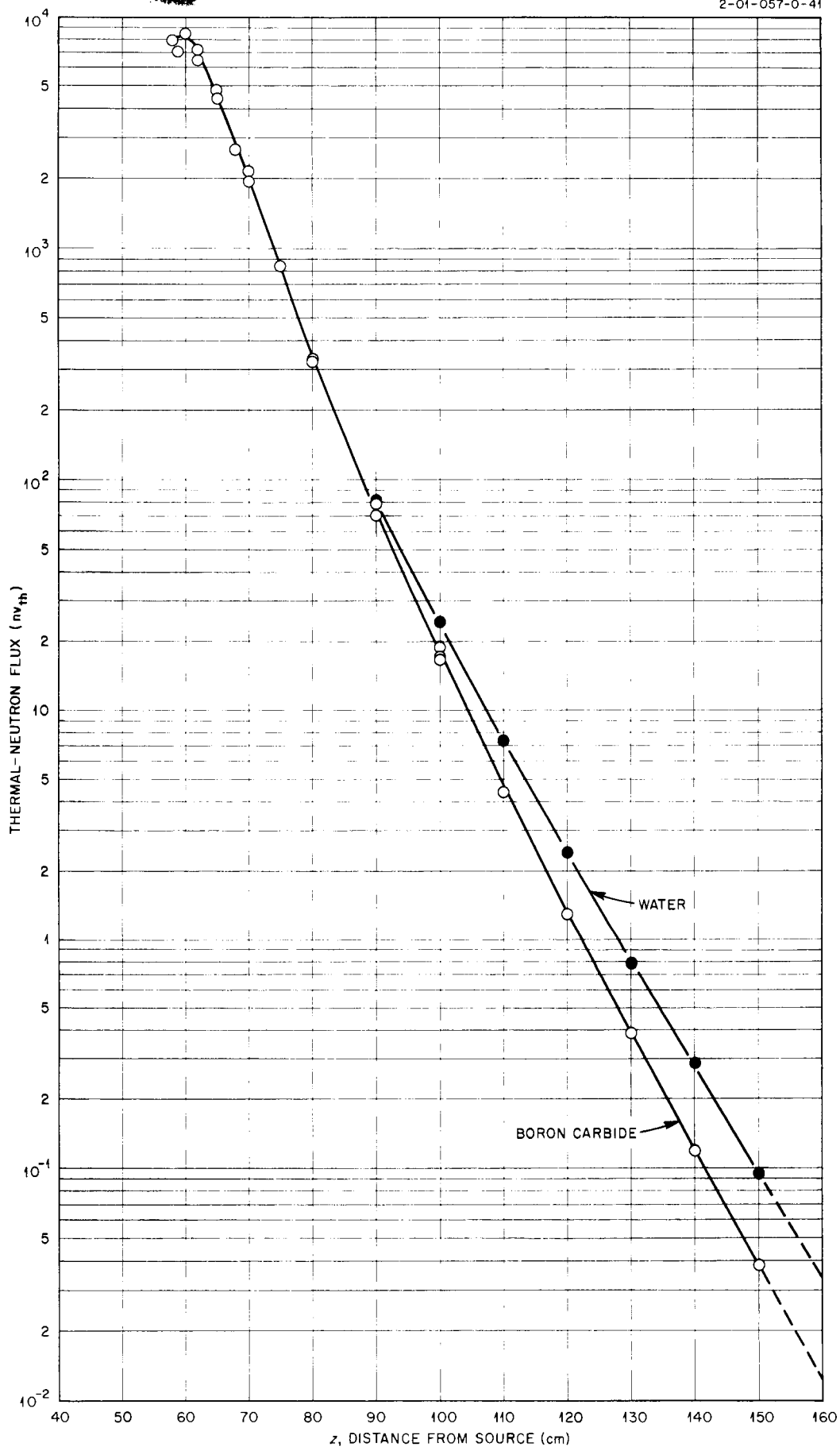


Fig. A-4. Thermal-Neutron Flux Beyond Bismuth.

Fig. A-5. Thermal-Neutron Flux Beyond Boric Acid ( $B_2O_3$ )

Fig. A-6 Thermal-Neutron Flux Beyond Boron Carbide ( $B_4C$ )

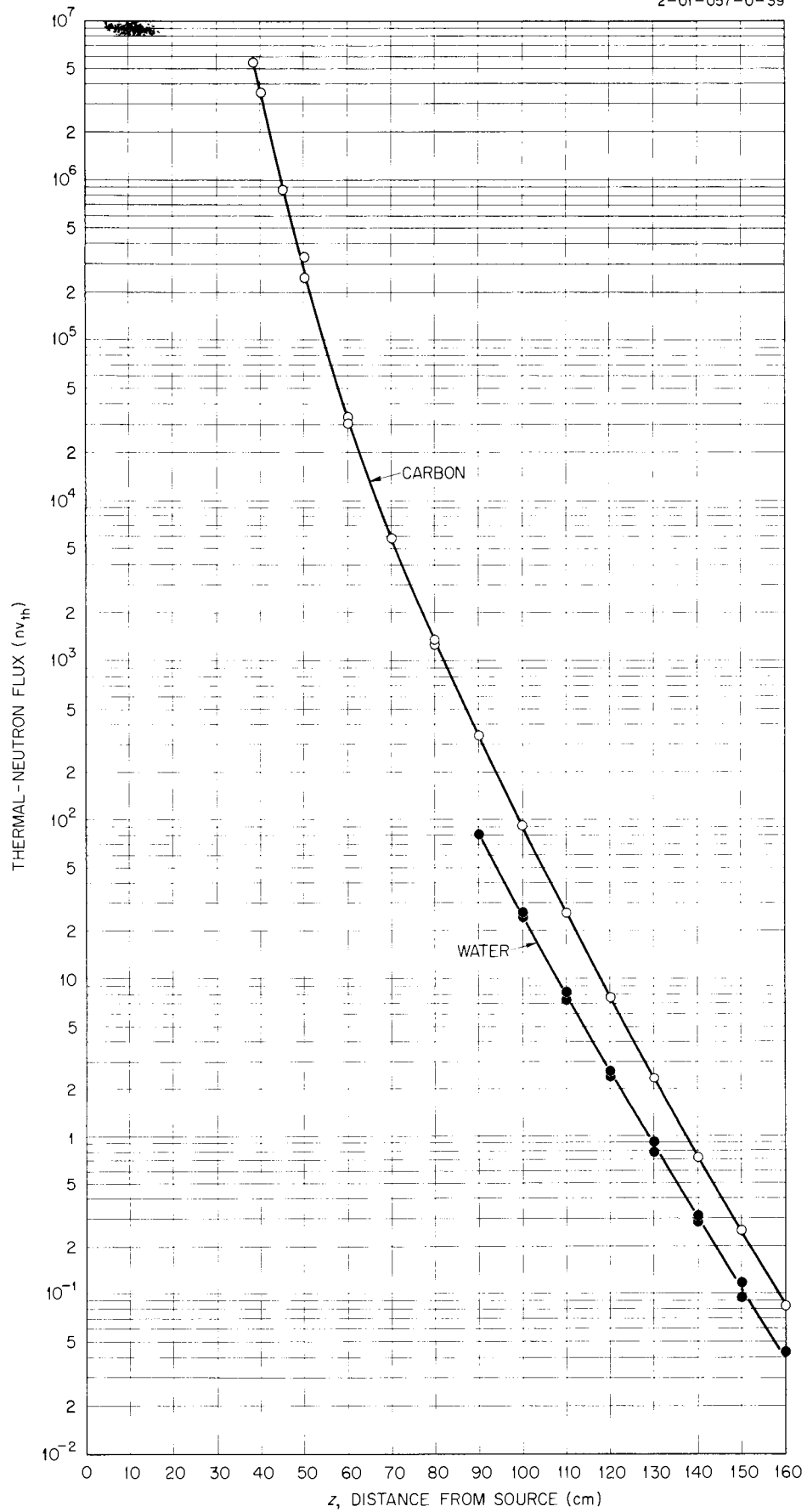


Fig. A-7. Thermal-Neutron Flux Beyond Carbon (AGHT)

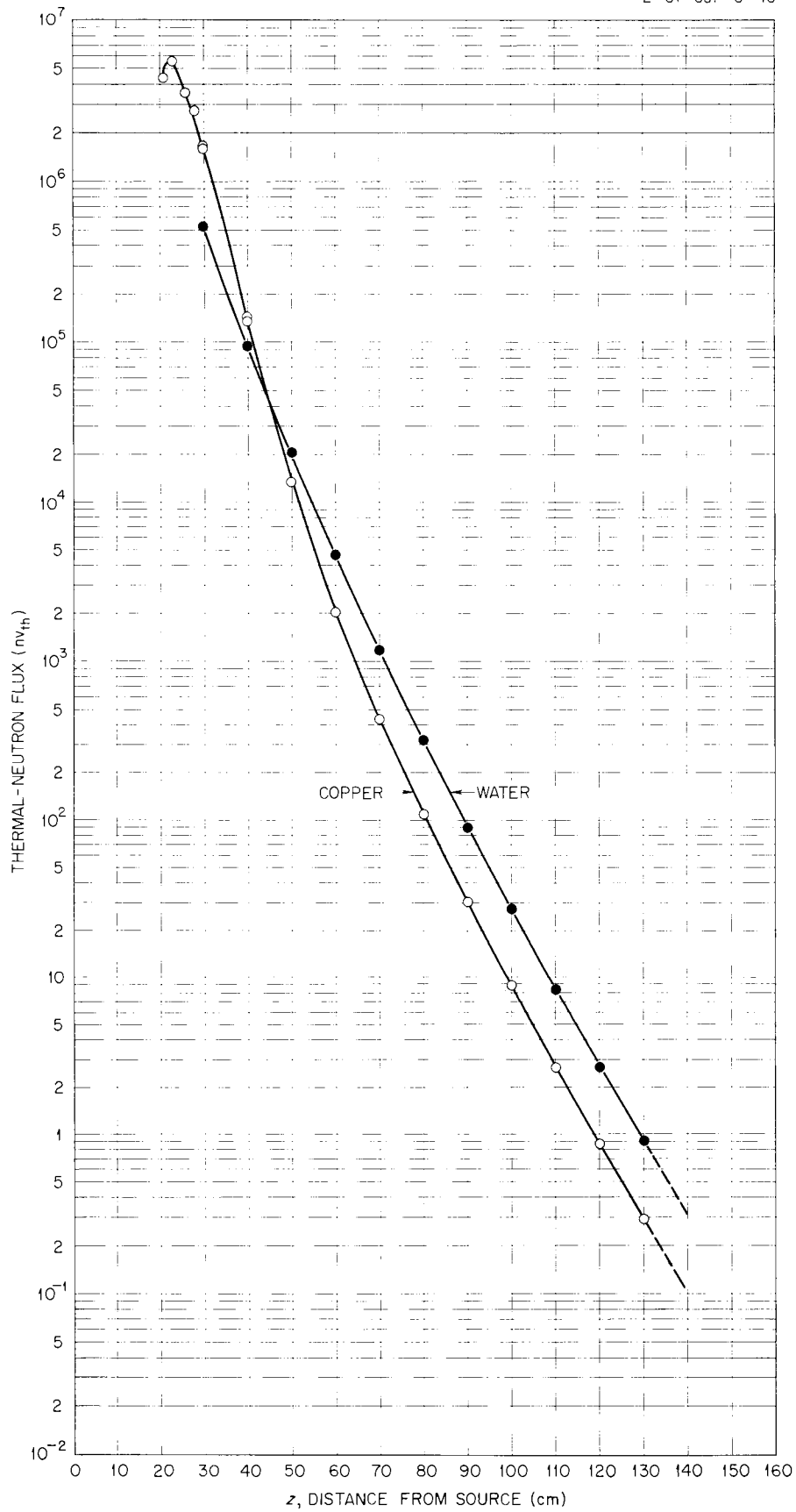
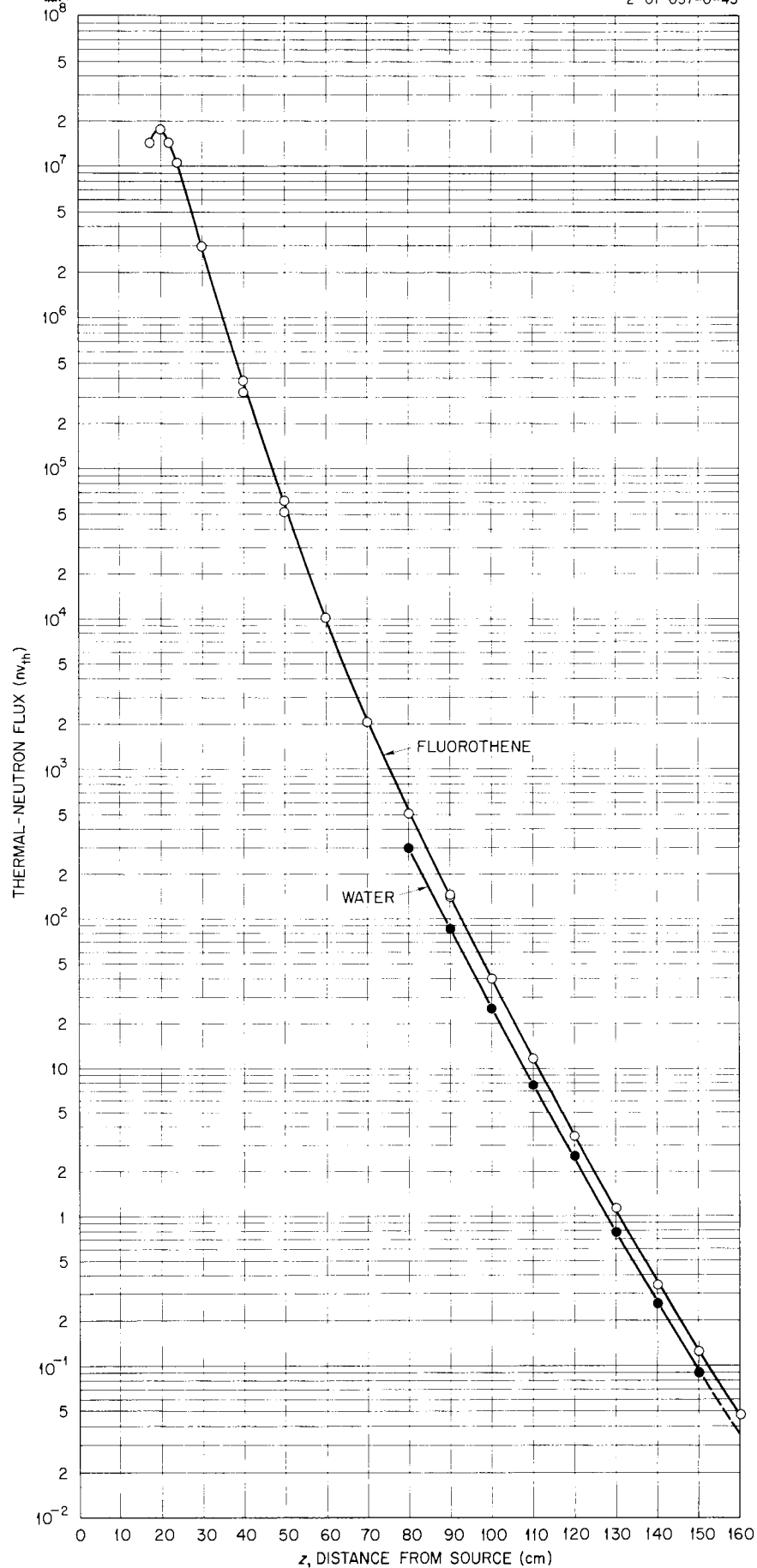
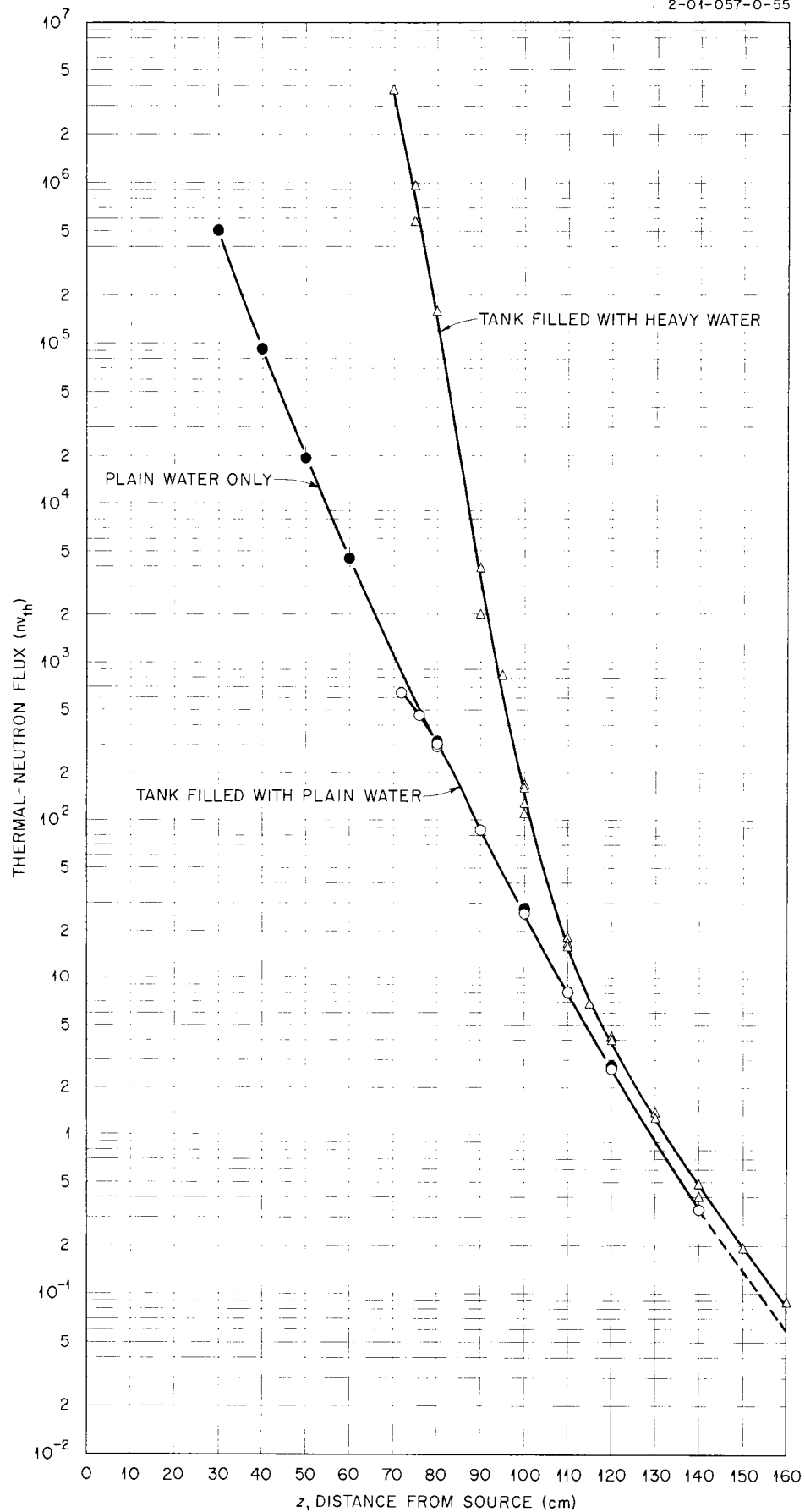


Fig. A-8. Thermal-Neutron Flux Beyond Copper

Fig. A-9. Thermal-Neutron Flux Beyond Fluorothene ( $C_2F_3Cl$ )



Fig. A-10. Thermal-Neutron Flux Beyond Heavy Water ( $D_2O$ )

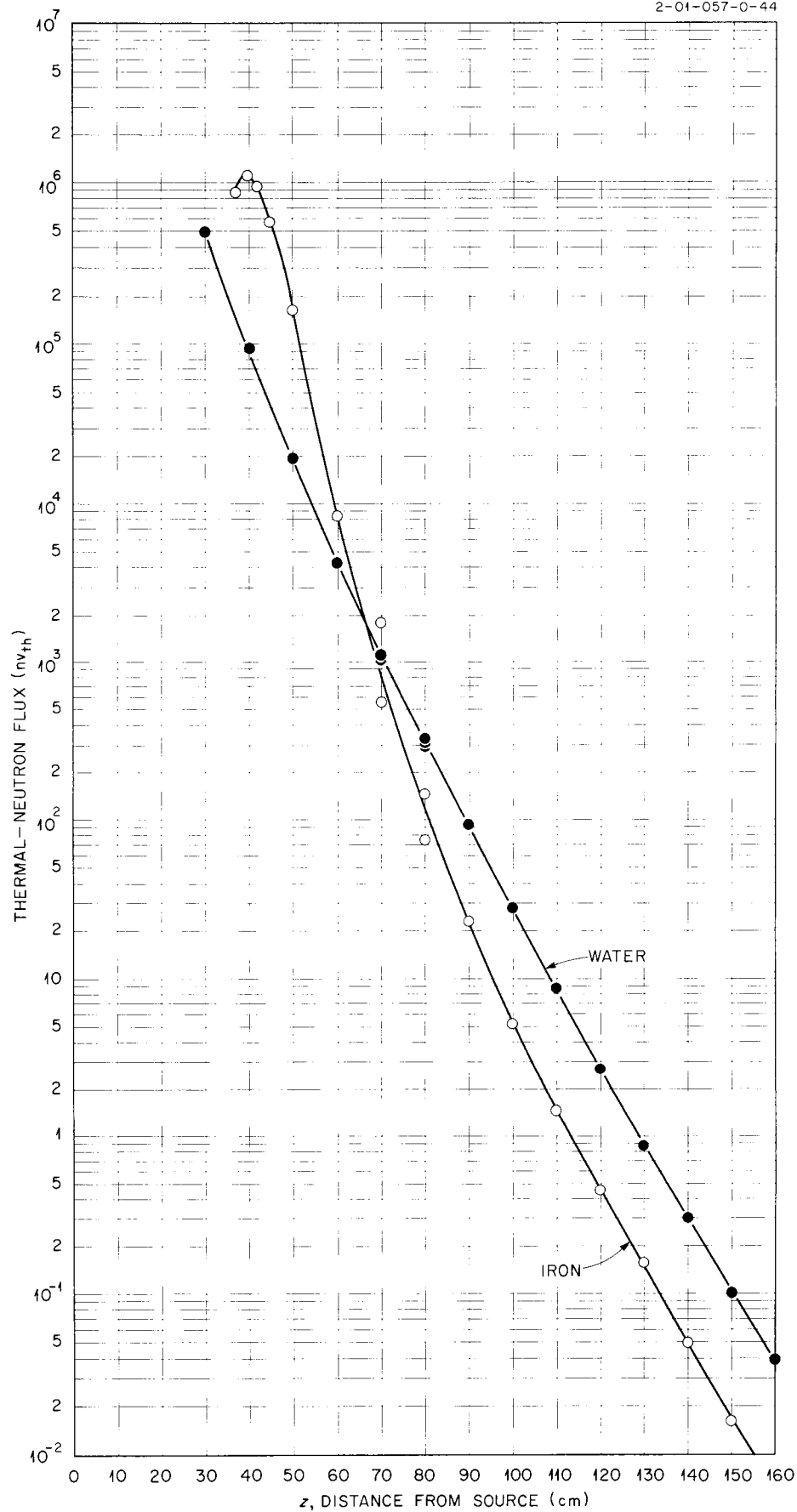


Fig. A-11. Thermal-Neutron Flux Beyond Iron

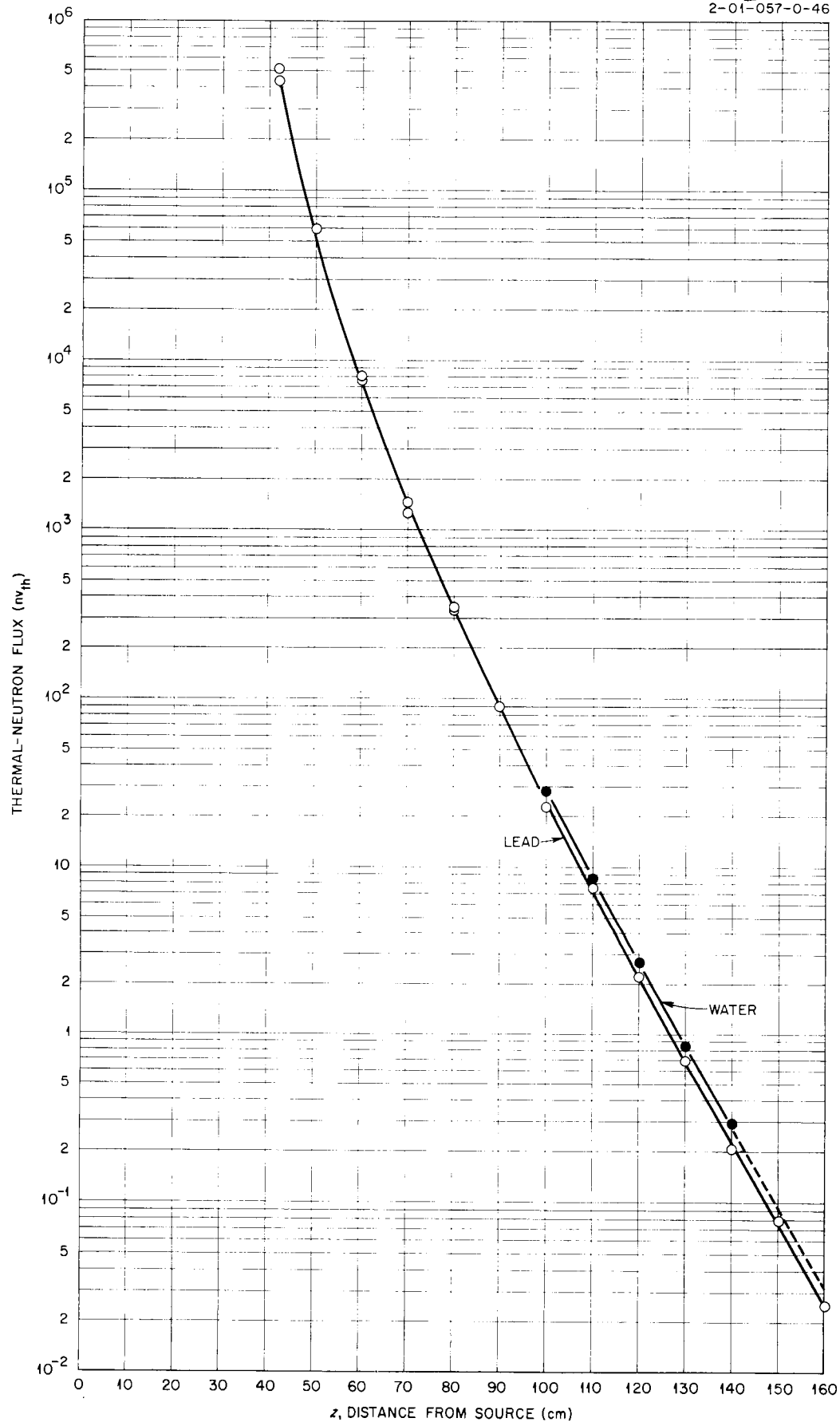


Fig. A-12. Thermal-Neutron Flux Beyond Lead

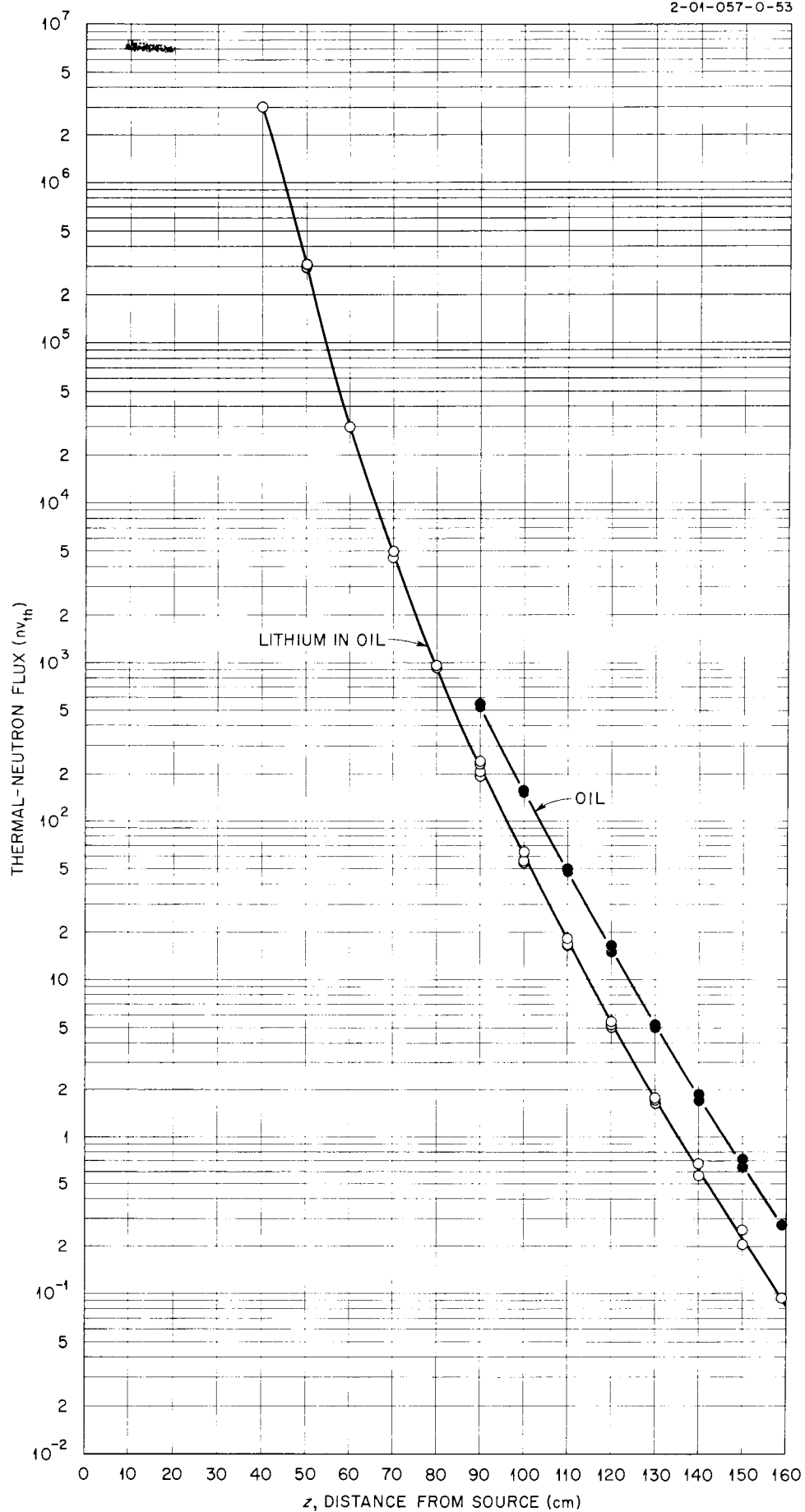


Fig. A-13. Thermal-Neutron Flux Beyond Lithium.

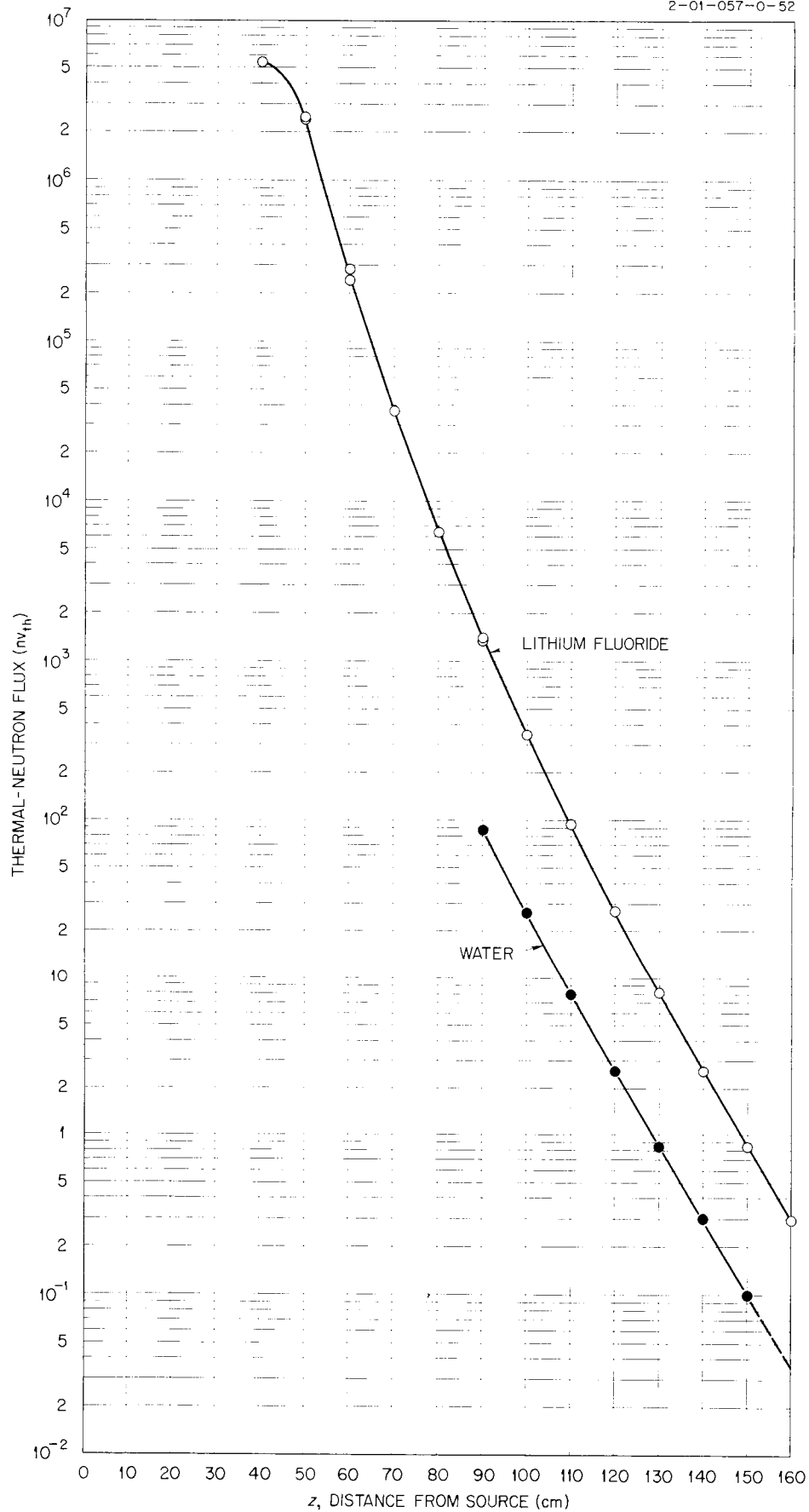


Fig. A-14. Thermal-Neutron Flux Beyond Lithium Fluoride (LiF)

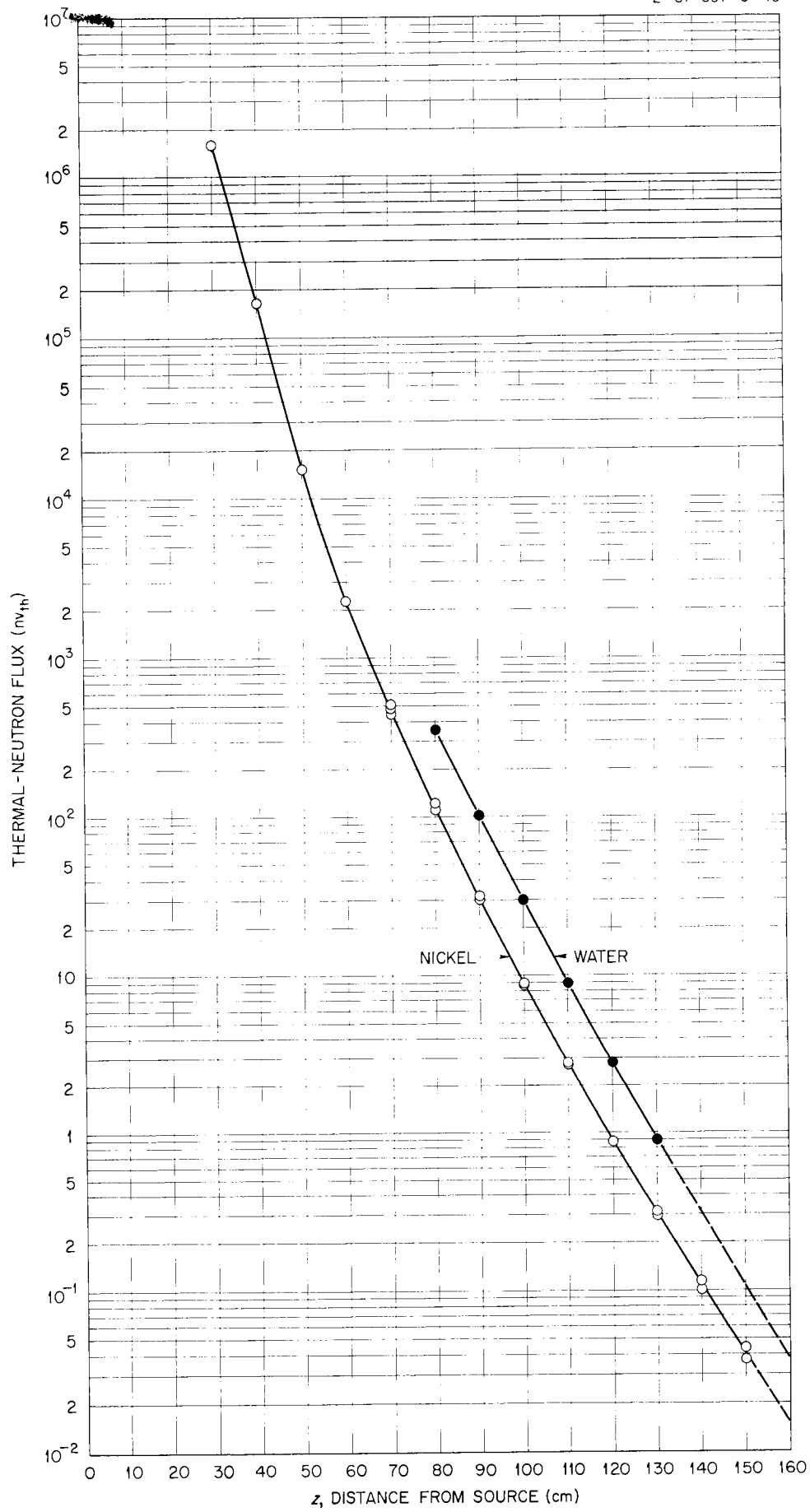
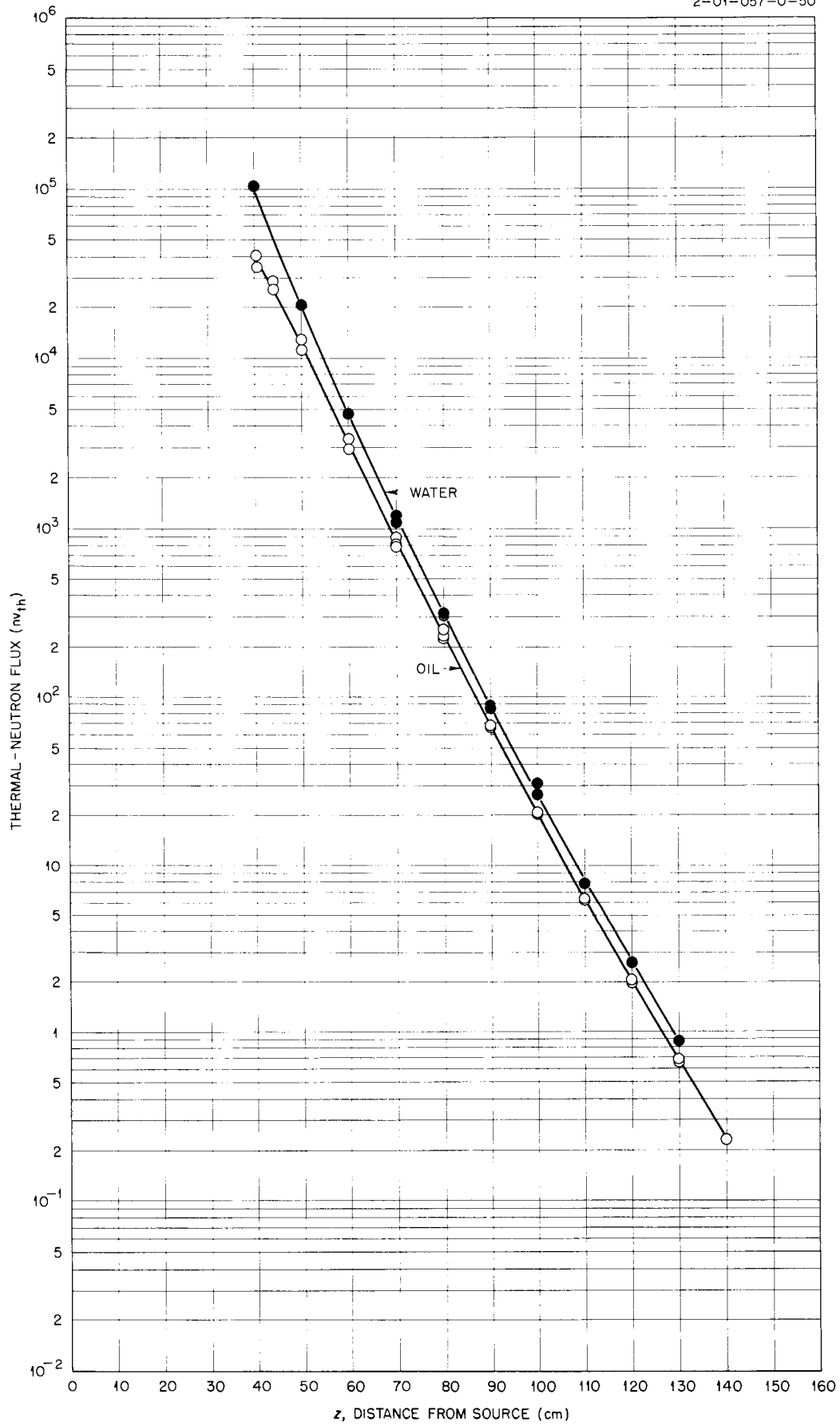


Fig. A-15. Thermal-Neutron Flux Beyond Nickel

Fig.A-16. Thermal-Neutron Flux Beyond Oil (CH<sub>2</sub>)

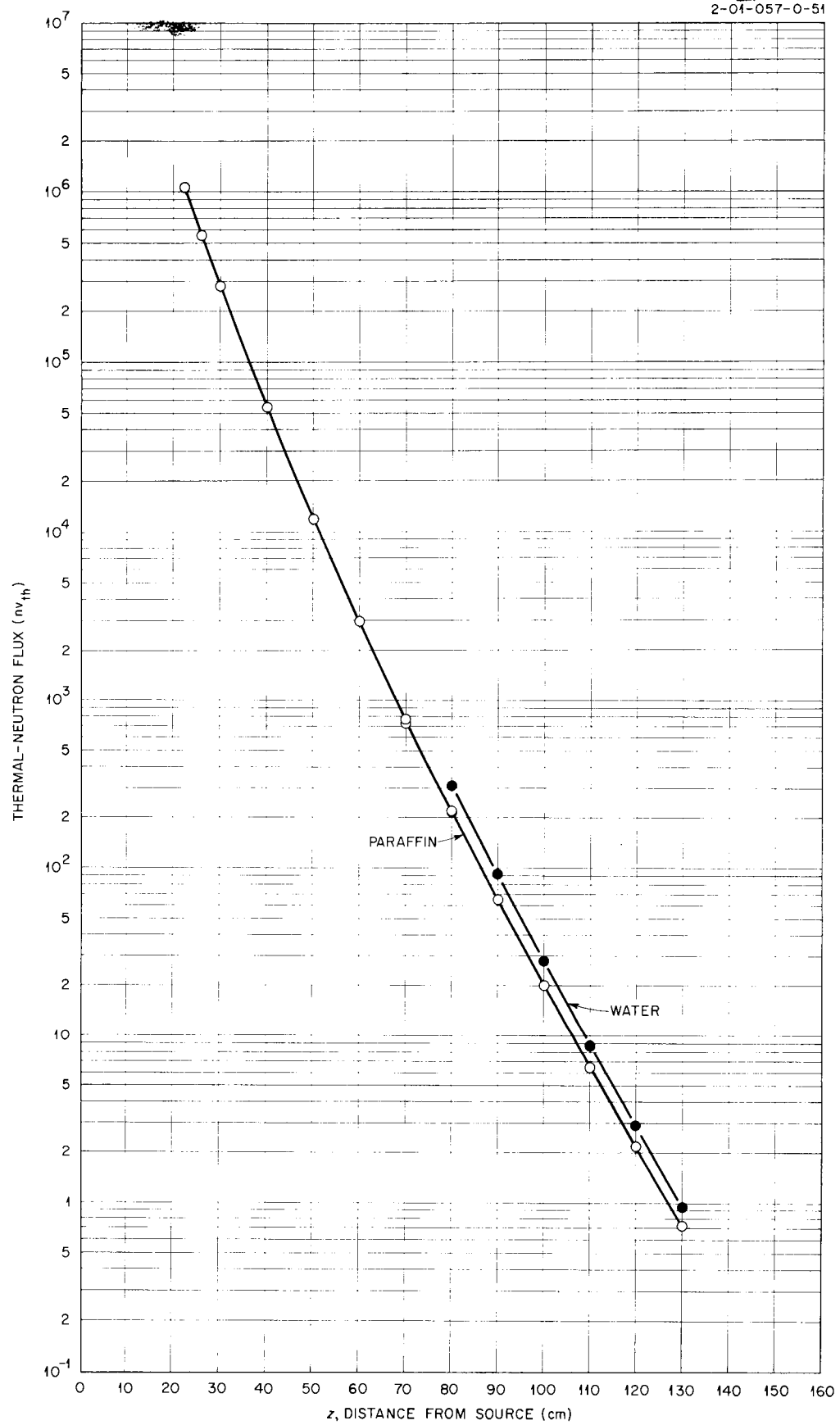
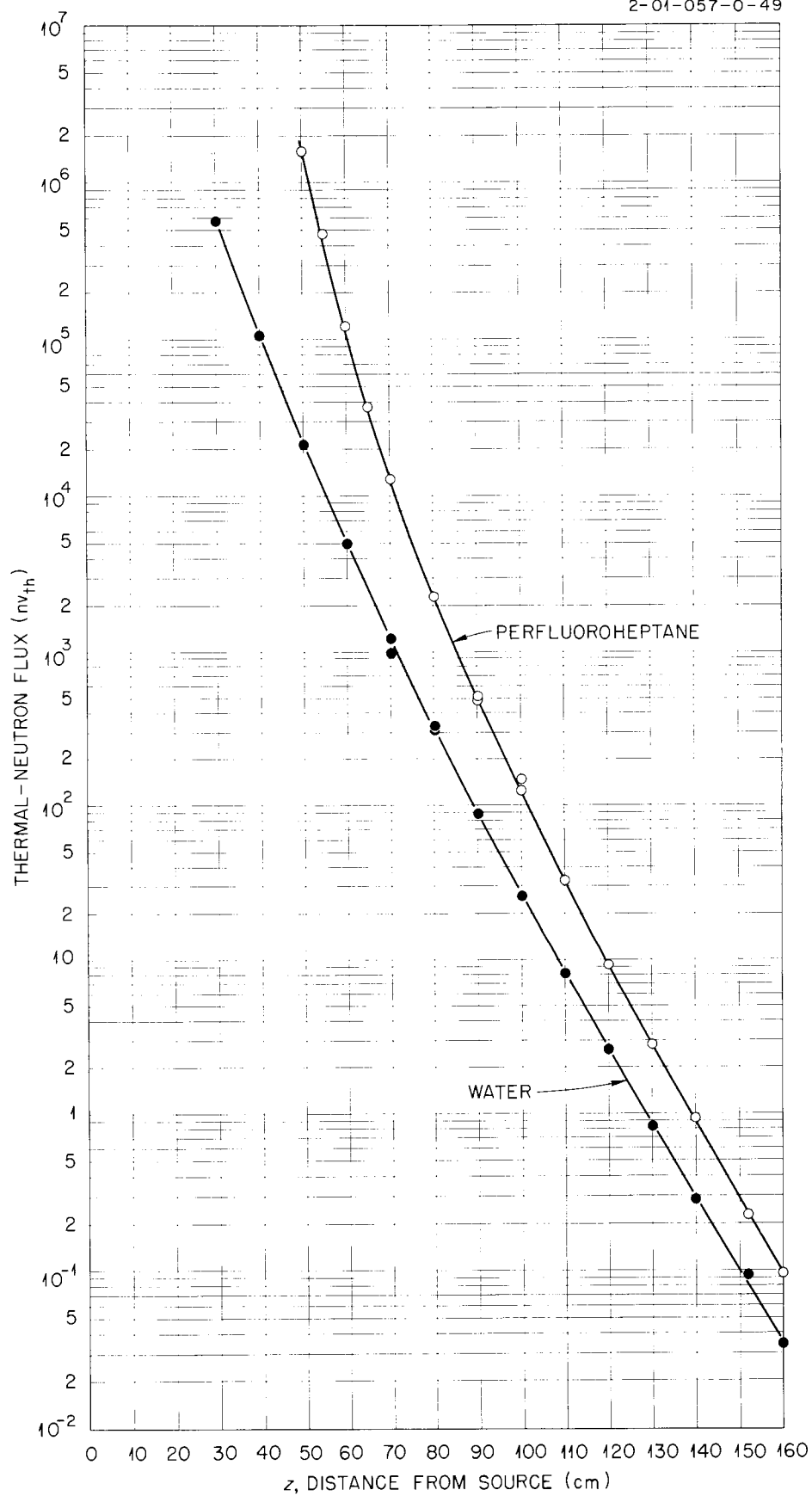


Fig. A-17. Thermal-Neutron Flux Beyond Paraffin (C<sub>30</sub>H<sub>62</sub>)



Fig. A-18. Thermal-Neutron Flux Beyond Perfluoroheptane ( $C_7F_{16}$ )

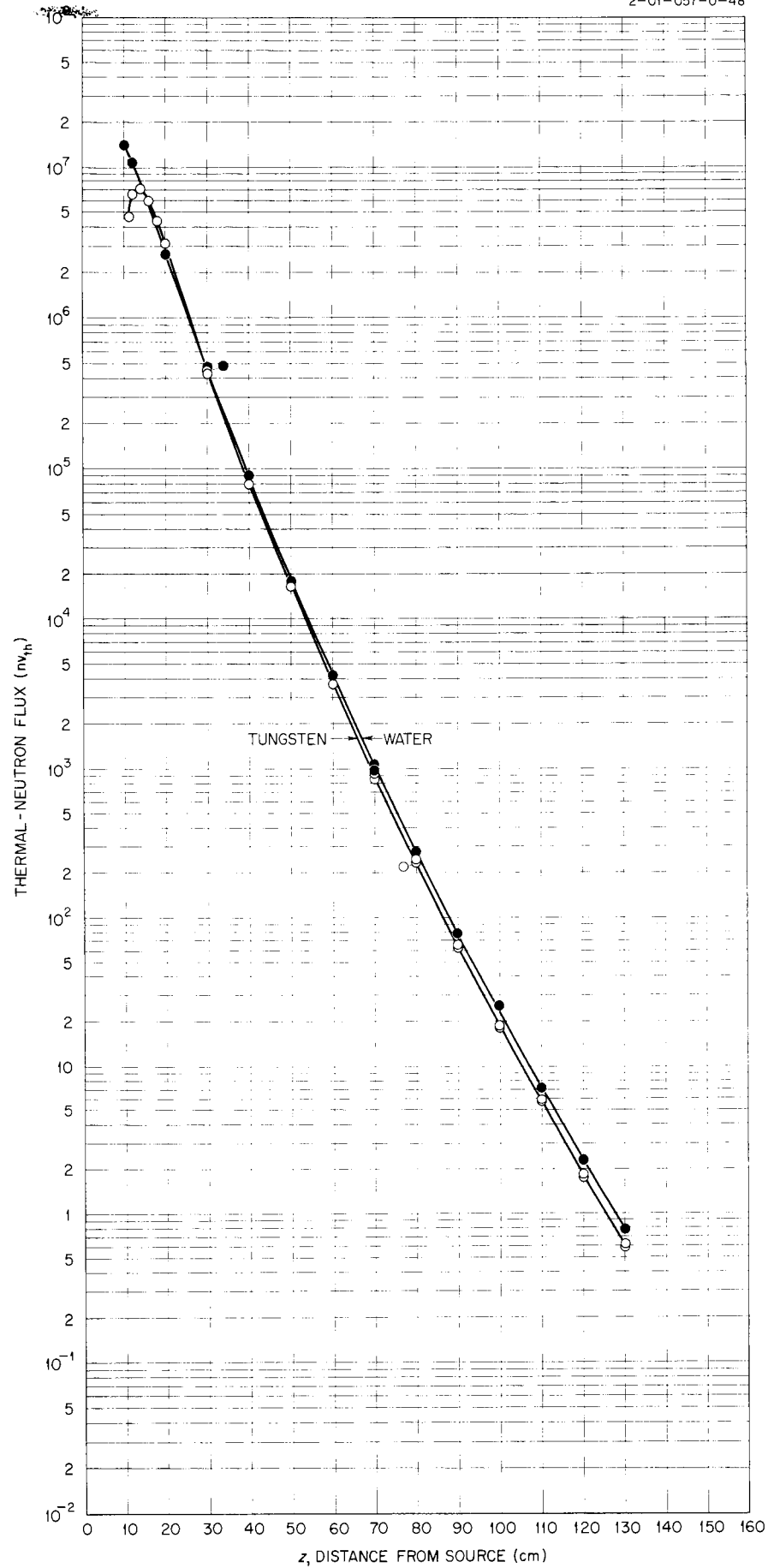


Fig. A-19. Thermal-Neutron Flux Beyond Tungsten

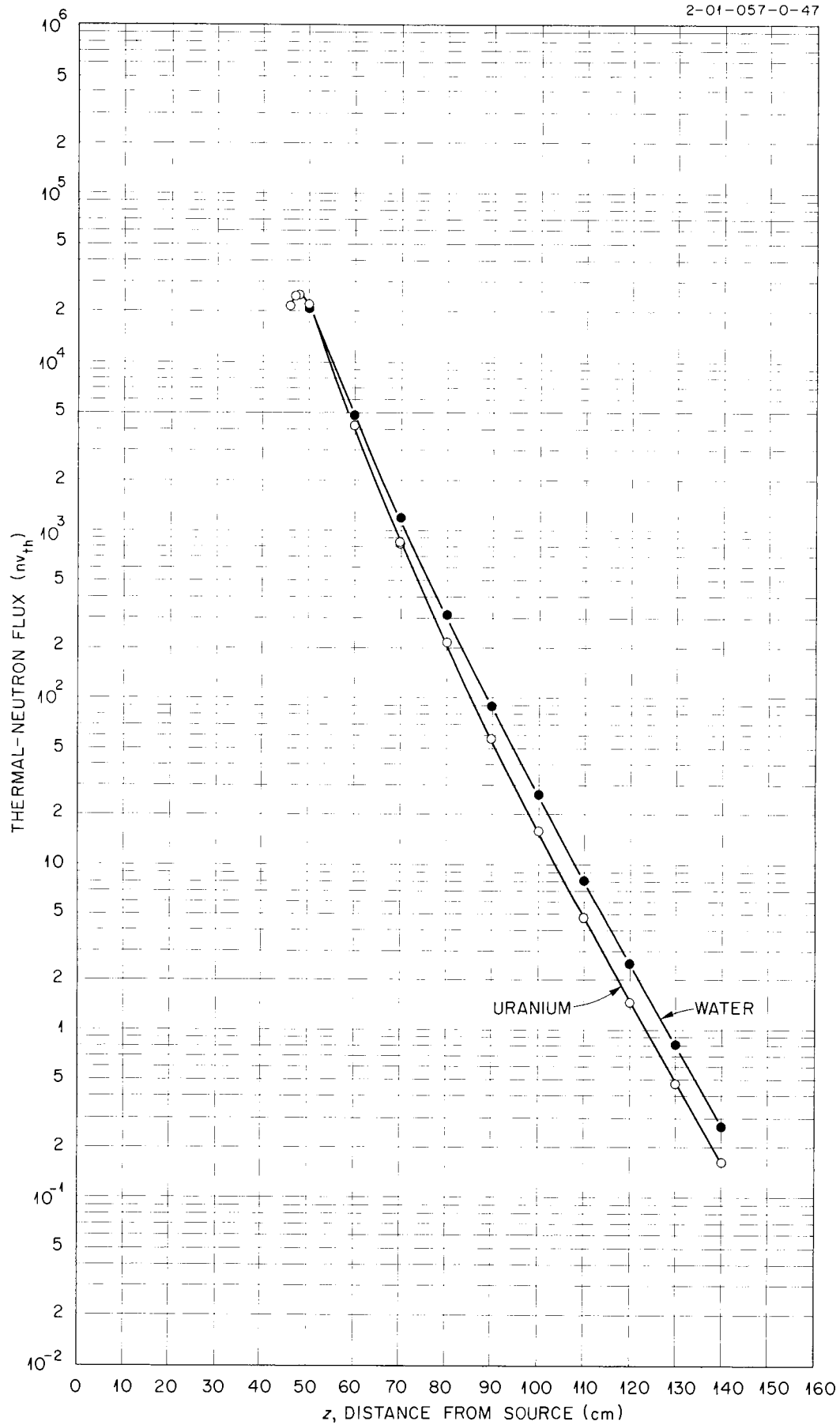


Fig. A-20. Thermal-Neutron Flux Beyond Uranium.

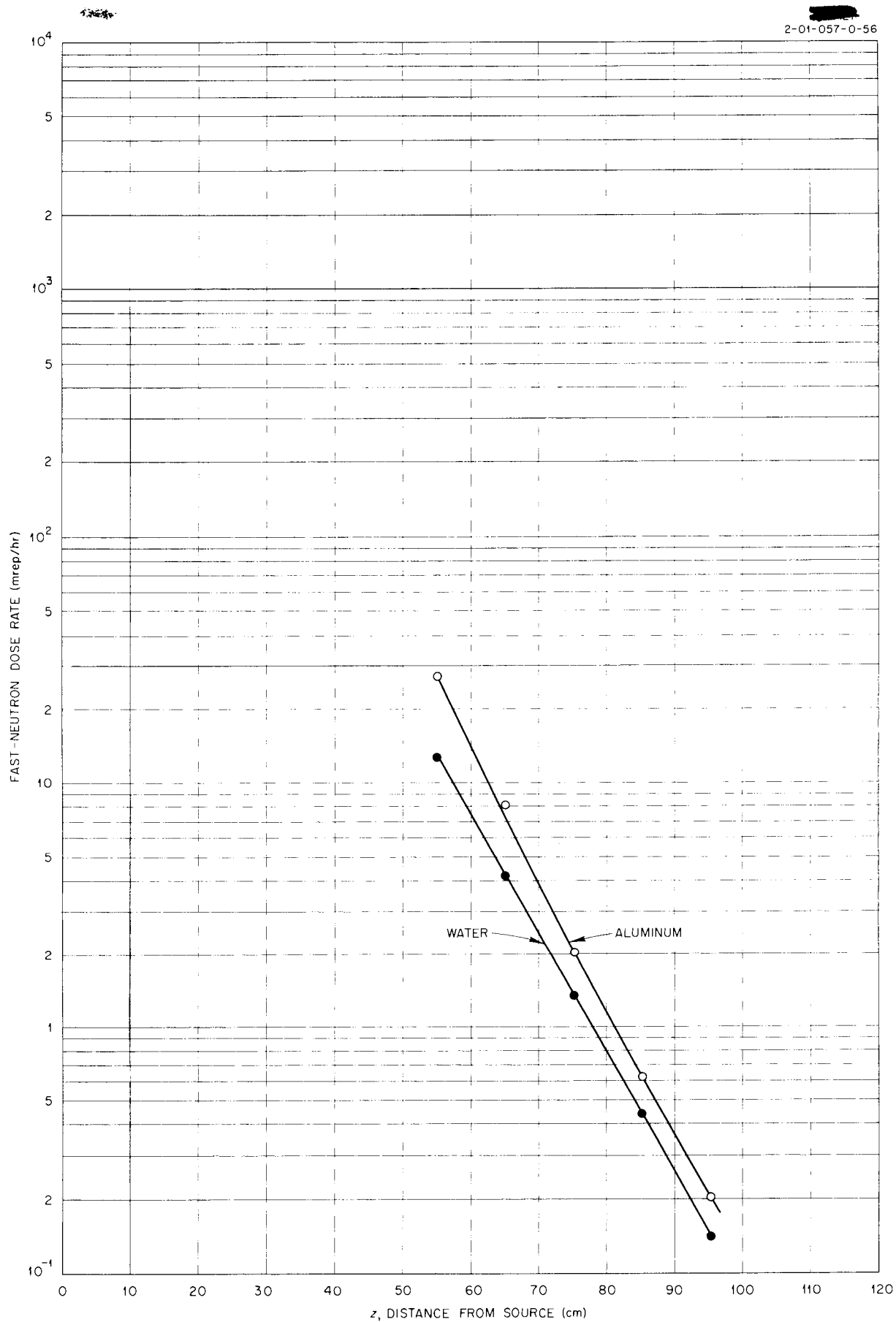


Fig. A-21. Fast-Neutron Dose Rate Beyond Aluminum.

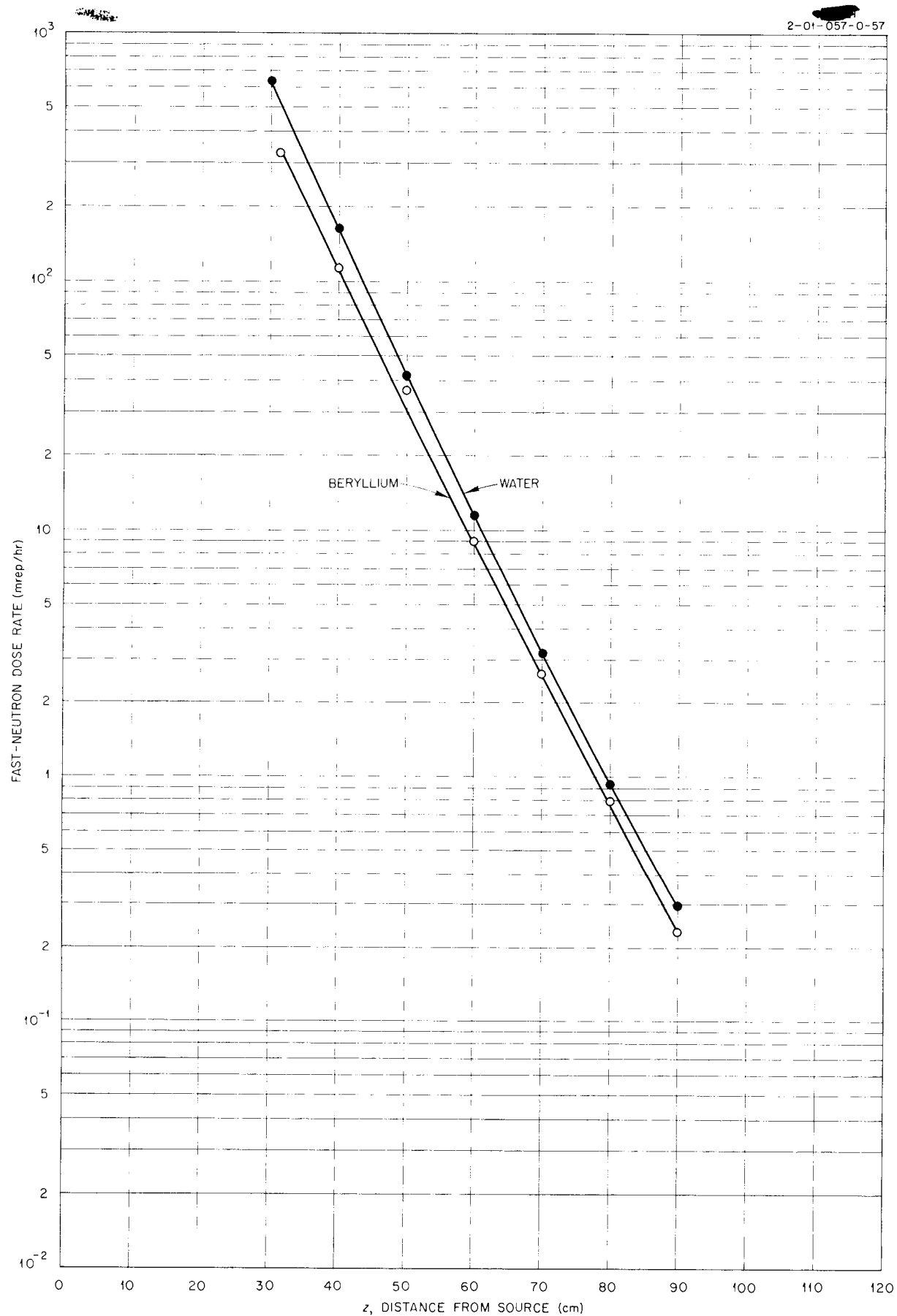


Fig. A-22. Fast-Neutron Dose Rate Beyond Beryllium Pellets.

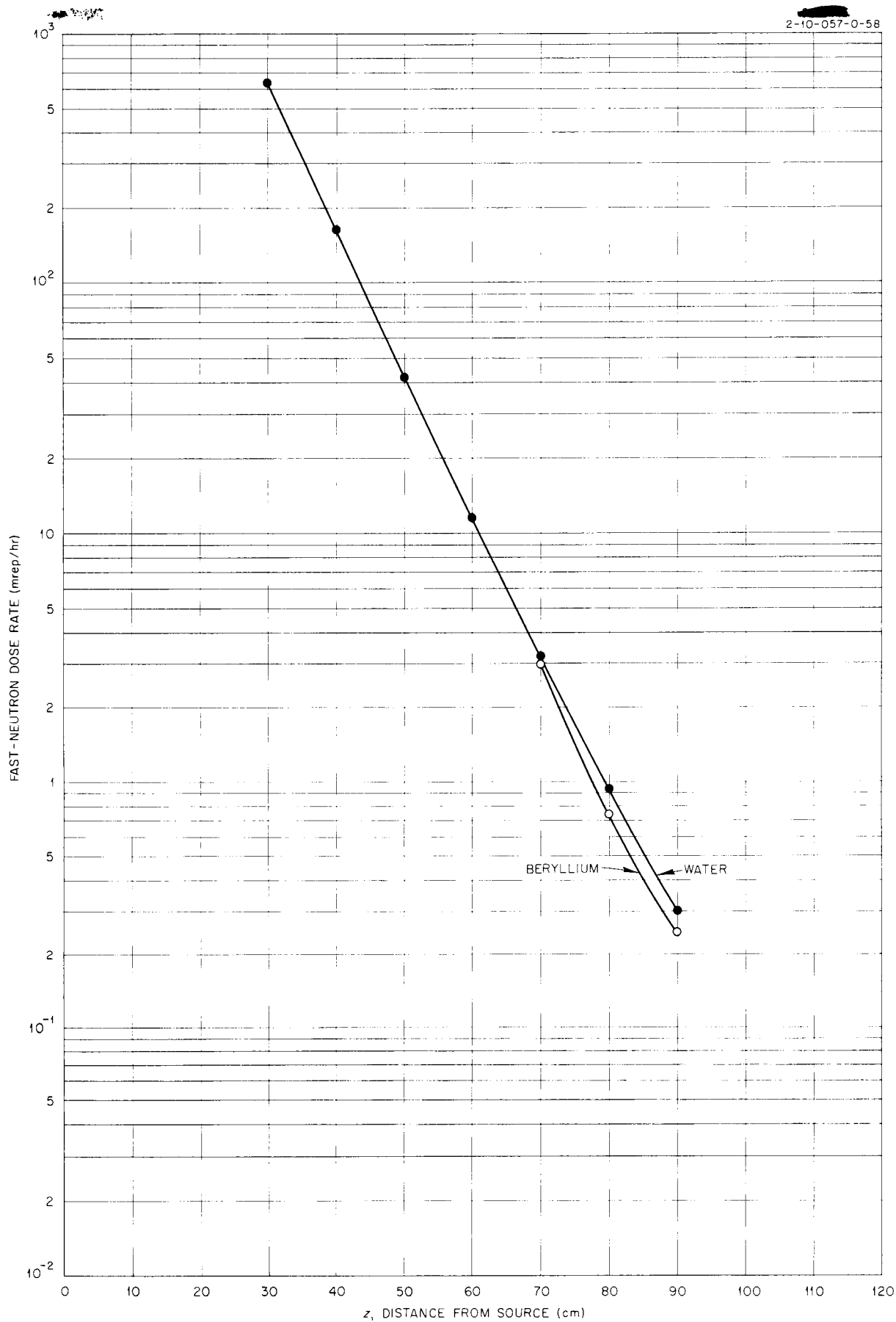
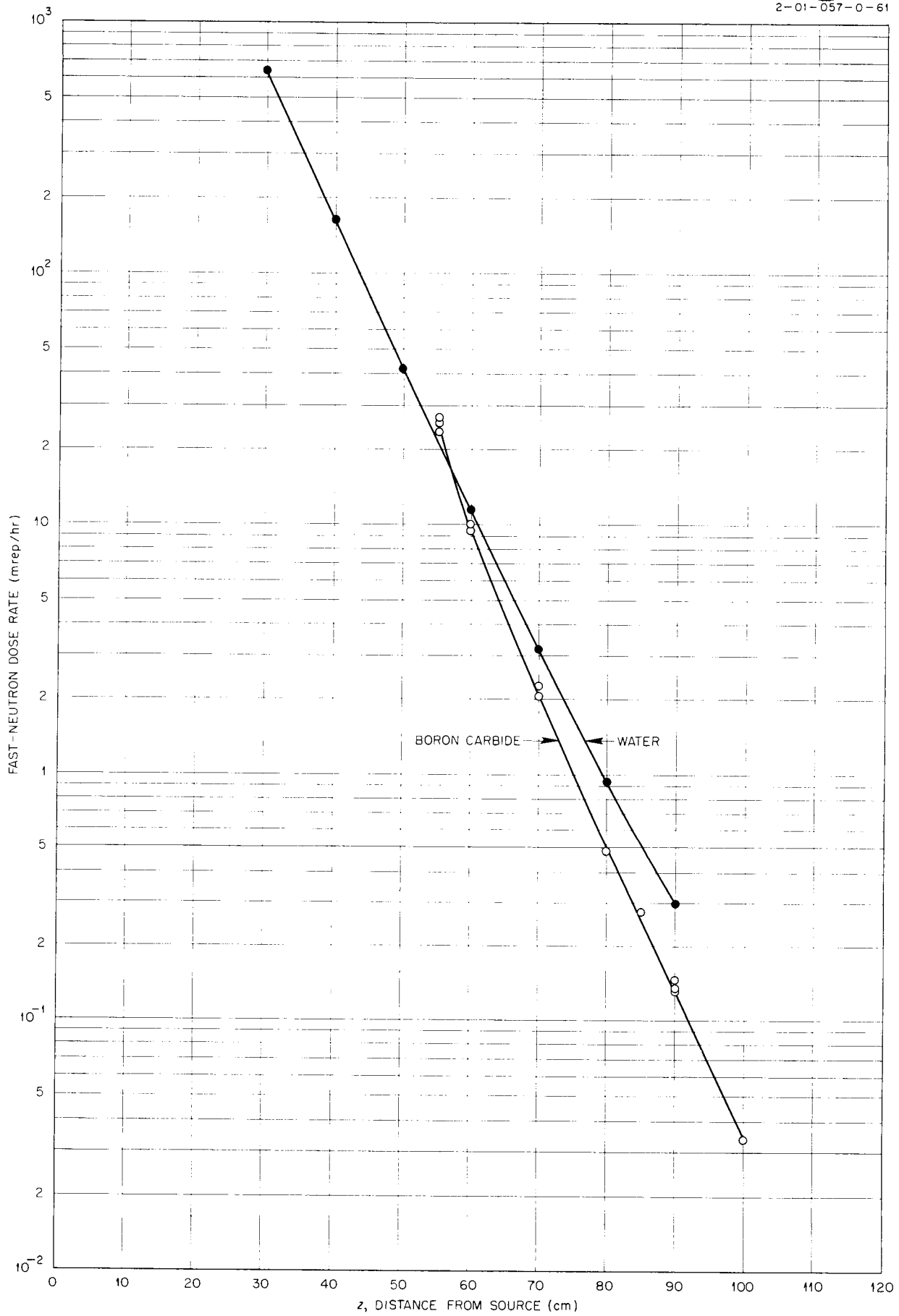


Fig. A-23. Fast-Neutron Dose Rate Beyond Solid Beryllium.

Fig. A-24. Fast-Neutron Dose Rate Beyond Boron Carbide ( $B_4C$ ).

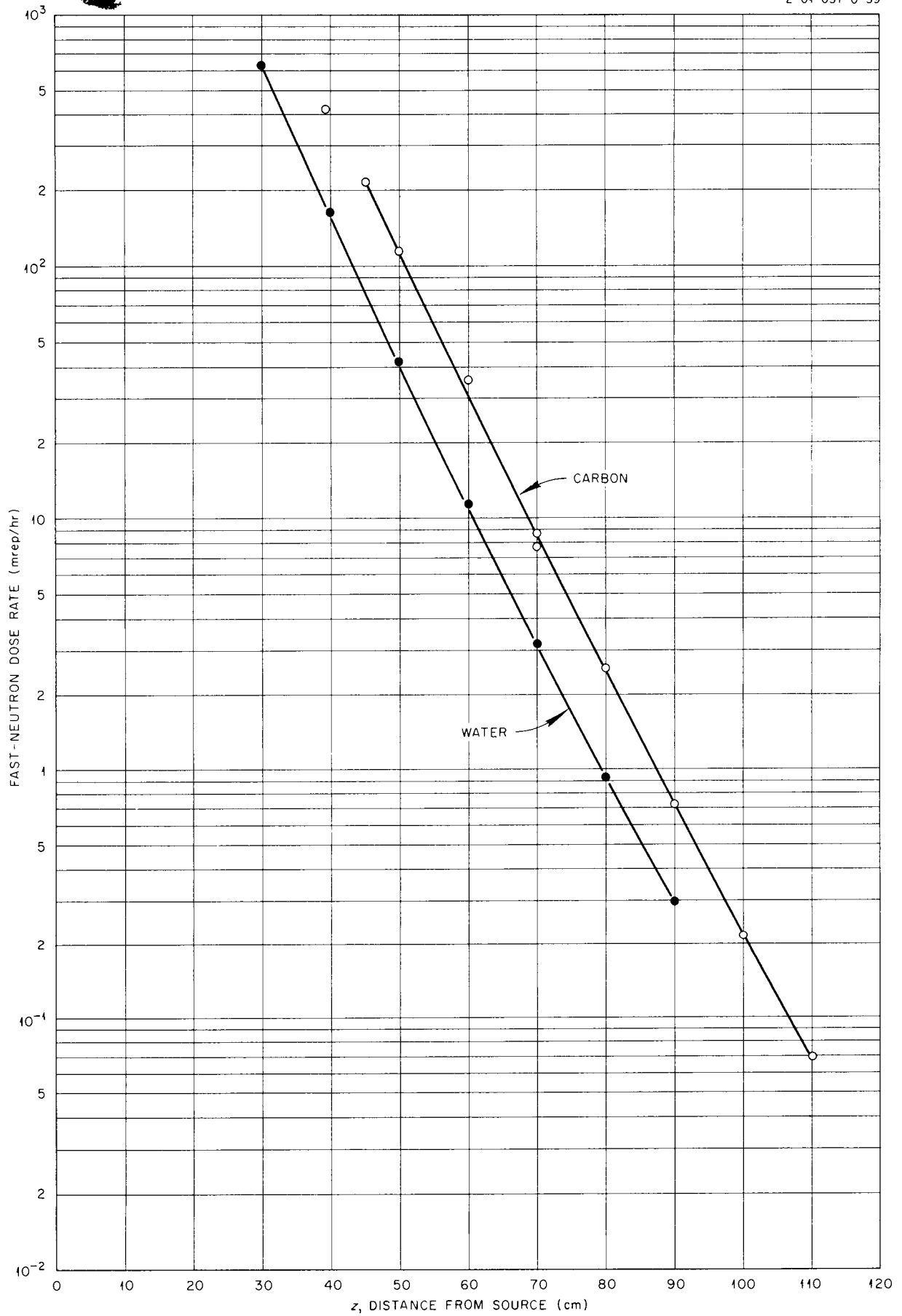


Fig. A-25. Fast-Neutron Dose Rate Beyond Carbon (AGHT).



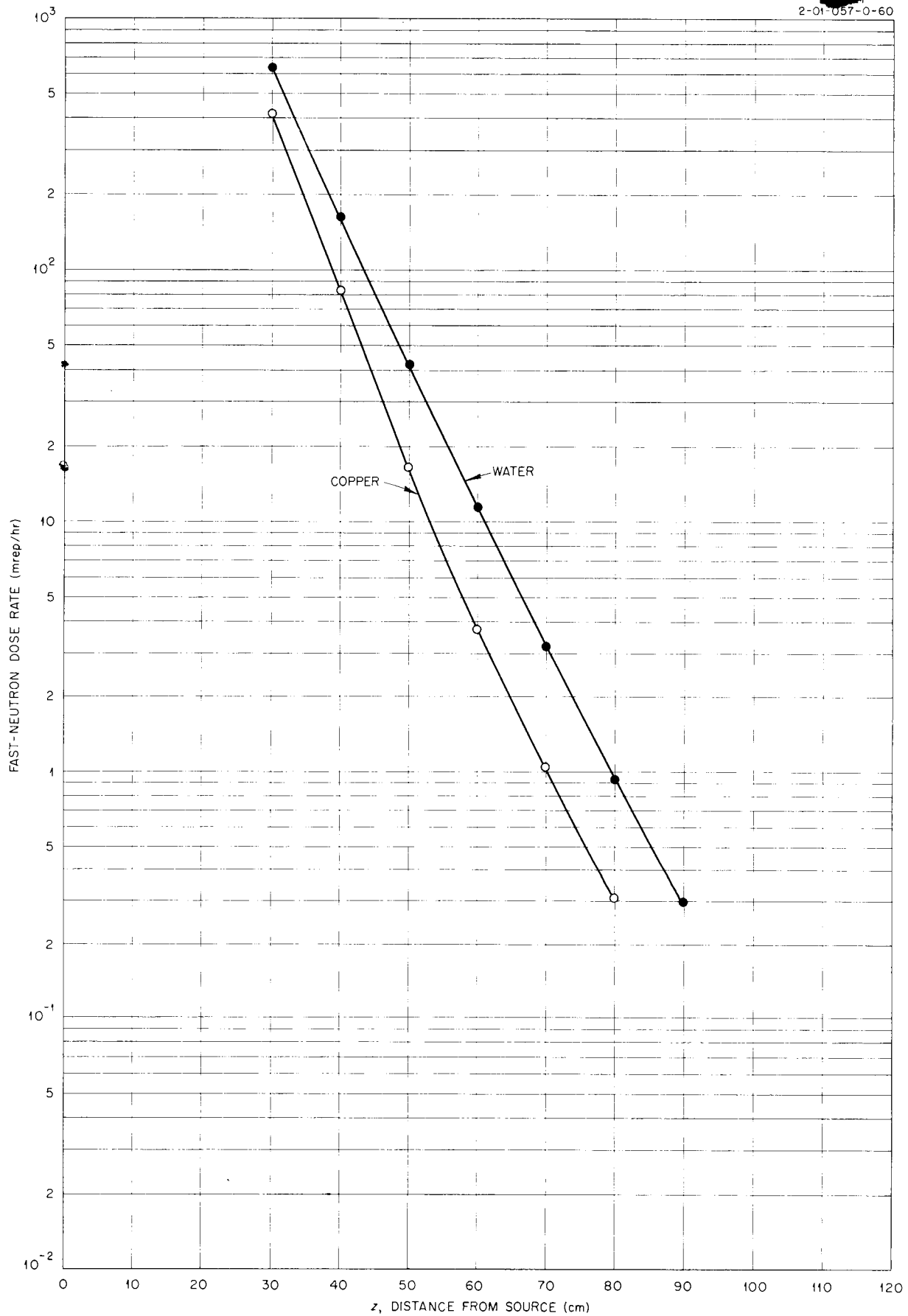
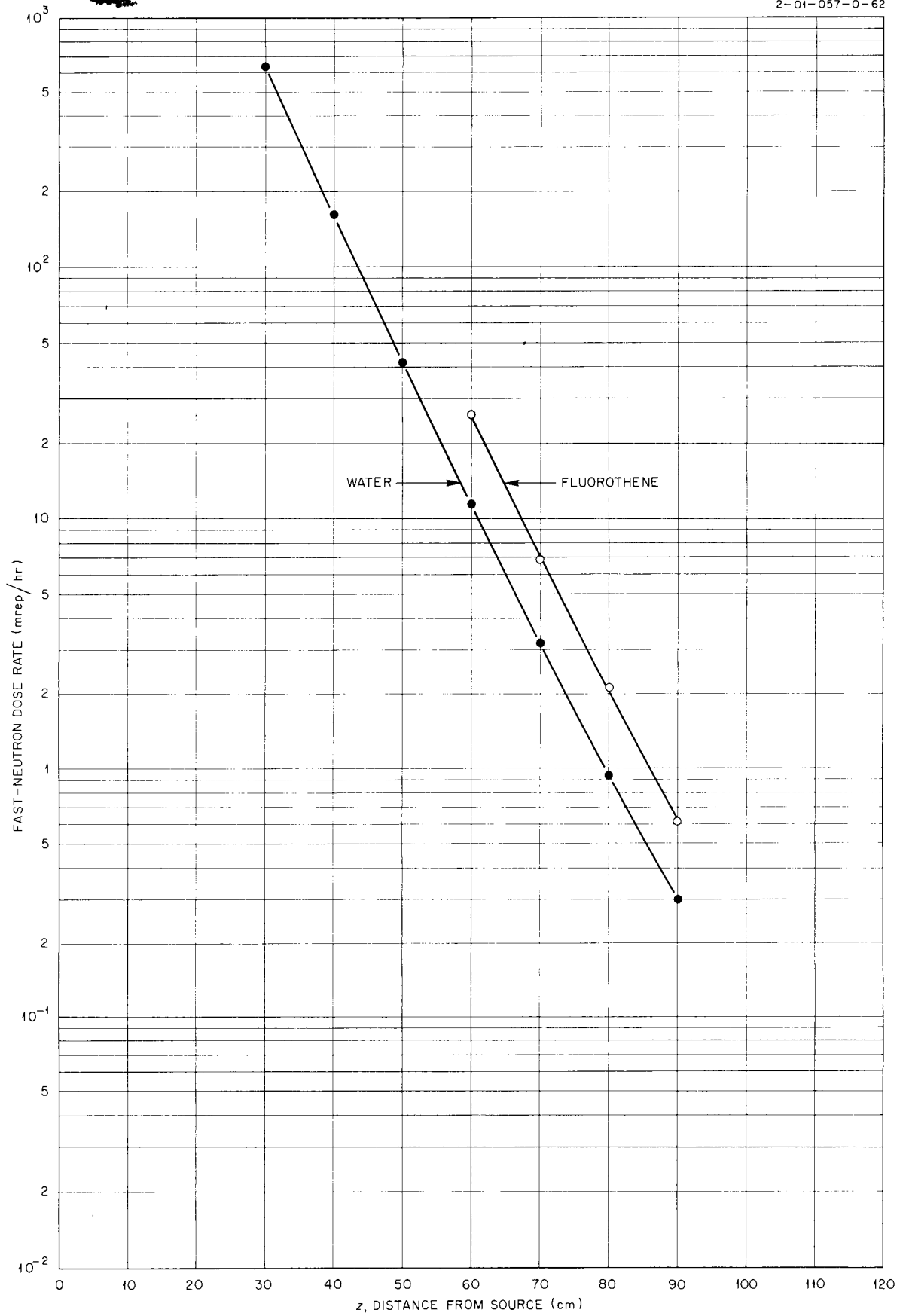


Fig. A-26. Fast-Neutron Dose Rate Beyond Copper.

Fig. A-27. Fast-Neutron Dose Rate Beyond Fluorothene ( $C_2F_3Cl$ )

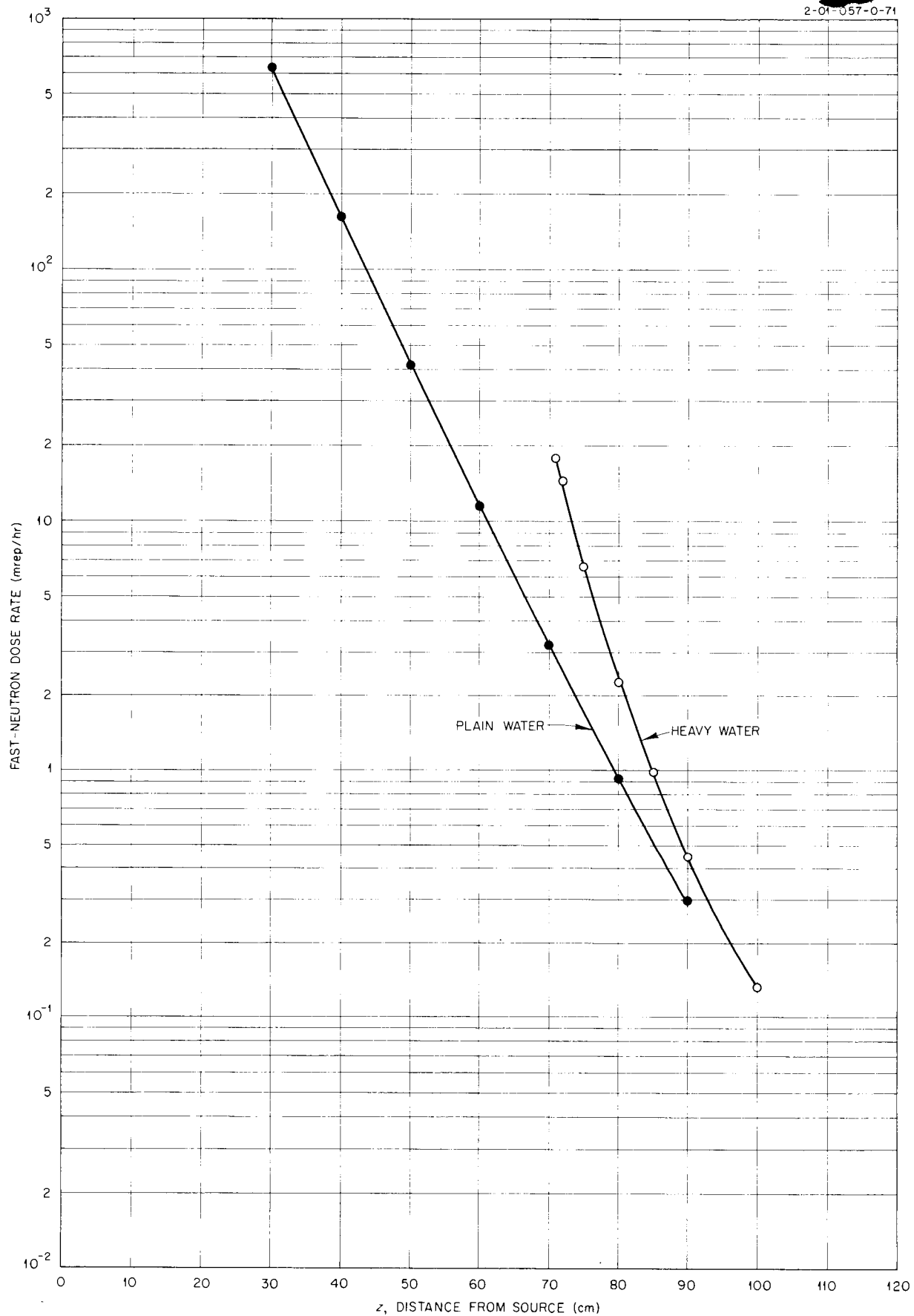


Fig. A-28. Fast-Neutron Dose Rate Beyond Heavy Water ( $D_2O$ ).

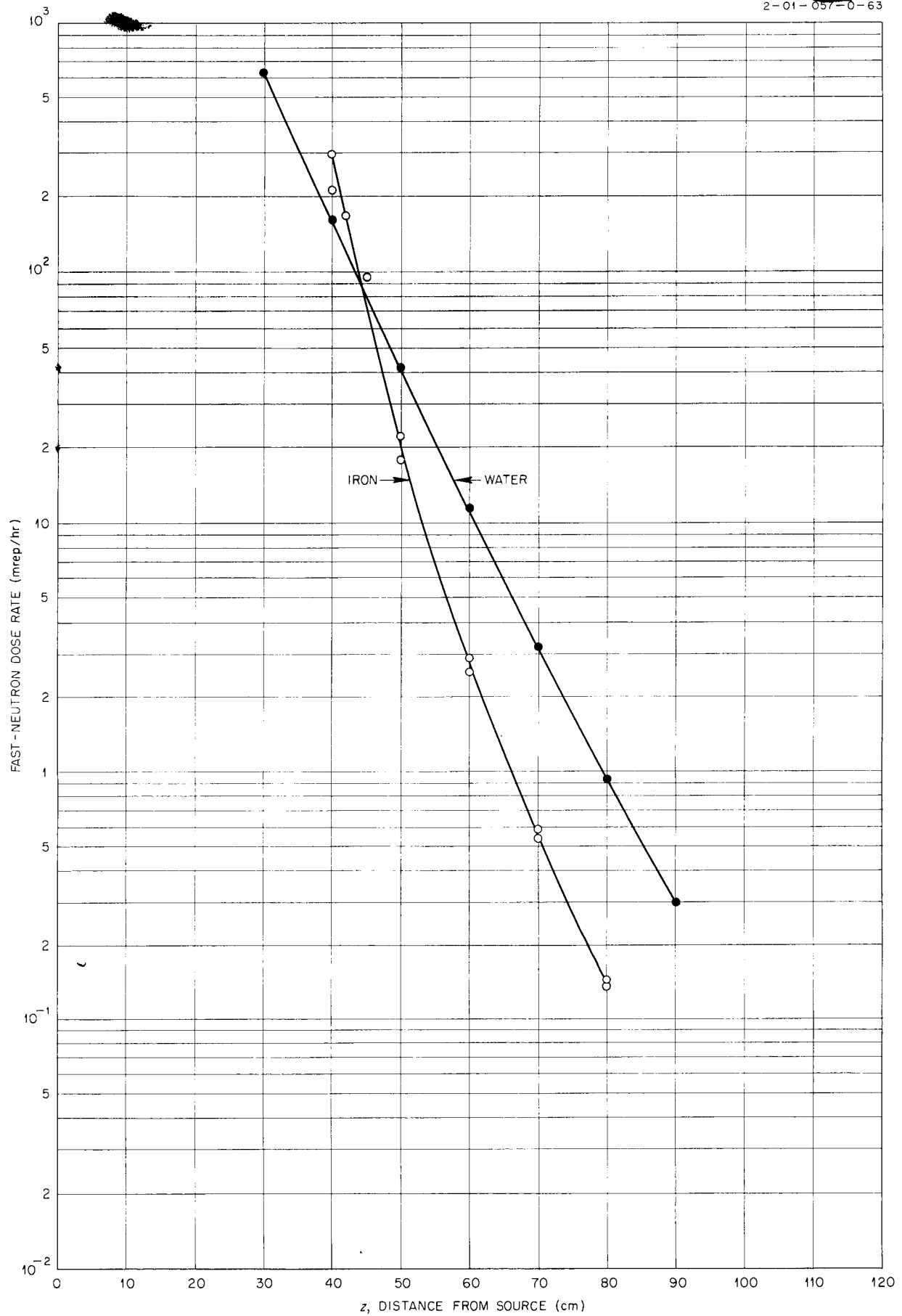


Fig. A-29. Fast-Neutron Dose Rate Beyond Iron.

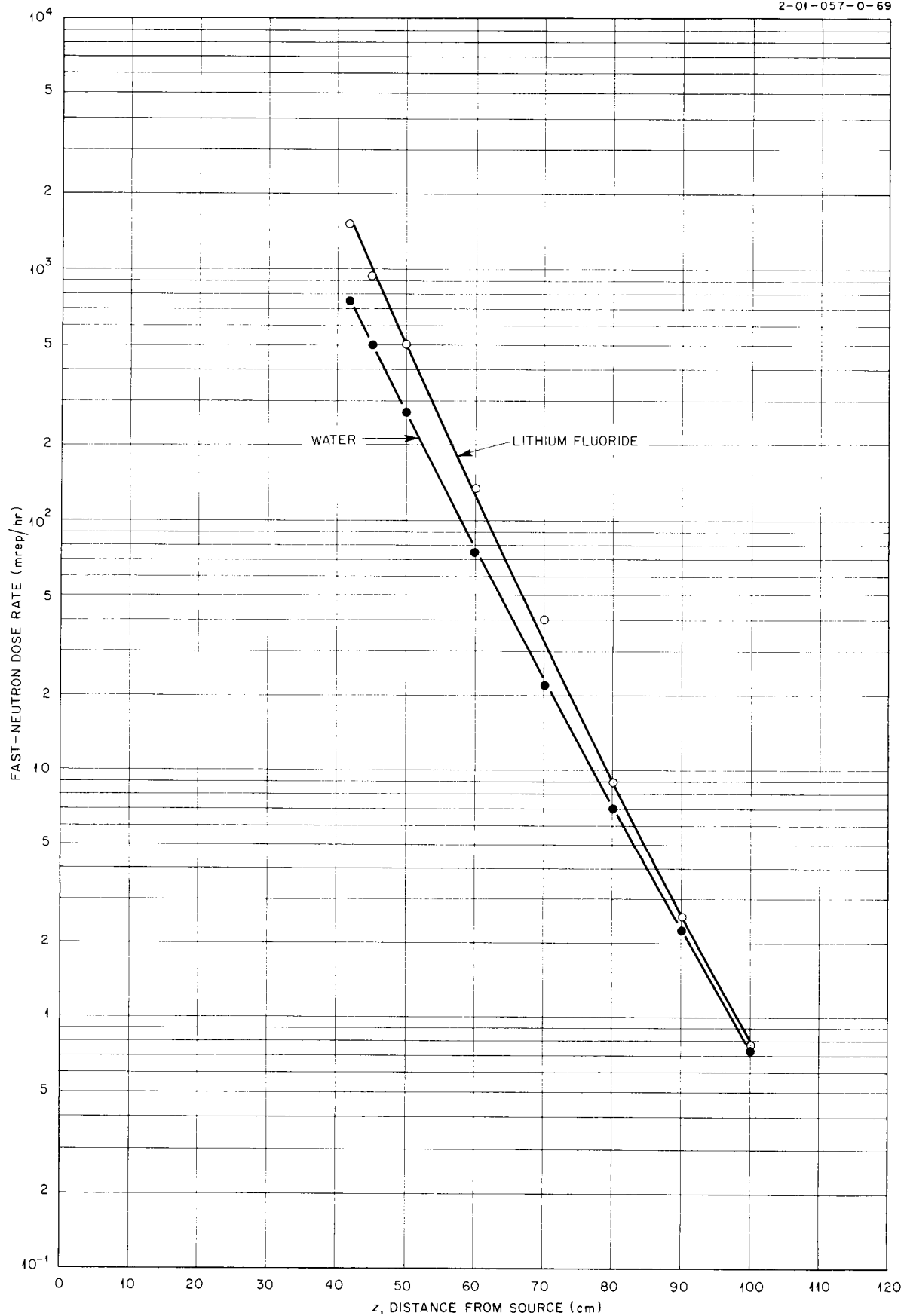


Fig. A-30. Fast-Neutron Dose Rate Beyond Lithium Fluoride

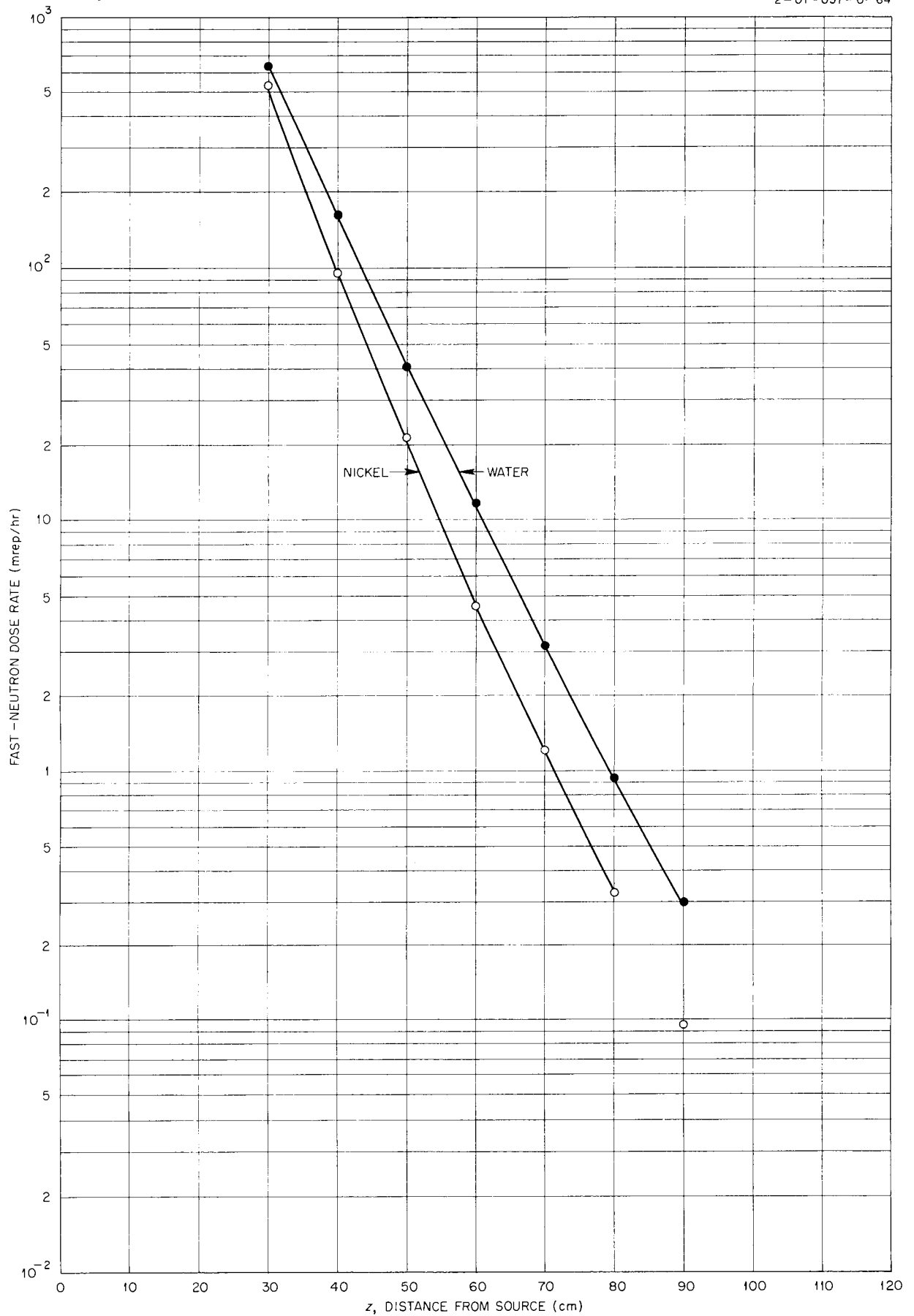
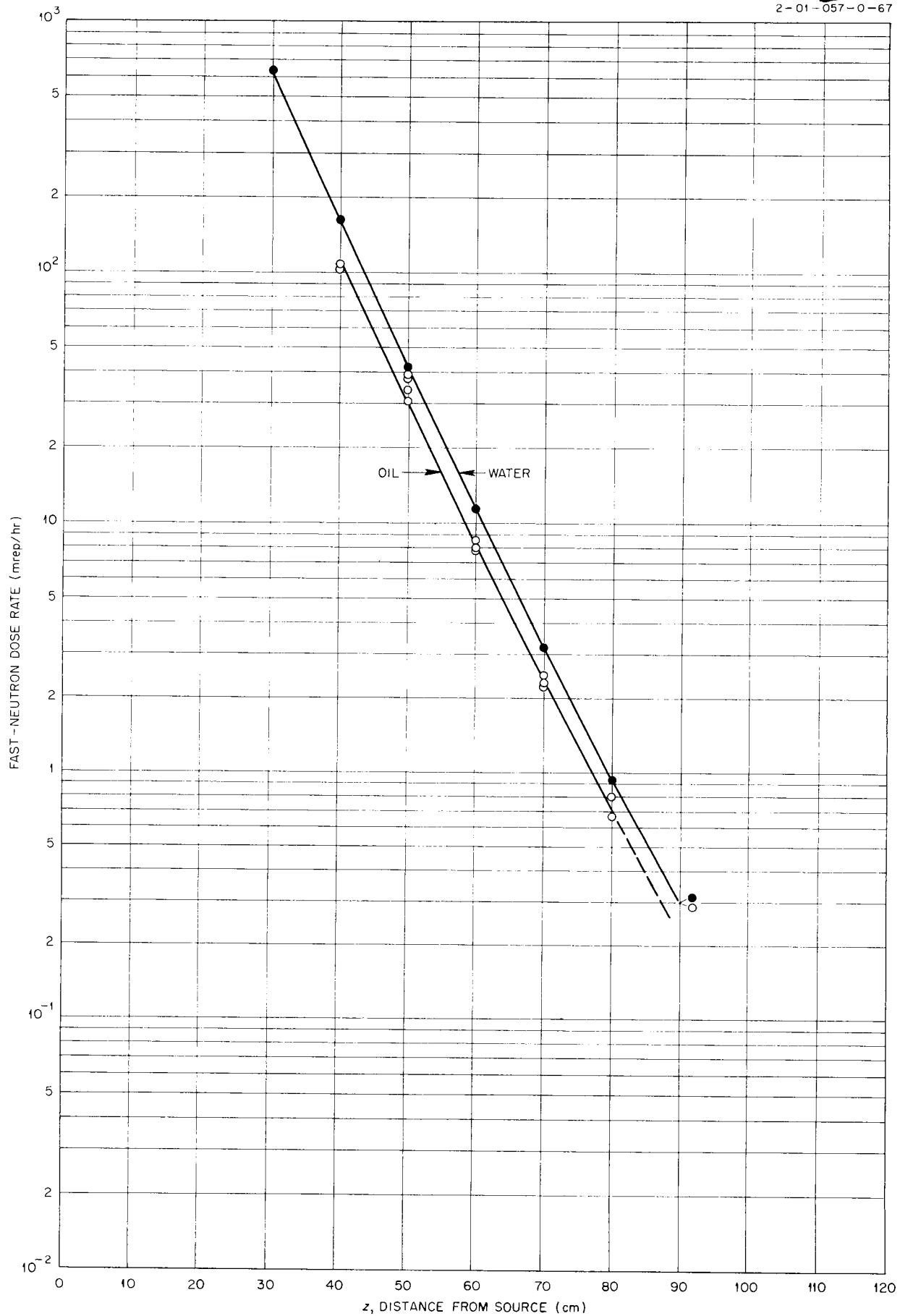


Fig. A-31. Fast-Neutron Dose Rate Beyond Nickel.

Fig. A-32. Fast-Neutron Dose Rate Beyond Oil ( $\text{CH}_2$ ).

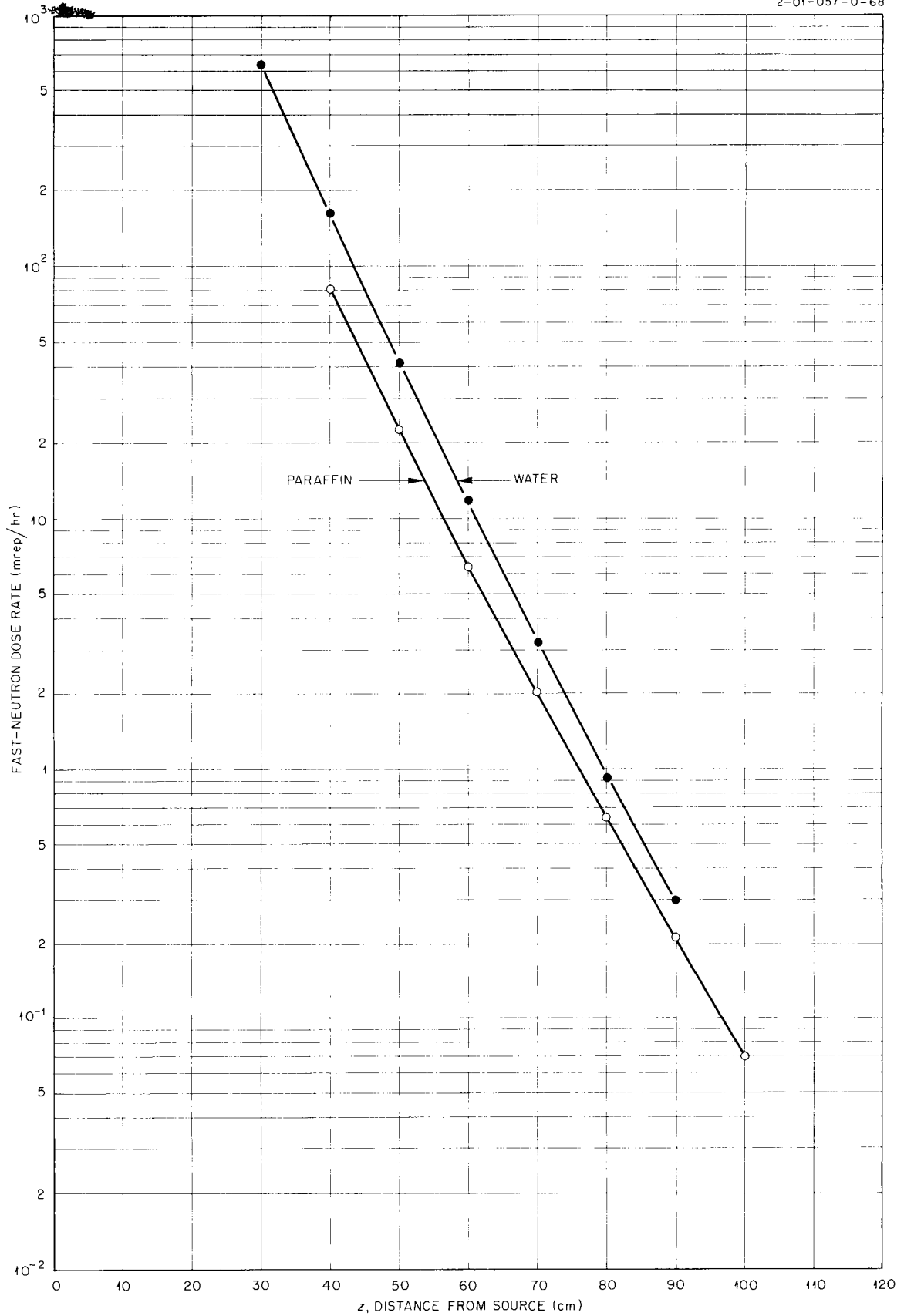


Fig. A-33. Fast-Neutron Dose Rate Beyond Paraffin ( $C_{30}H_{62}$ )



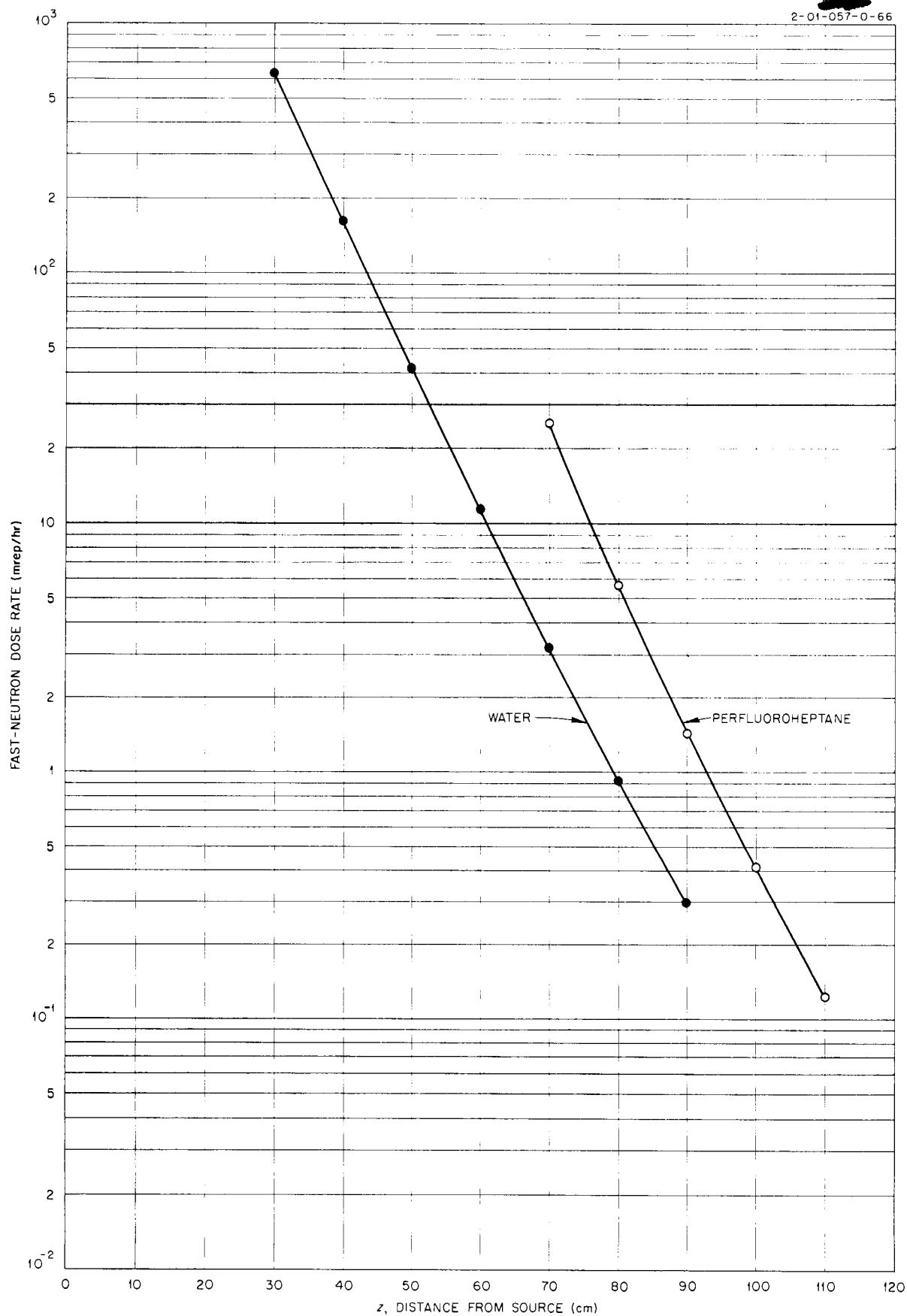


Fig. A-34. Fast-Neutron Dose Rate Beyond Perfluoroheptane ( $C_7F_{16}$ ).

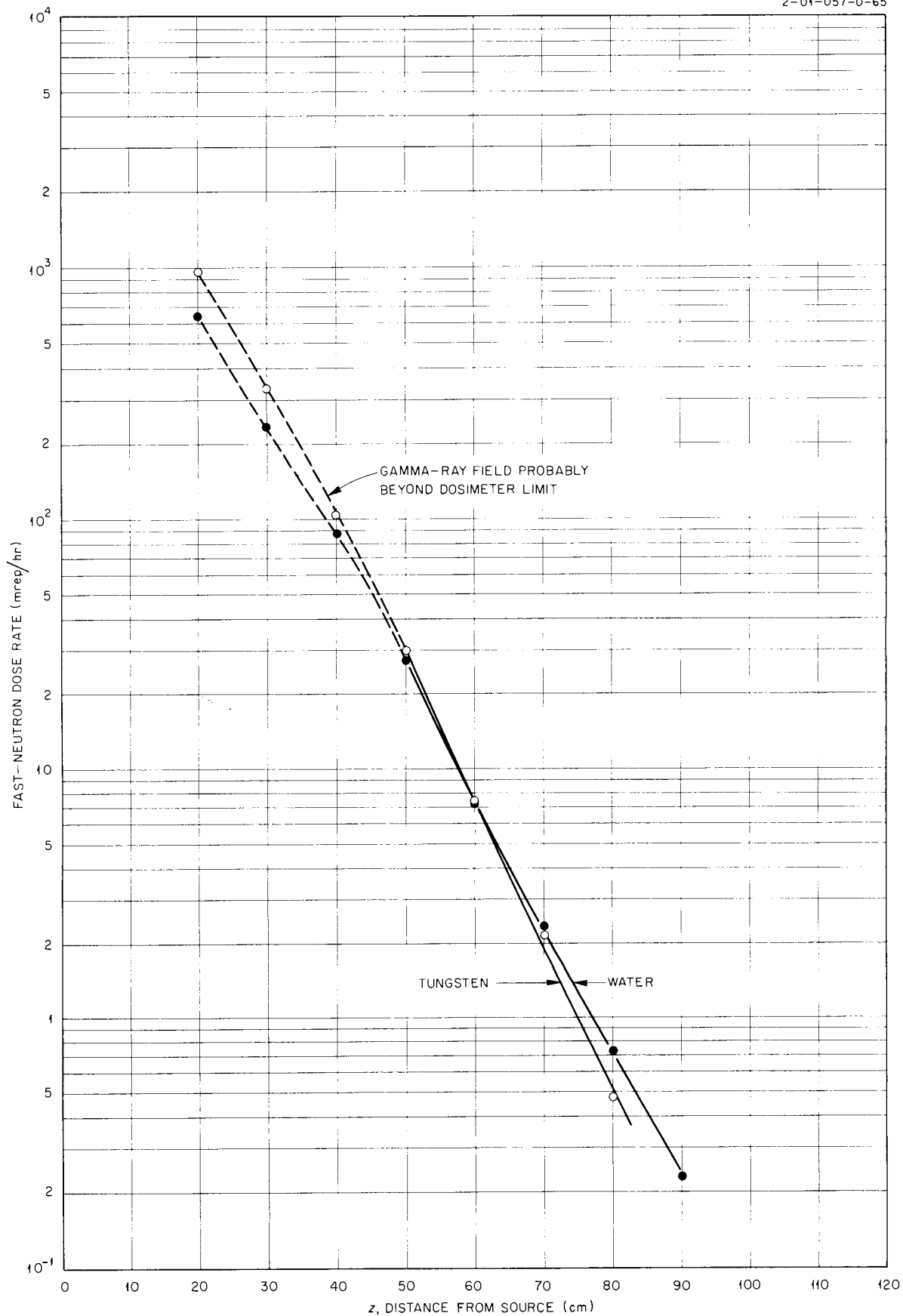


Fig. A-35. Fast-Neutron Dose Rate Beyond Tungsten.

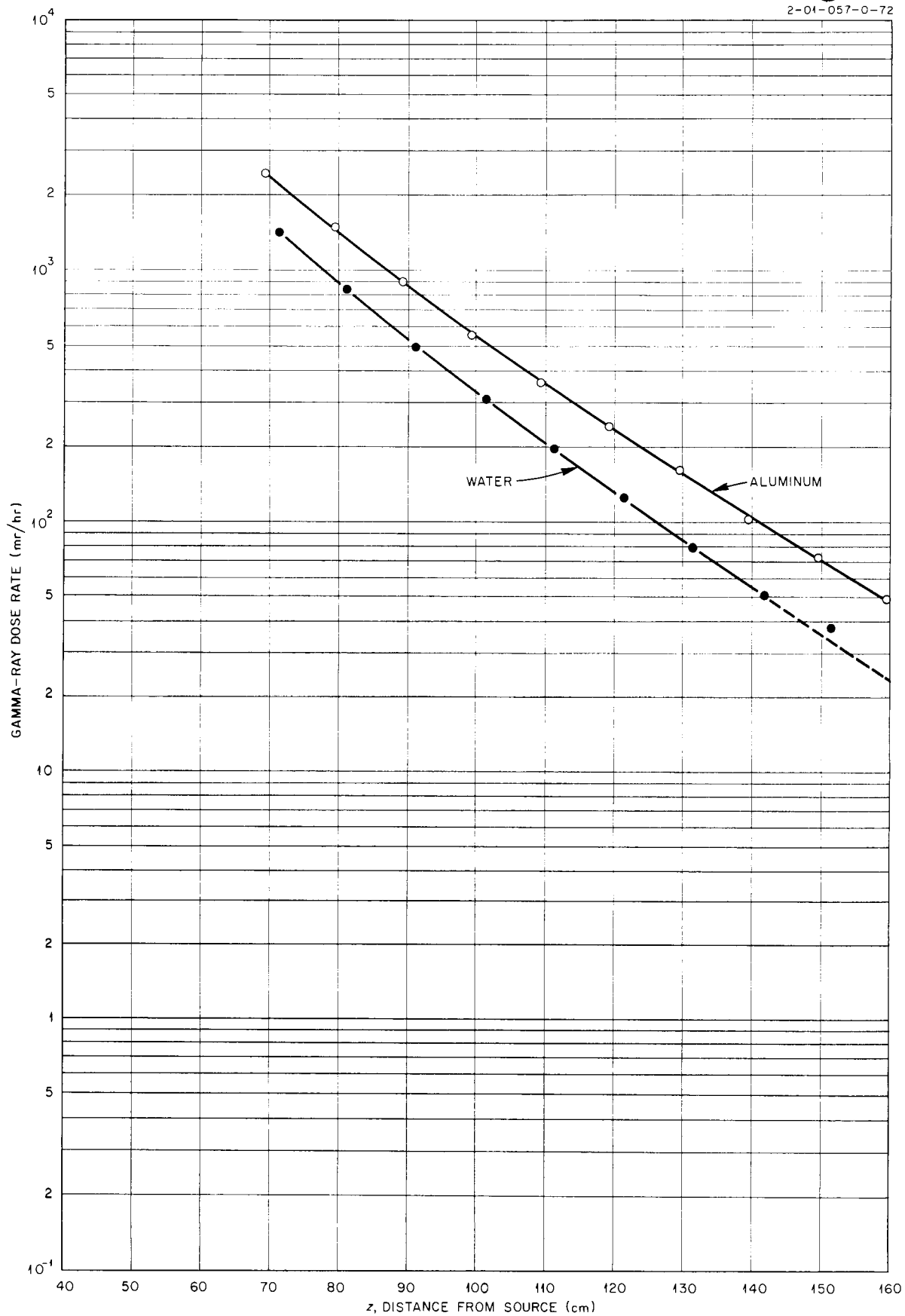


Fig. A-36. Gamma-Ray Dose Rate Beyond Aluminum.

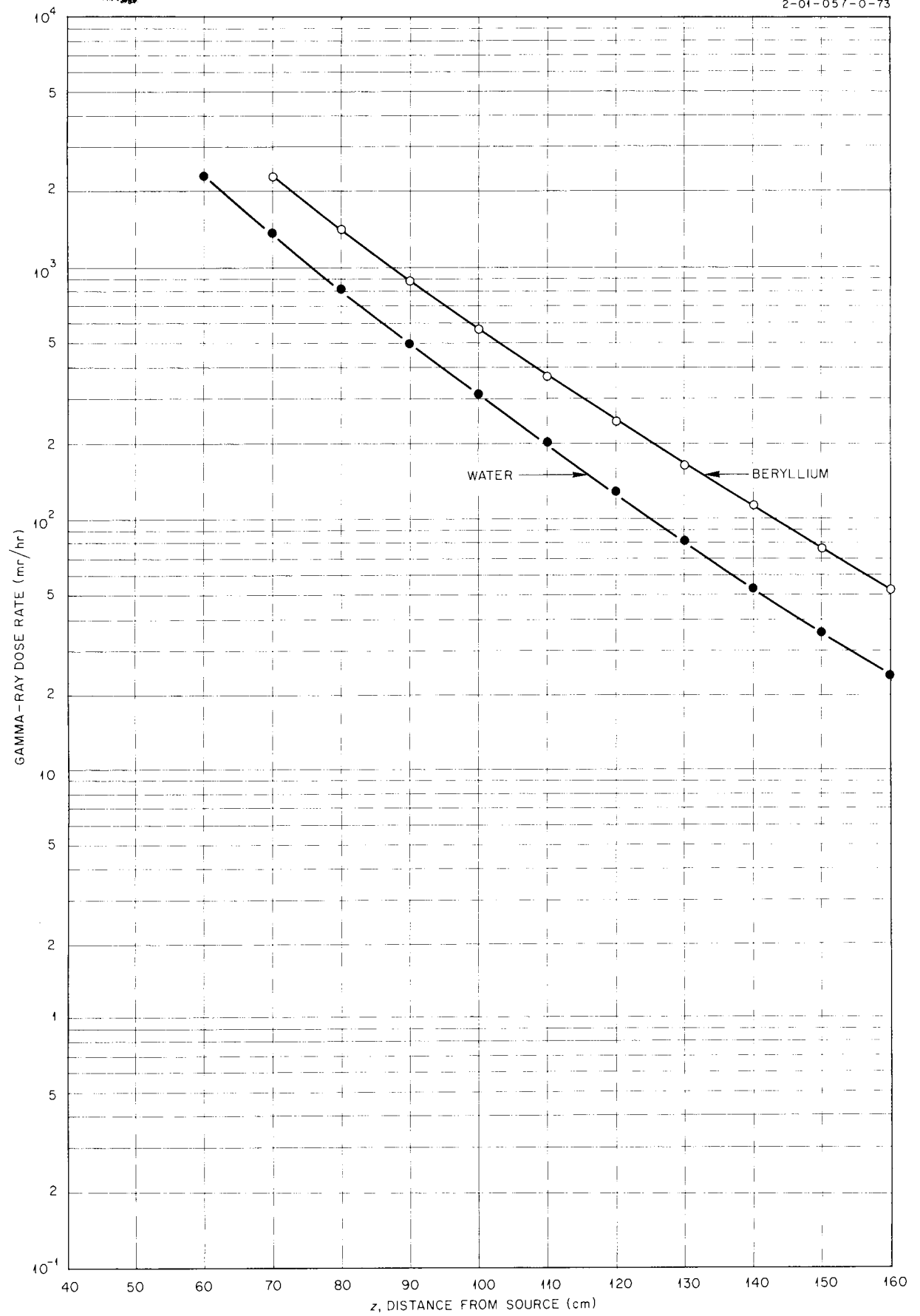


Fig. A-37. Gamma-Ray Dose Rate Beyond Beryllium Pellets.

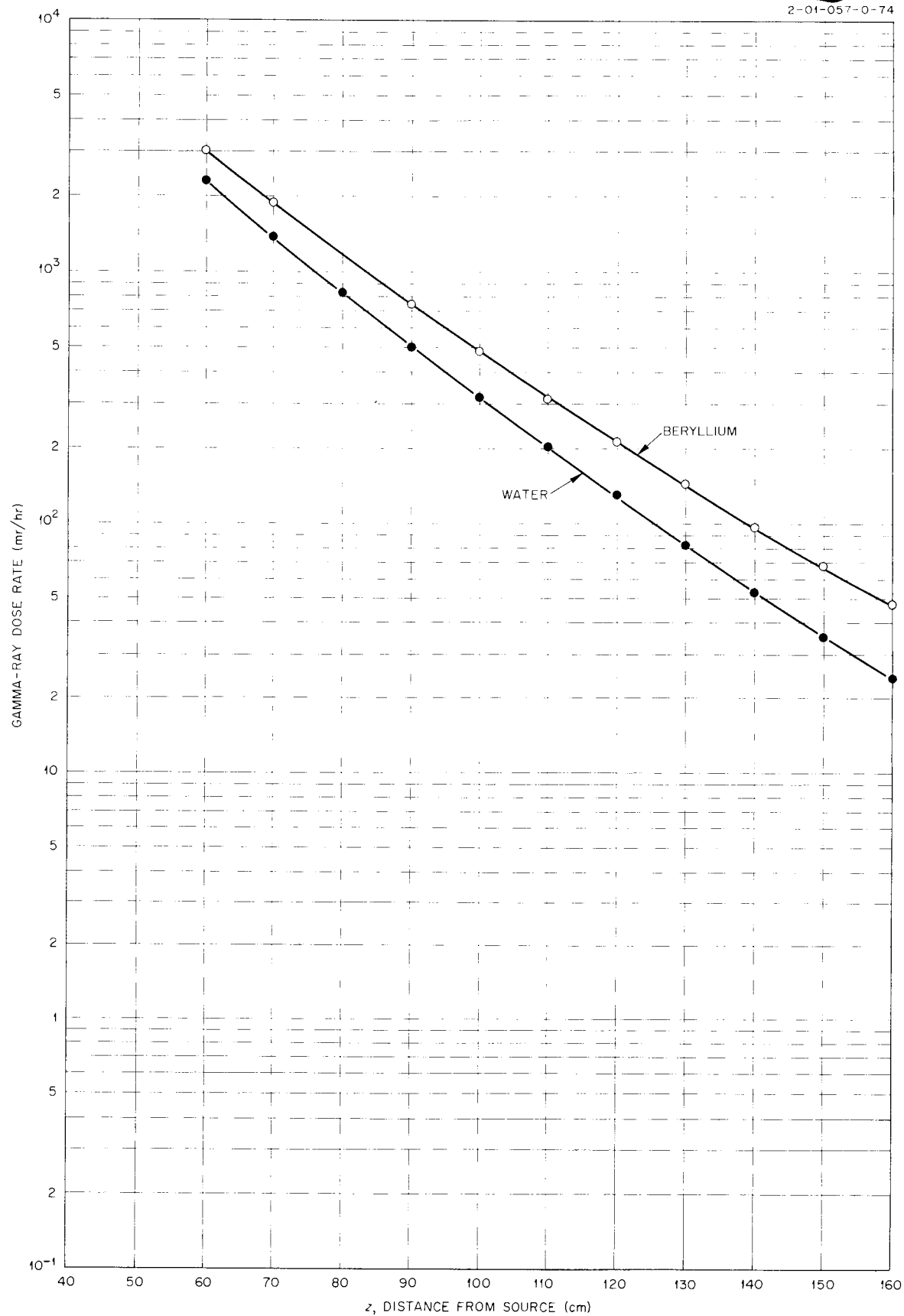


Fig. A-38. Gamma-Ray Dose Rate Beyond Solid Beryllium.

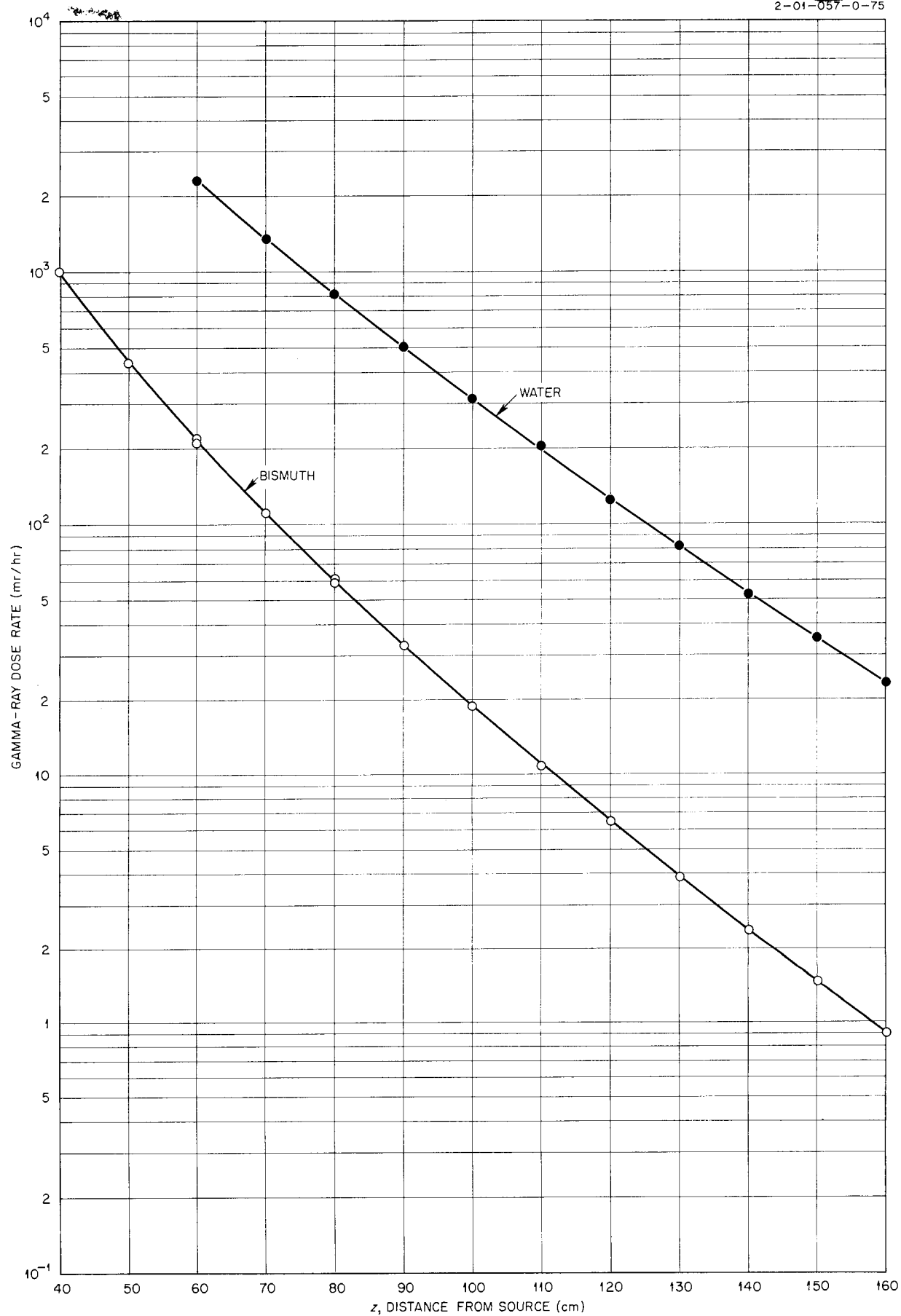
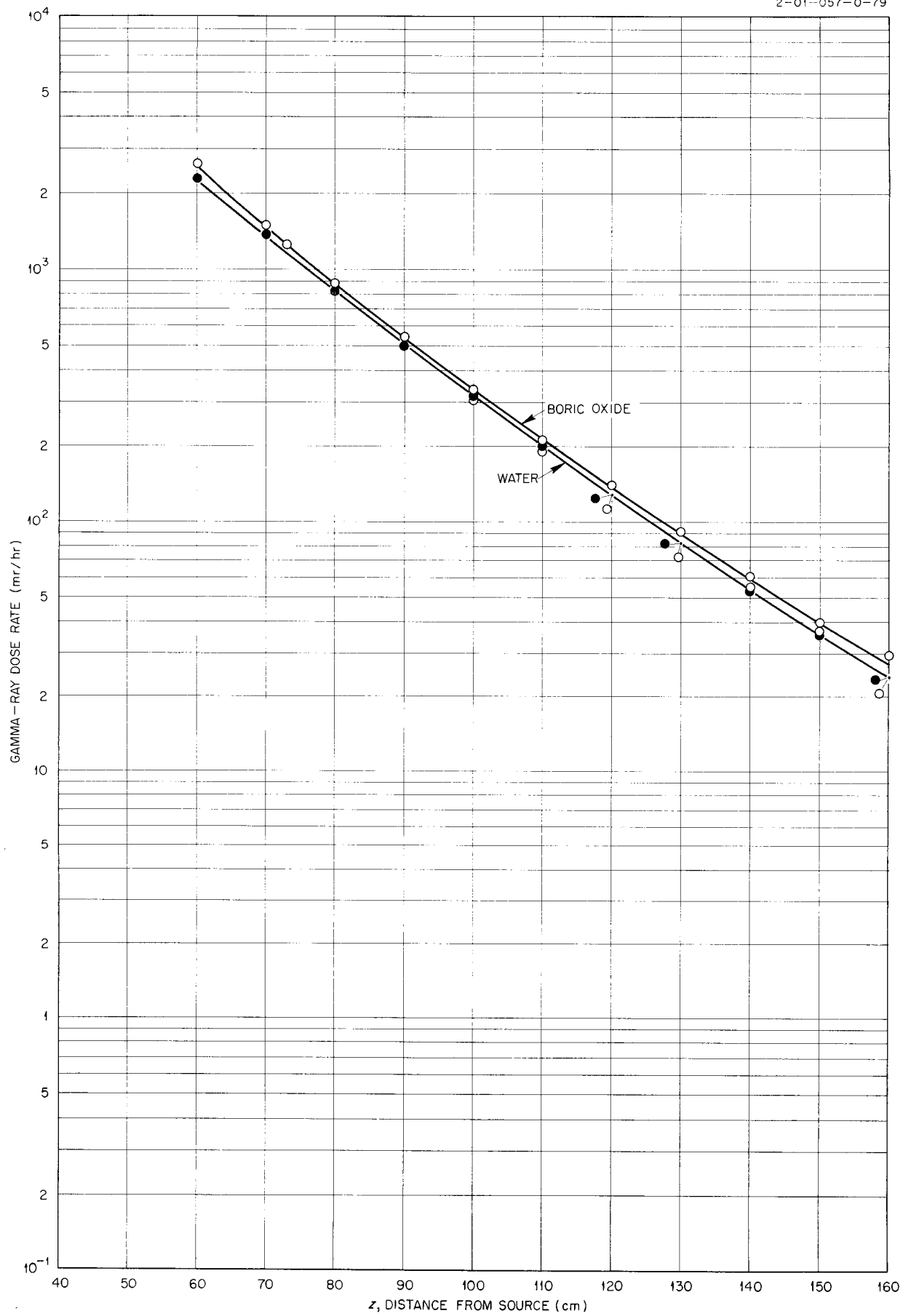
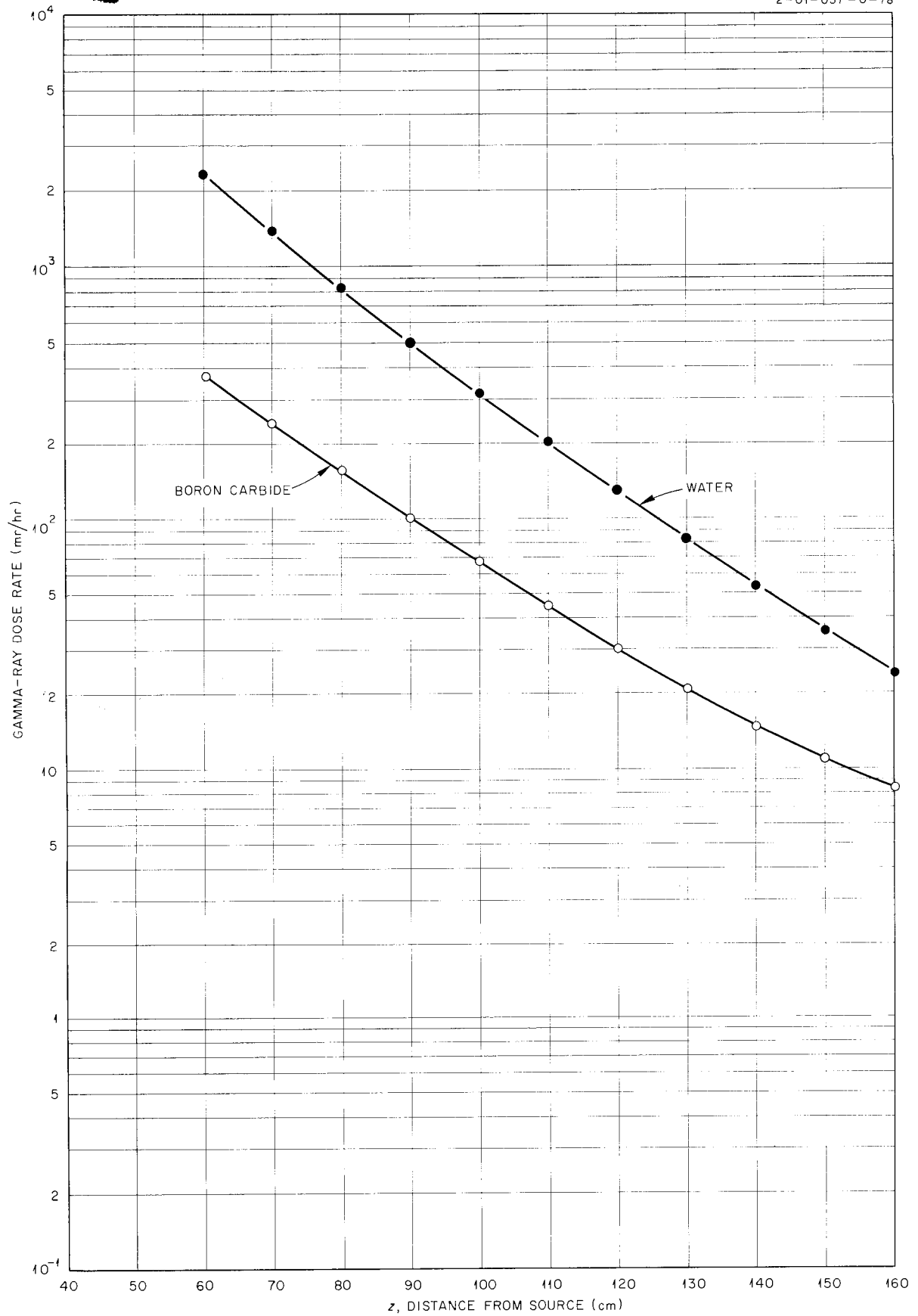


Fig. A-39. Gamma-Ray Dose Rate Beyond Bismuth.

Fig. A-40. Gamma-Ray Dose Rate Beyond Boric Oxide ( $B_2O_3$ )

Fig. A-41. Gamma-Ray Dose Rate Beyond Boron Carbide ( $B_4C$ )



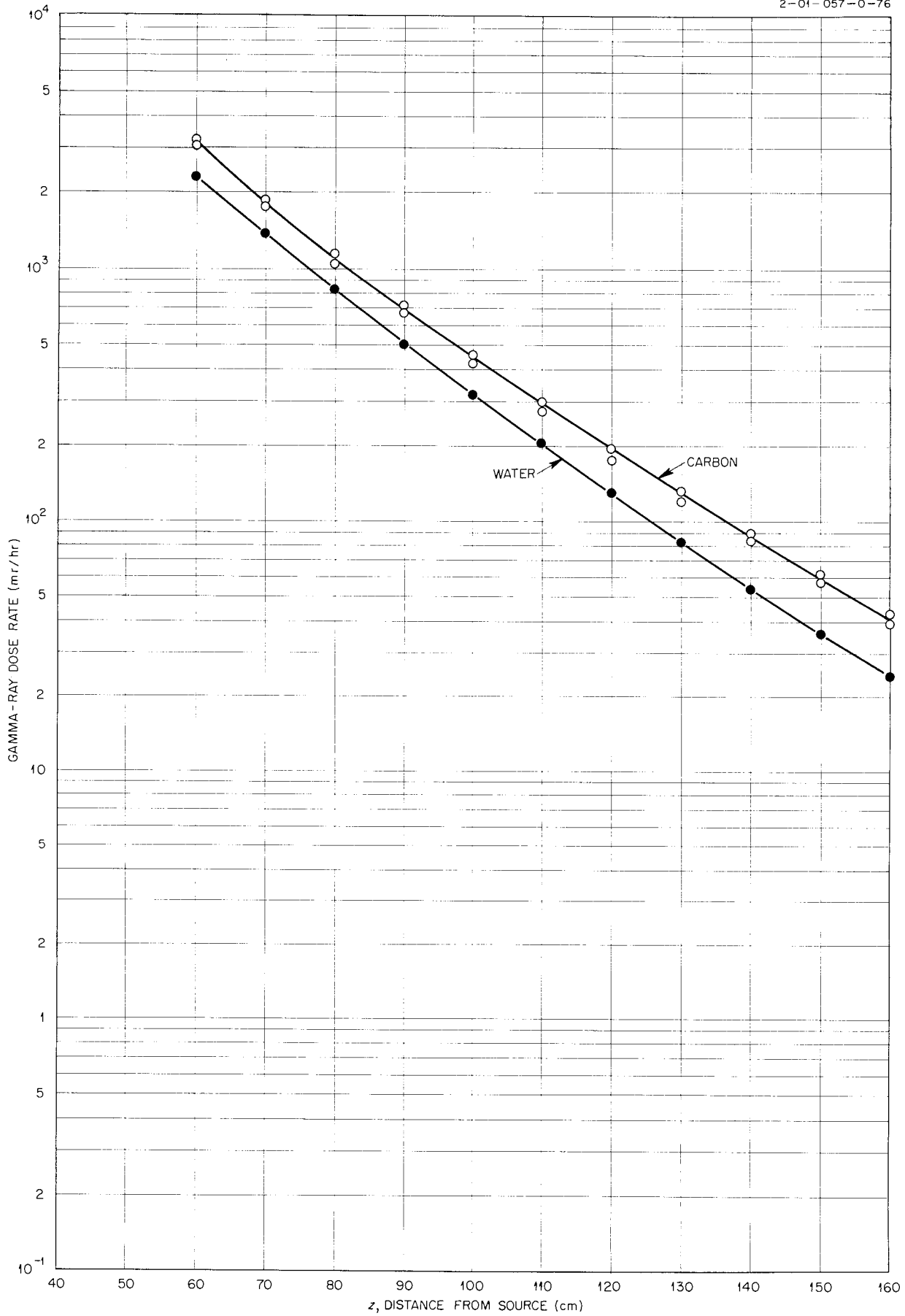


Fig. A-42. Gamma-Ray Dose Rate Beyond Carbon.

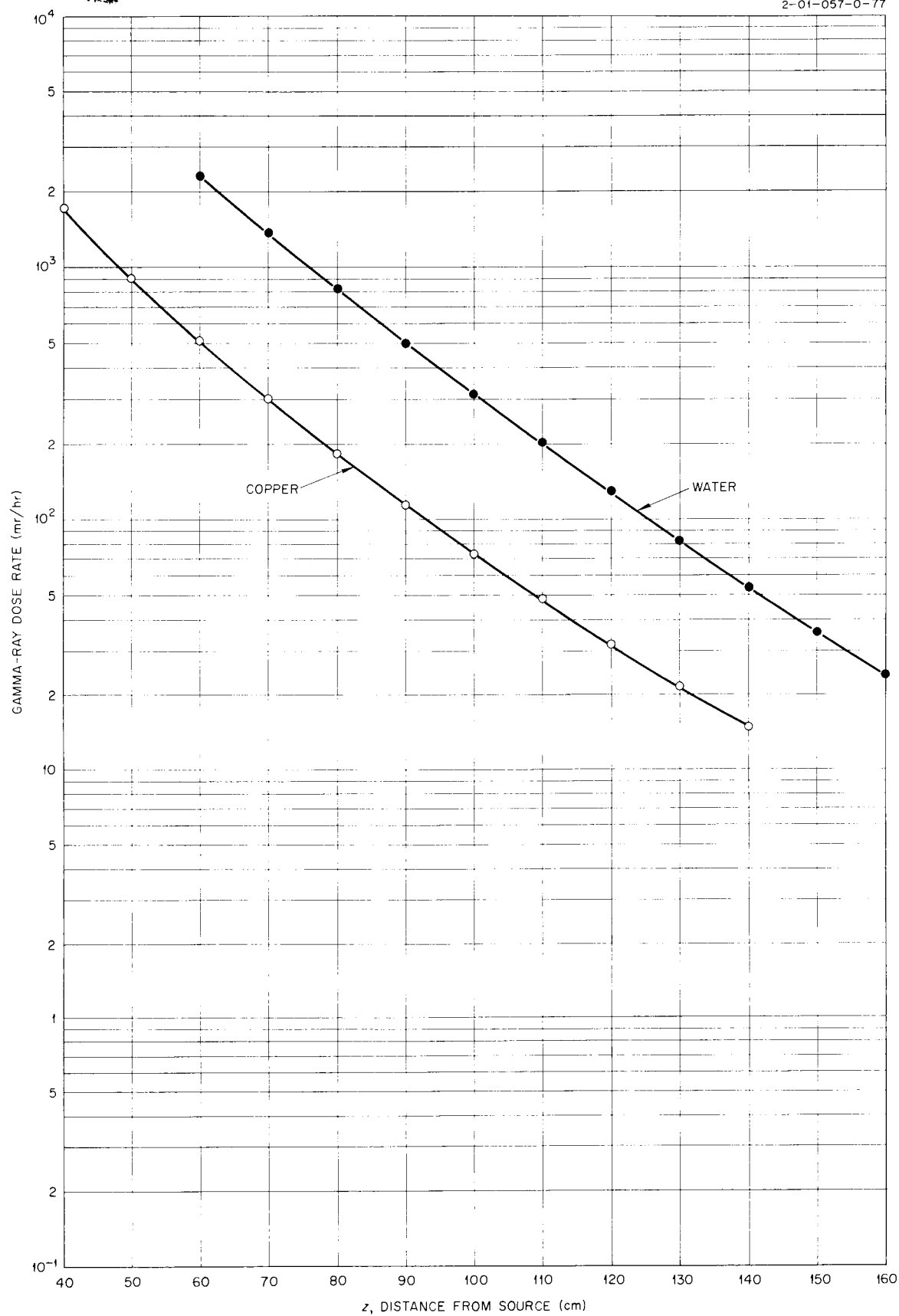
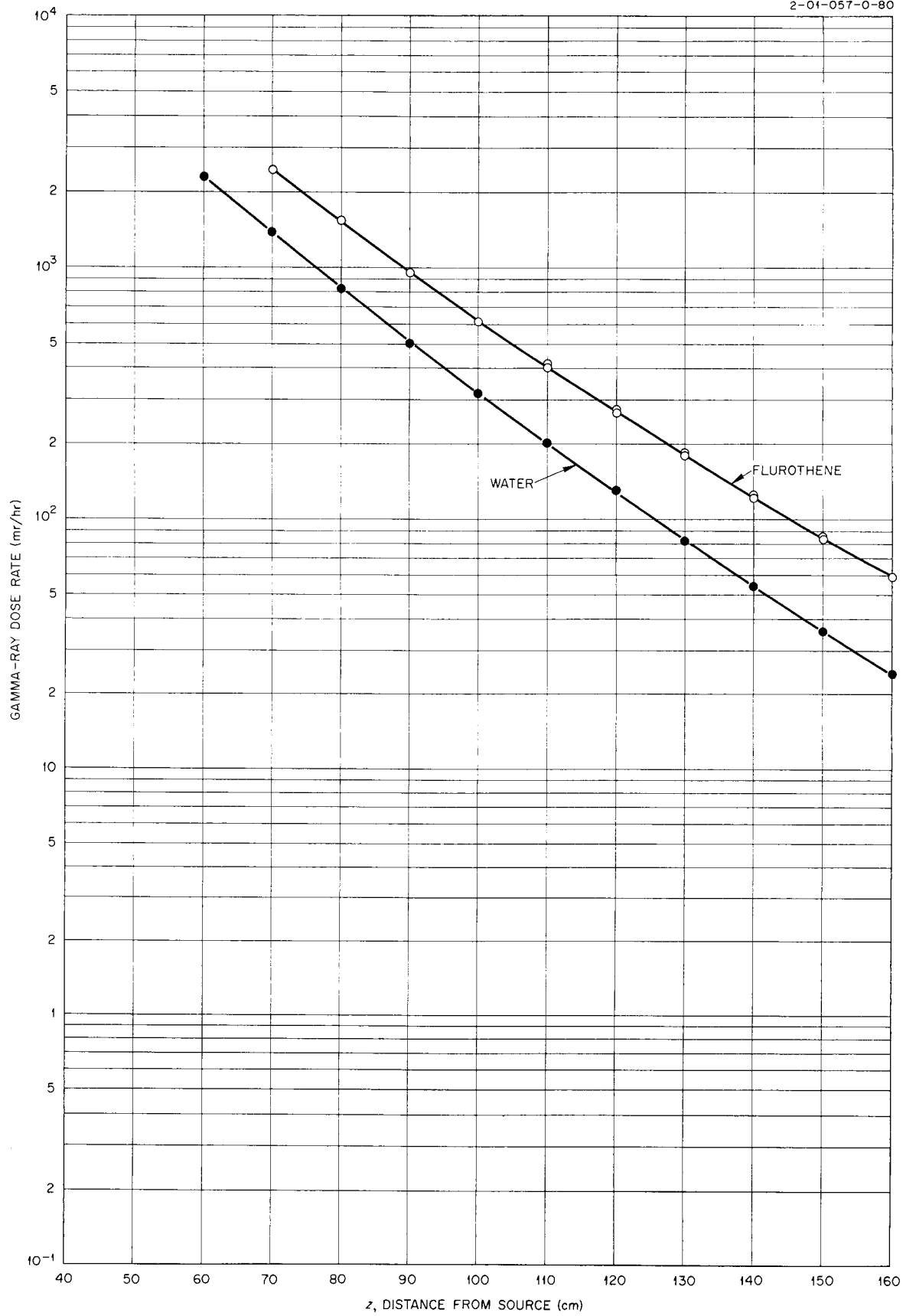


Fig. A-43. Gamma-Ray Dose Rate Beyond Copper.

Fig. A-44. Gamma-Ray Dose Rate Beyond Fluorothene ( $C_2ClF_3$ )

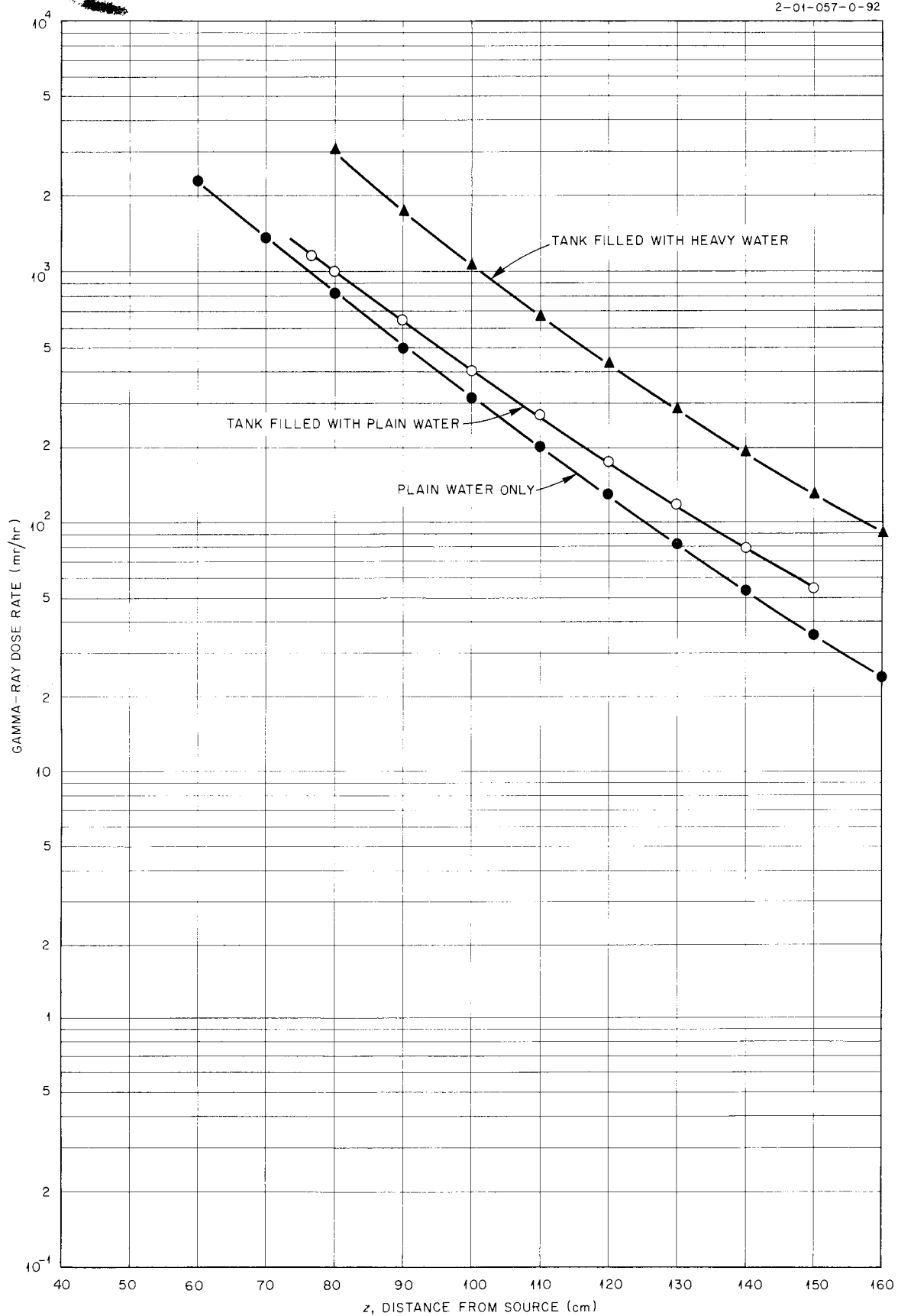


Fig. A-45. Gamma-Ray Dose Rate Beyond Heavy Water

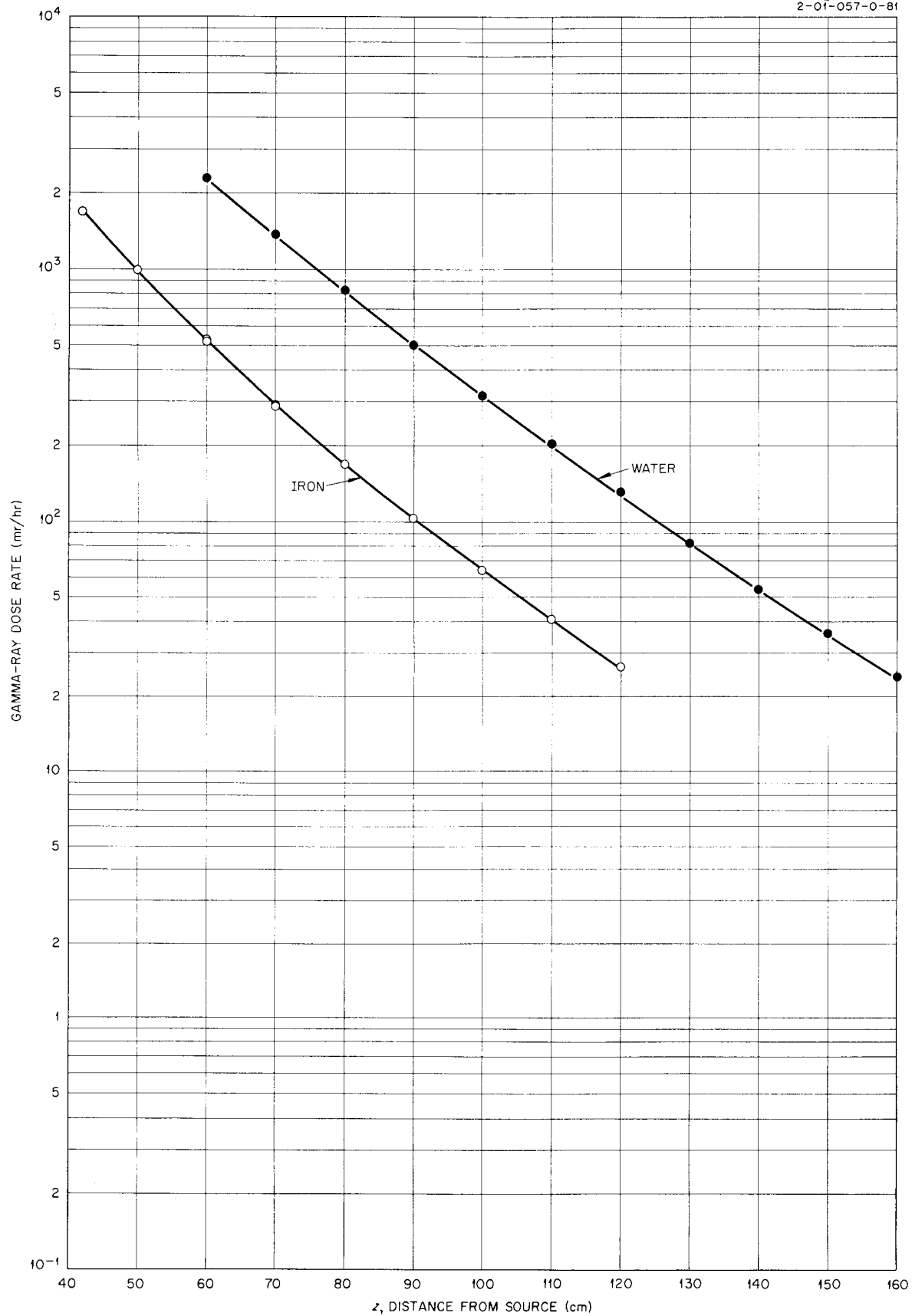


Fig. A-46. Gamma-Ray Dose Rate Beyond Iron.

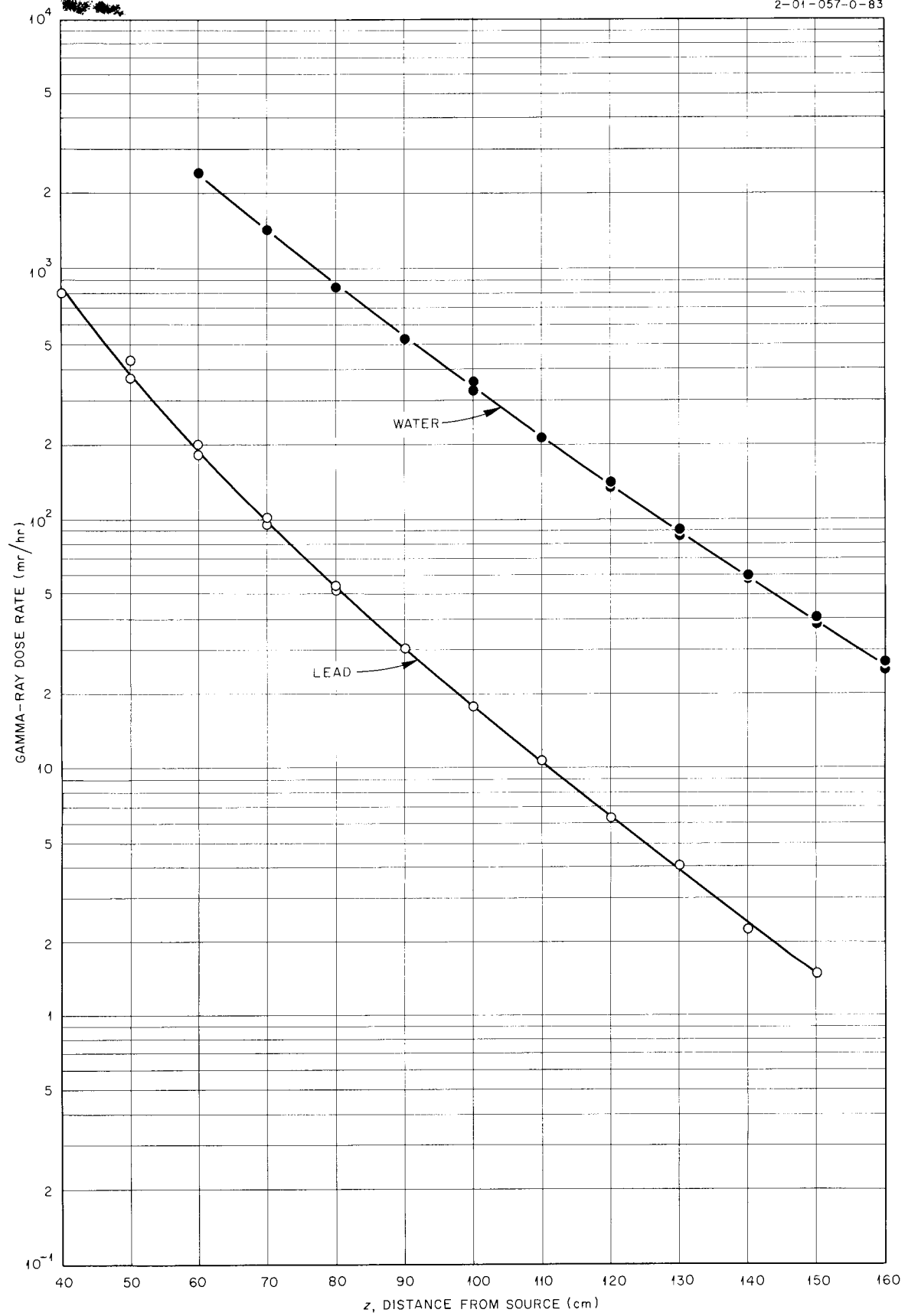


Fig. A-47. Gamma-Ray Dose Rate Beyond Lead

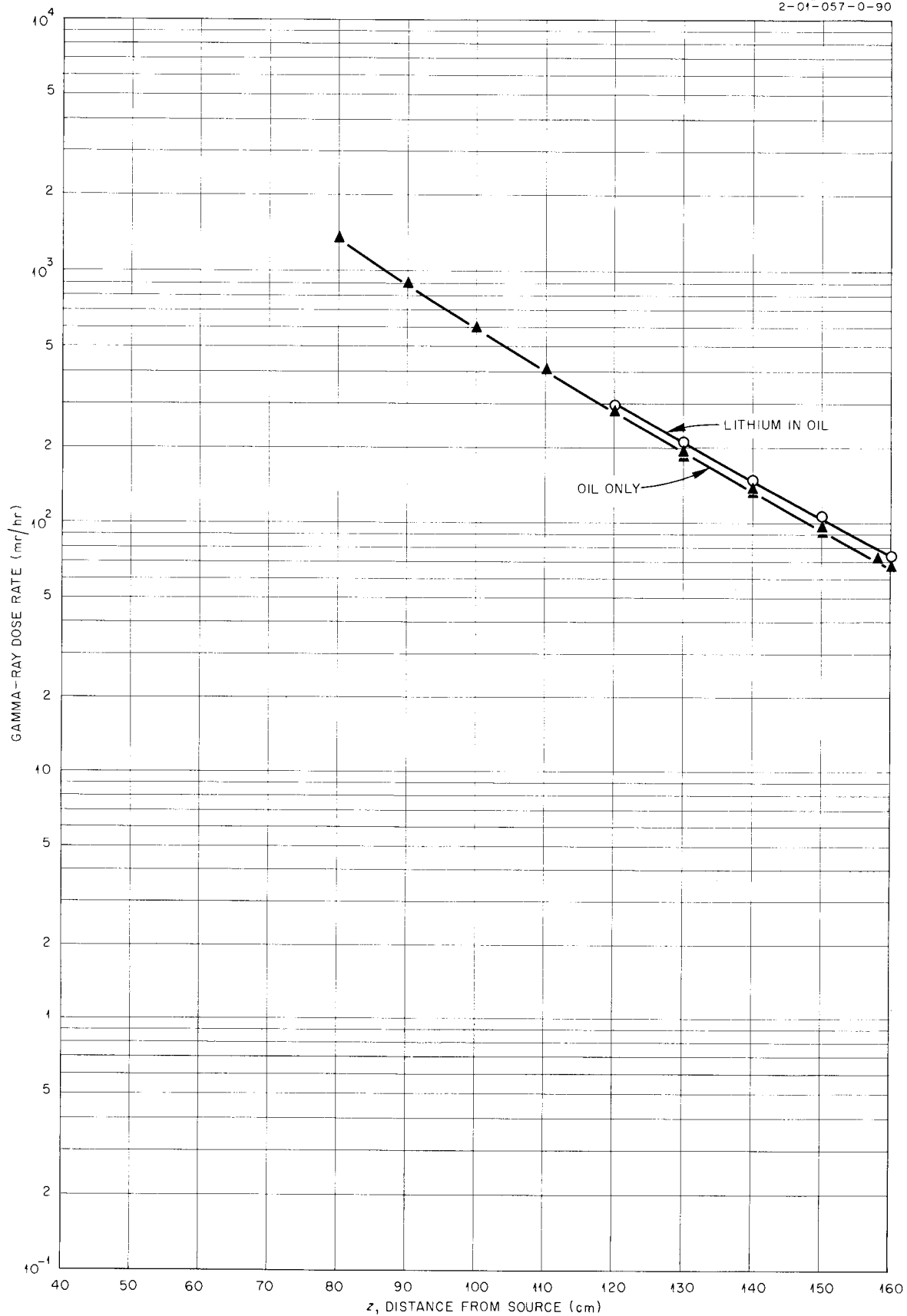


Fig. A-48. Gamma-Ray Dose Rate in Oil Beyond Lithium

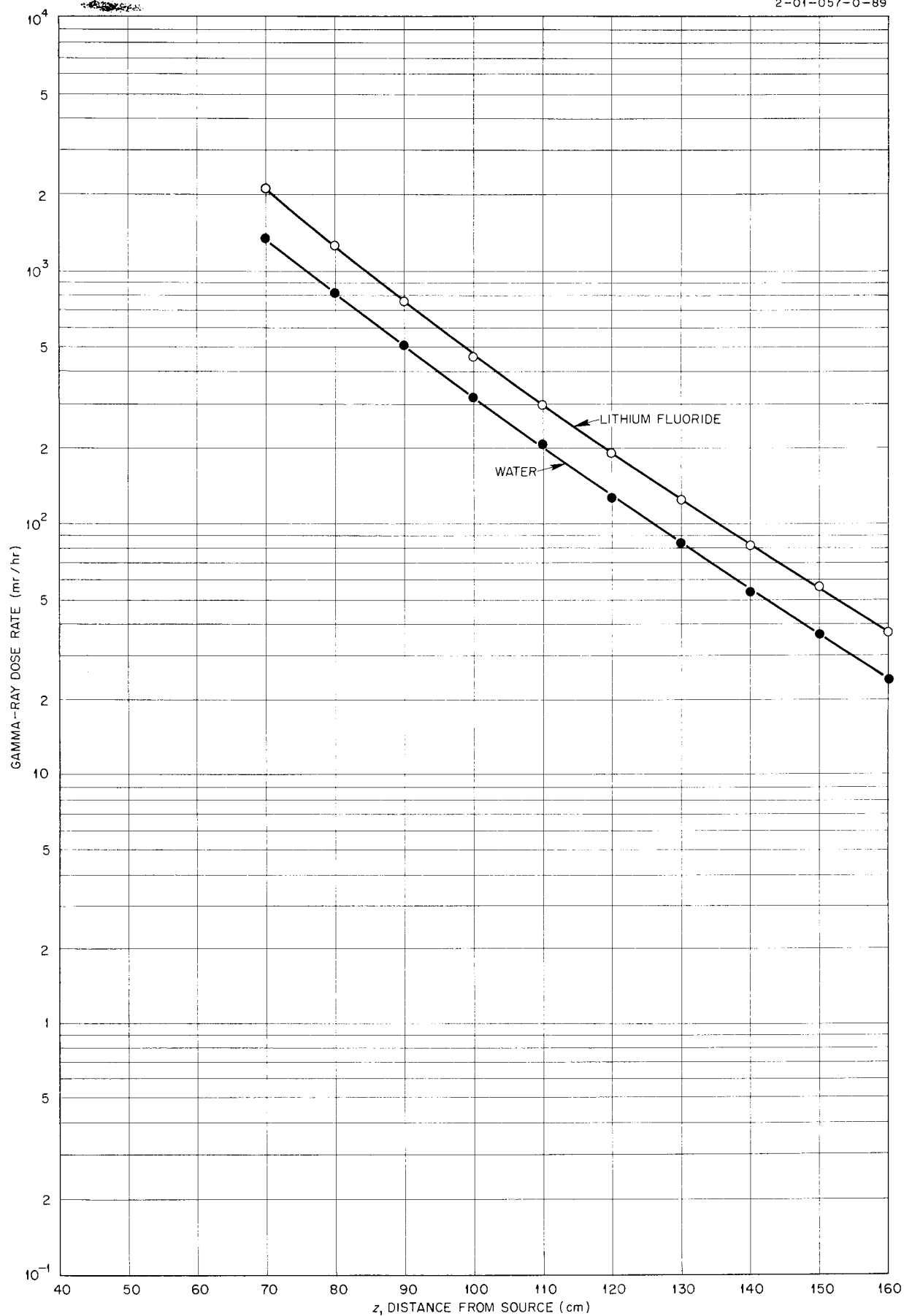


Fig. A-49 Gamma-Ray Dose Rate Beyond Lithium Fluoride (LiF)



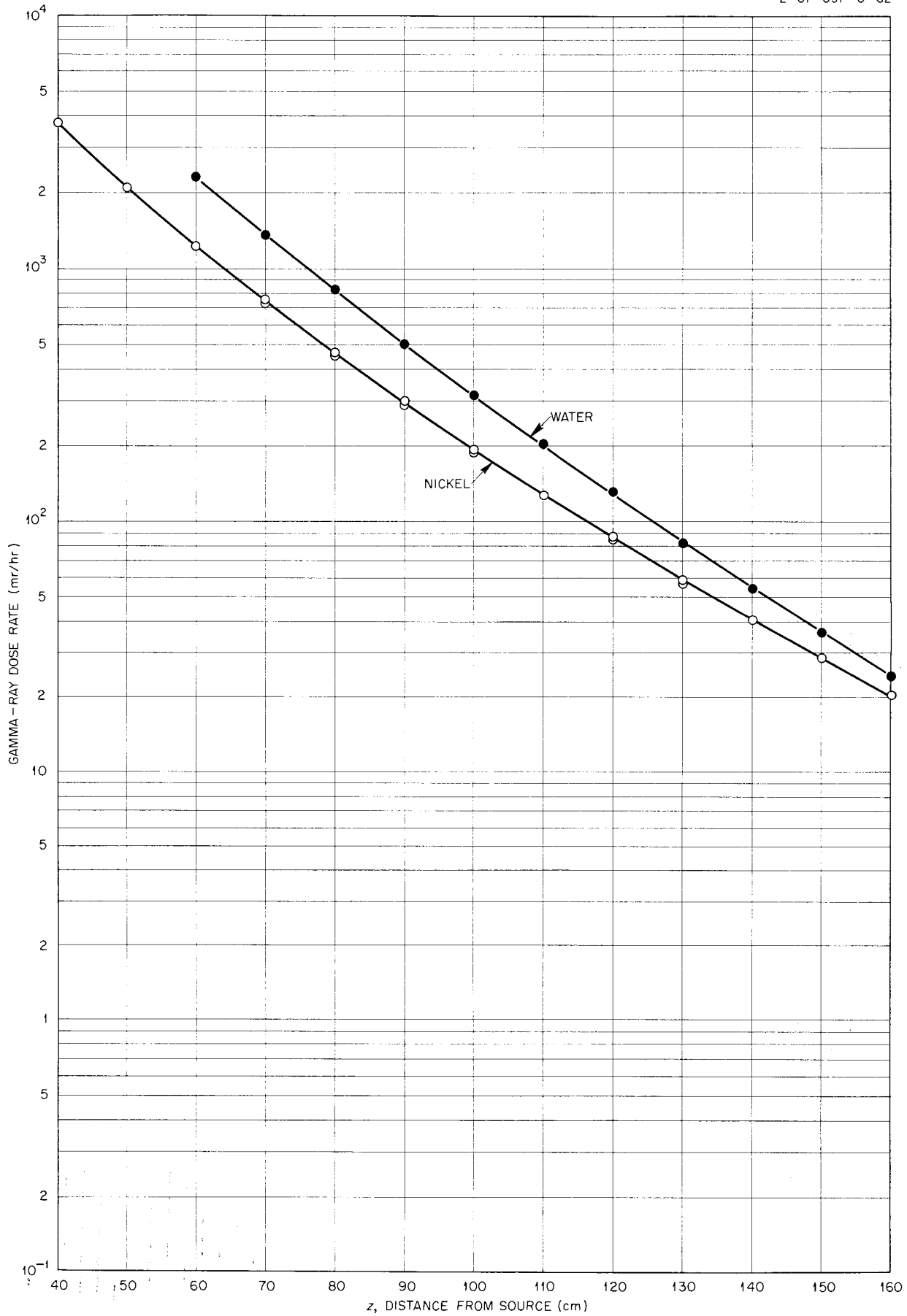


Fig. A-50. Gamma-Ray Dose Rate Beyond Nickel

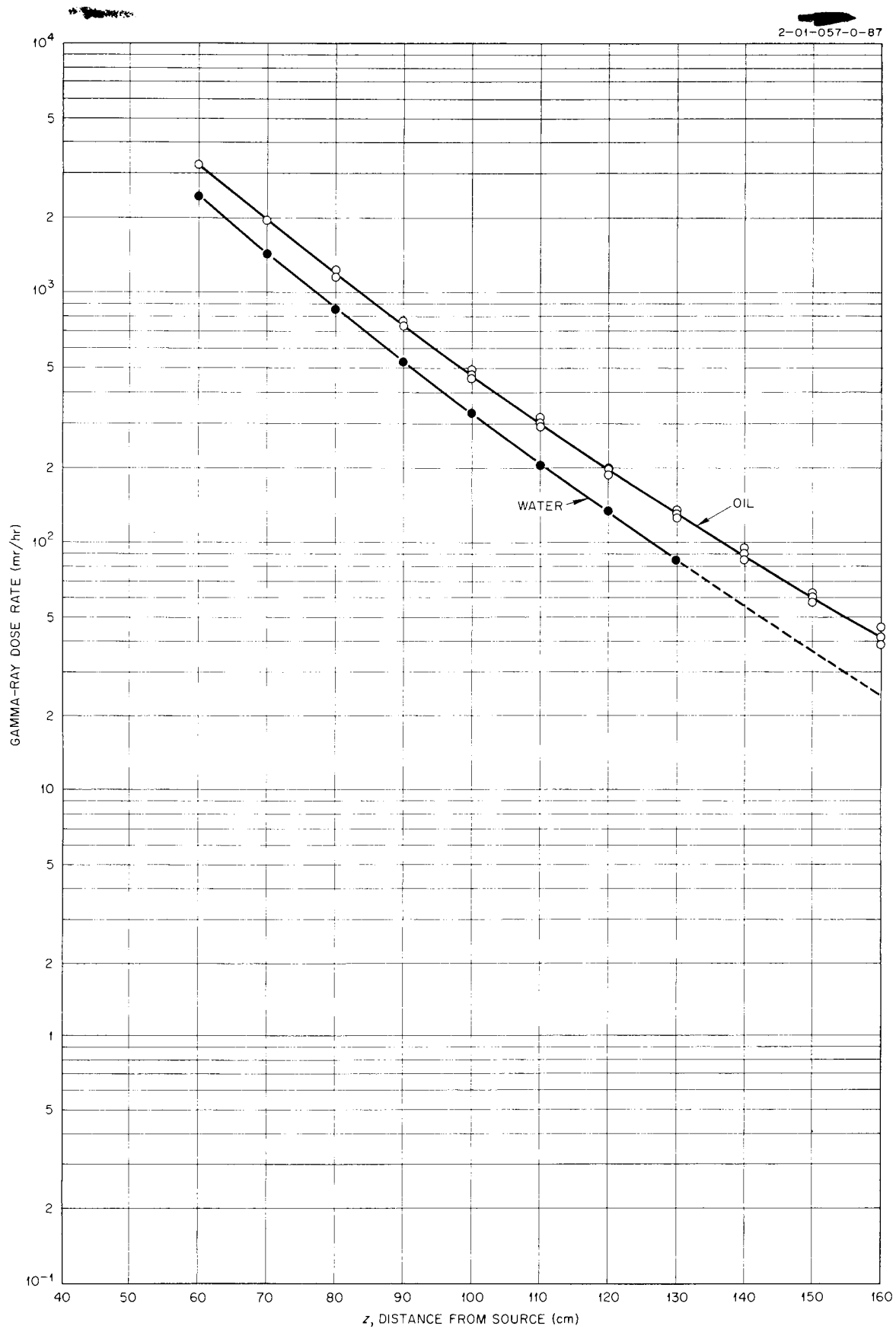


Fig. A-51. Gamma-Ray Dose Rate Beyond Oil ( $\text{CH}_2$ )

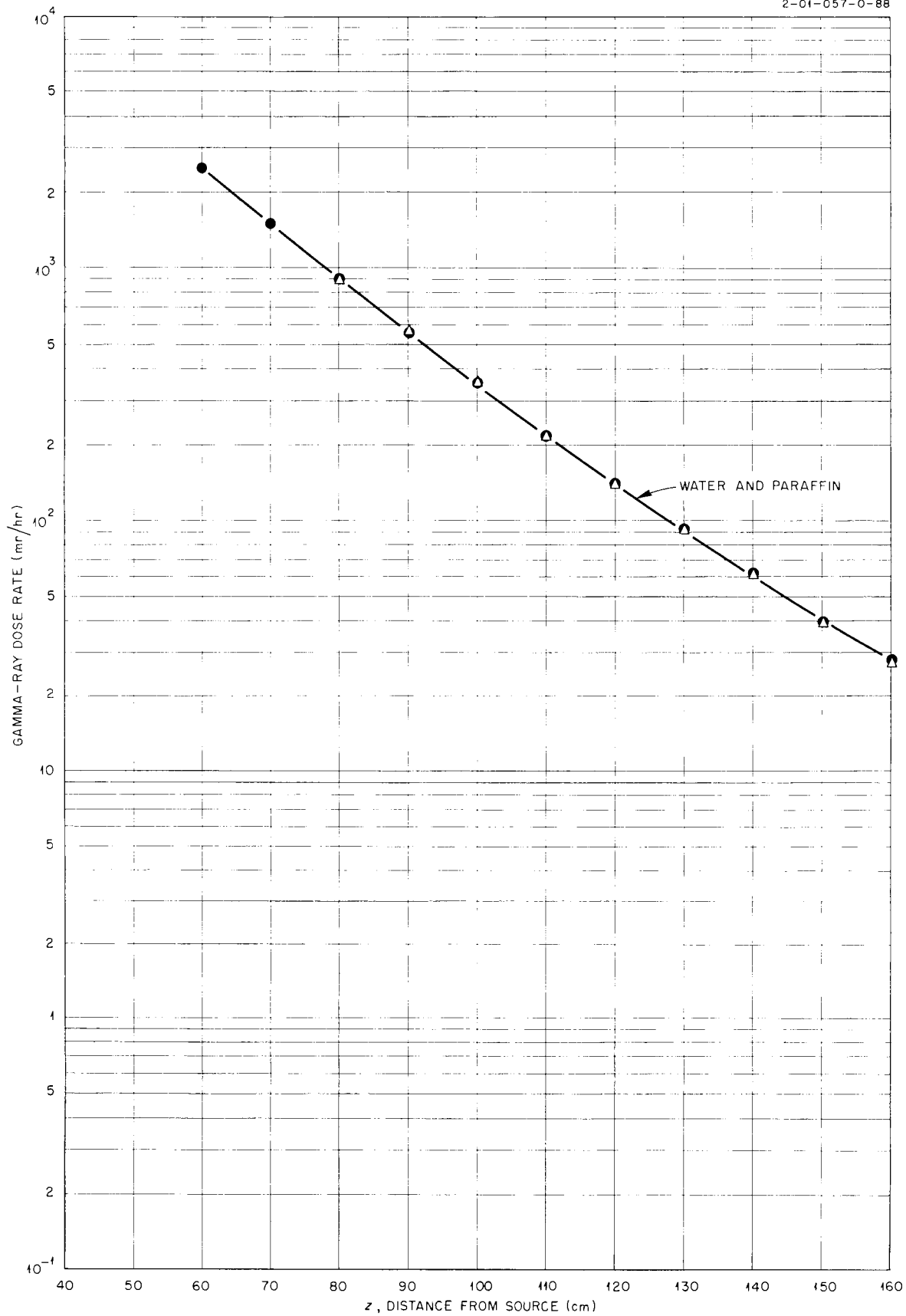
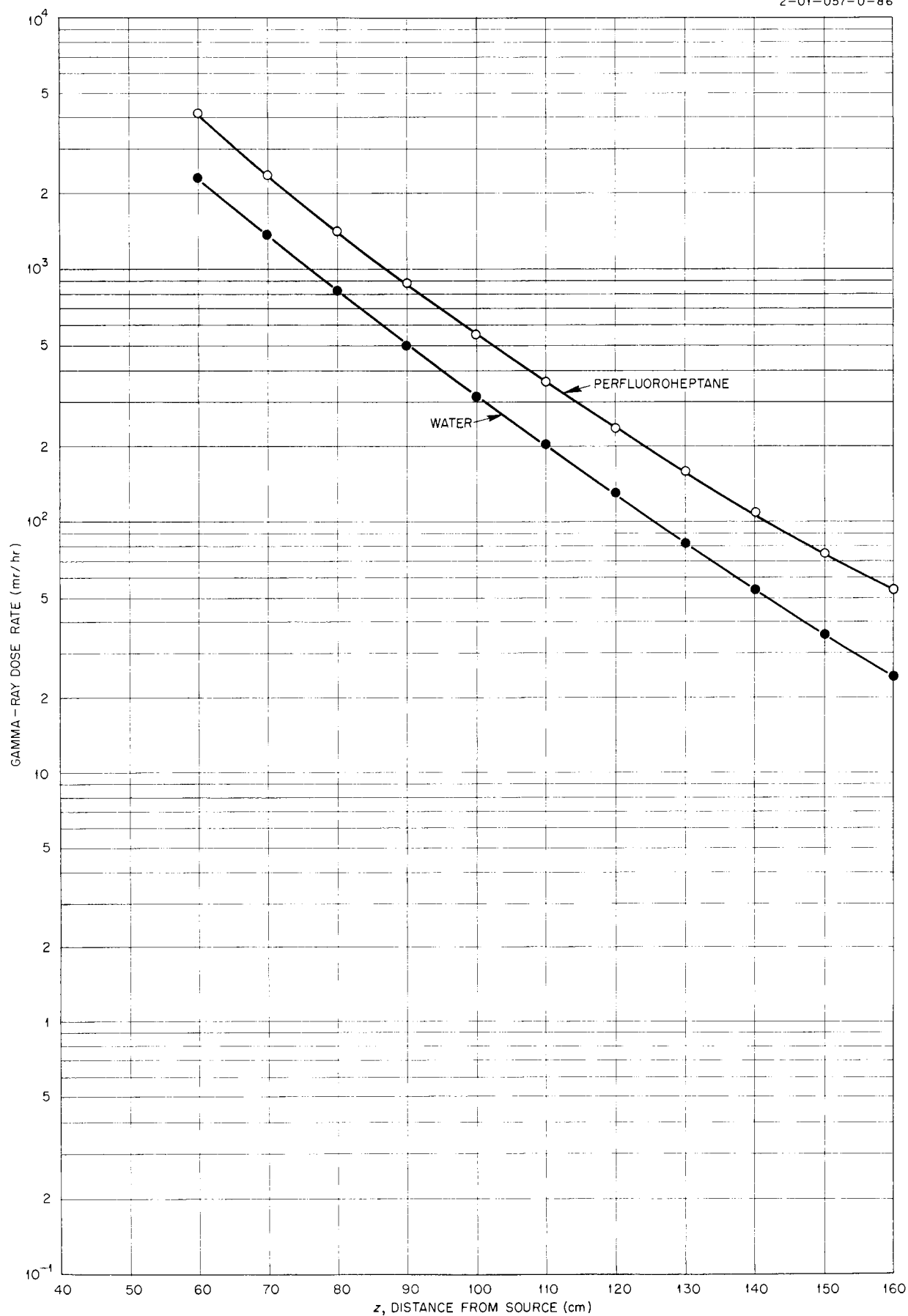


Fig. A-52. Gamma-Ray Dose Rate Beyond Paraffin ( $C_{30}H_{62}$ )

Fig. A-53. Gamma-Ray Dose Rate Beyond Perfluoroheptane ( $C_7F_{16}$ ).

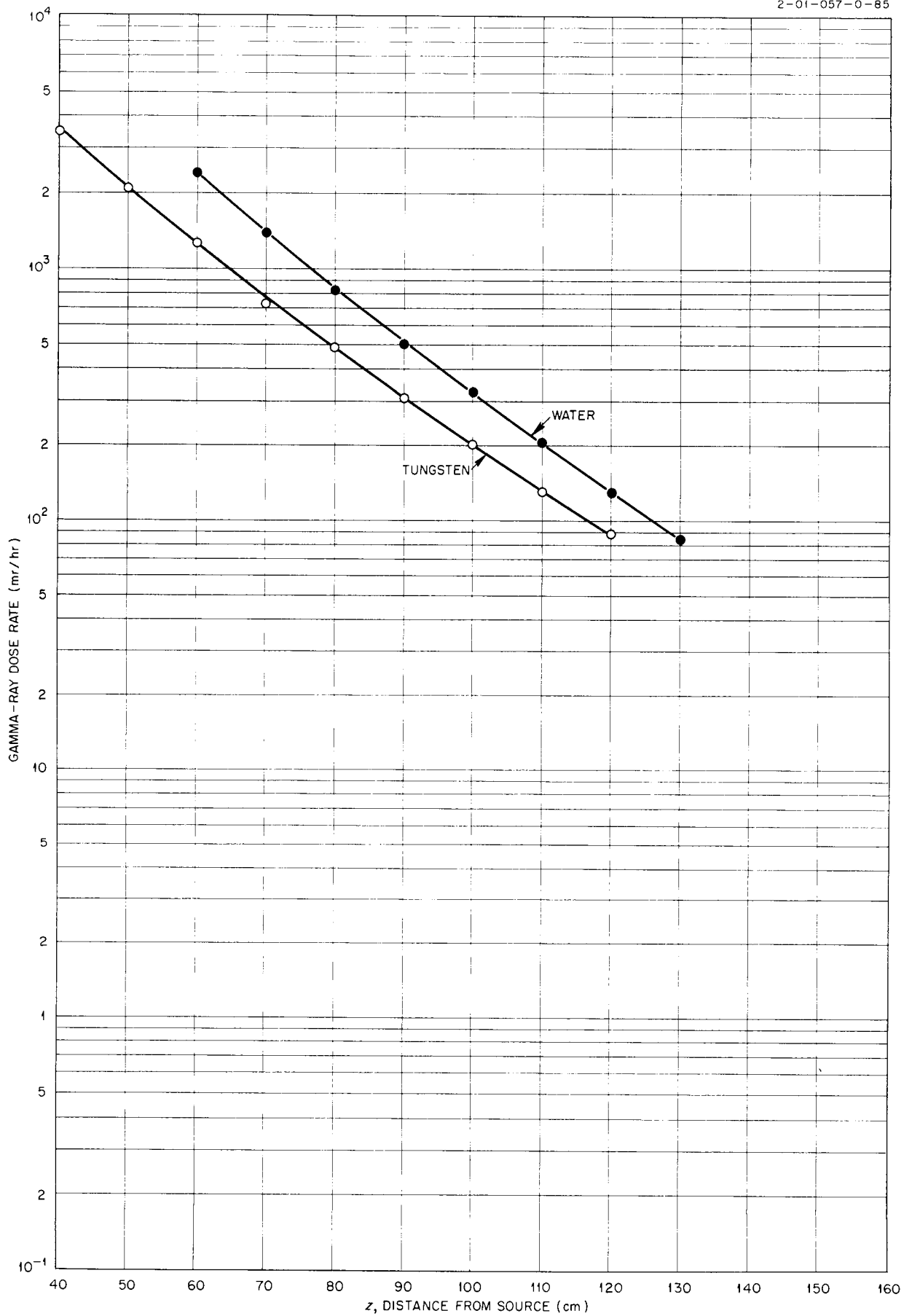


Fig. A-54. Gamma-Ray Dose Rate Beyond Tungsten

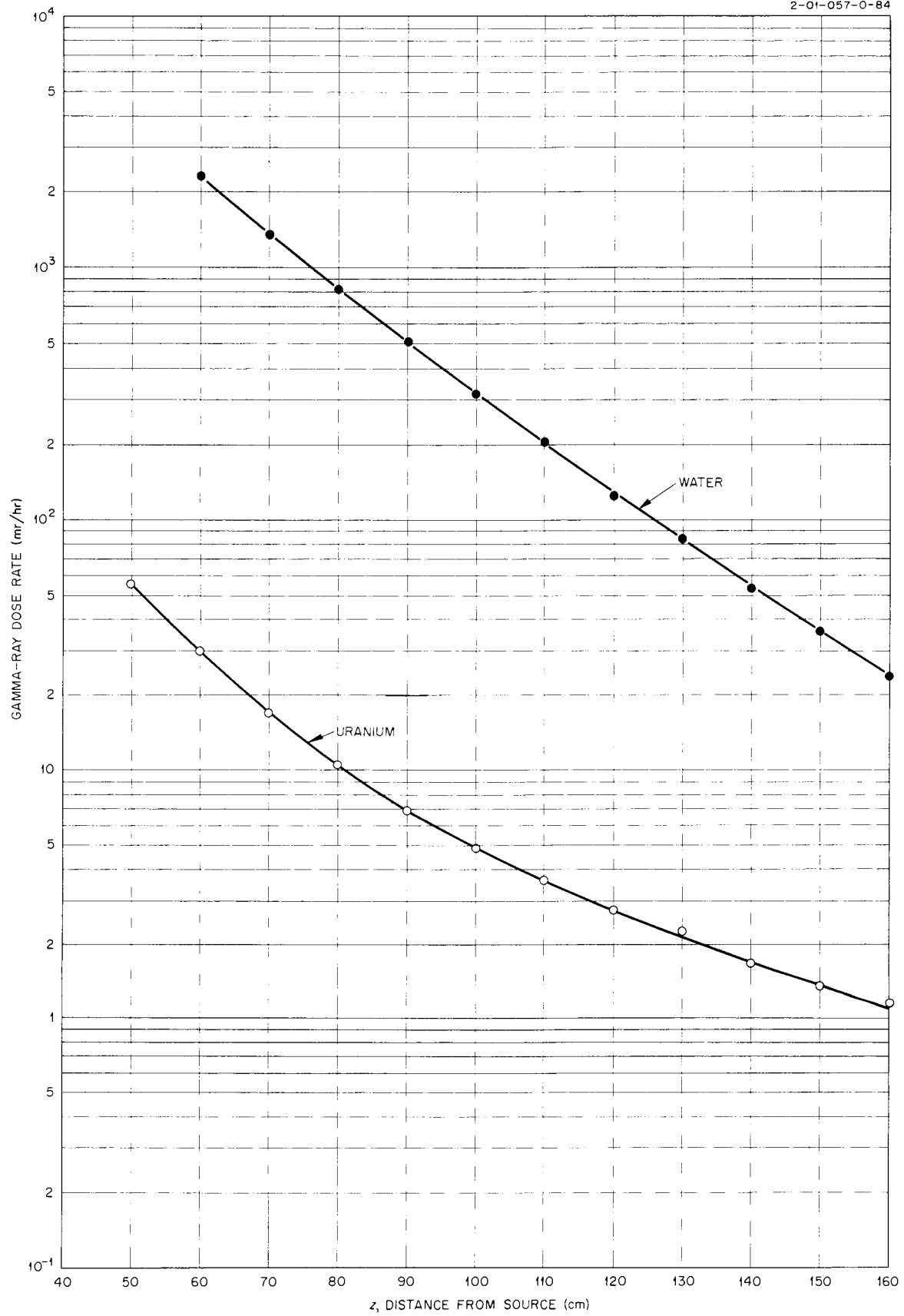


Fig. A-55. Gamma-Ray Dose Rate Beyond Uranium.

Table A-1

Aluminum -- Thermal-Neutron Flux

z, Distance from Source (cm)	Thermal-Neutron Flux (neutrons/cm <sup>2</sup> /sec)		
	Aluminum		Water, BF <sub>3</sub> (SB)
	3FC	BF <sub>3</sub> (SB)	
30	$2.99 \times 10^6$		
40	$3.17 \times 10^5$		
50	$4.58 \times 10^4$		
60	$8.44 \times 10^3$ $8.48 \times 10^3$		
70	$1.87 \times 10^3$		
80	$4.42 \times 10^2$		
83.7		$3.11 \times 10^2$	$1.86 \times 10^2$
93.7		$8.45 \times 10^1$	$5.40 \times 10^1$
103.7		$2.45 \times 10^1$	$1.67 \times 10^1$
113.7		$7.38 \times 10^0$	$5.06 \times 10^0$
123.7		$2.25 \times 10^0$	$1.67 \times 10^0$
133.7		$7.55 \times 10^{-1}$	$5.44 \times 10^{-1}$
143.7		$2.62 \times 10^{-1}$	$1.90 \times 10^{-1}$
153.7		$8.49 \times 10^{-2}$	

Table A-2

Aluminum -- Fast-Neutron Dose Rate

z, Distance from Source (cm)	Fast-Neutron Dose Rate (mrep/hr), HD	
	Aluminum	Water
55	$2.71 \times 10^1$	$1.28 \times 10^1$
65	$7.12 \times 10^0$	$4.16 \times 10^0$
75	$2.01 \times 10^0$	$1.34 \times 10^0$
85	$6.17 \times 10^{-1}$	$4.38 \times 10^{-1}$
95	$2.02 \times 10^{-1}$	$1.40 \times 10^{-1}$

Table A-3

Aluminum -- Gamma-Ray Dose Rate

z, Distance from Source (cm)	Gamma-Ray Dose Rate (mr/hr), ASC	
	Aluminum	Water
69.3	$2.42 \times 10^3$	
71.2		$1.41 \times 10^3$
79.3	$1.50 \times 10^3$	
81.2		$8.56 \times 10^2$
89.3	$9.10 \times 10^2$	
91.2		$4.98 \times 10^2$
99.3	$5.58 \times 10^2$	
101.2		$3.12 \times 10^2$
109.3	$3.58 \times 10^2$	
111.2		$1.97 \times 10^2$
119.3	$2.40 \times 10^2$	
121.2		$1.26 \times 10^2$
129.3	$1.60 \times 10^2$	
131.2		$7.91 \times 10^1$
139.3	$1.02 \times 10^2$	
141.2		$5.03 \times 10^1$
149.3	$7.22 \times 10^1$	
151.2		$3.80 \times 10^1$
159.3	$4.94 \times 10^1$	



Table A-4

## Beryllium (Pellets) -- Thermal-Neutron Flux

z, Distance from Source (cm)	Thermal-Neutron Flux (neutrons/cm <sup>2</sup> /sec)					
	Beryllium				Water	
	1/2 FC	3FC	8BF <sub>3</sub>	BF <sub>3</sub> (SB)	BF <sub>3</sub> (SB)	BF <sub>3</sub> (DB)
30	$1.706 \times 10^7$					
40	$1.035 \times 10^6$	$1.460 \times 10^6$				
50	$7.115 \times 10^4$	$8.788 \times 10^4$				
60		$9.391 \times 10^3$	$1.022 \times 10^4$			
70		$1.679 \times 10^3$	$1.637 \times 10^3$	$1.518 \times 10^3$		
80		$4.072 \times 10^2$	$3.852 \times 10^2$	$3.767 \times 10^2$		
90				$9.892 \times 10^1$	$8.078 \times 10^1$	
100				$2.738 \times 10^1$	$2.428 \times 10^1$	$2.608 \times 10^1$
110				$8.096 \times 10^0$	$7.390 \times 10^0$	$8.162 \times 10^0$
120				$2.455 \times 10^0$	$2.399 \times 10^0$	$2.644 \times 10^0$
130				$9.169 \times 10^{-1}$	$7.838 \times 10^{-1}$	$9.098 \times 10^{-1}$
140				$2.947 \times 10^{-1}$	$2.818 \times 10^{-1}$	$3.126 \times 10^{-1}$
150				$1.054 \times 10^{-1}$	$9.440 \times 10^{-2}$	$1.160 \times 10^{-1}$
160						$4.285 \times 10^{-2}$

Table A-5

Beryllium (Pellets) -- Fast-Neutron Dose Rate

z, Distance from Source (cm)	Fast-Neutron Dose Rate (mrep/hr), HD	
	Beryllium	Water
30		$2.34 \times 10^2$
31.2	$3.30 \times 10^2$	
40	$1.13 \times 10^2$	$8.80 \times 10^1$
50	$3.66 \times 10^1$	$2.72 \times 10^1$
60	$9.05 \times 10^0$	$7.19 \times 10^0$
70	$2.62 \times 10^0$	$2.31 \times 10^0$
80	$7.95 \times 10^{-1}$	$7.23 \times 10^{-1}$
90	$2.32 \times 10^{-1}$	$2.29 \times 10^{-1}$

Table A-6

Beryllium (Pellets) -- Gamma-Ray Dose Rate

z, Distance from Source (cm)	Gamma-Ray Dose Rate (mr/hr)	
	Beryllium	Water
70	$2.29 \times 10^3$	$1.34 \times 10^3$
80	$1.42 \times 10^3$	$8.68 \times 10^2$
90	$8.91 \times 10^2$	$5.31 \times 10^2$
100	$5.70 \times 10^2$	$3.29 \times 10^2$
110	$3.69 \times 10^2$	$2.16 \times 10^2$
120	$2.46 \times 10^2$	$1.37 \times 10^2$
130	$1.66 \times 10^2$	$8.80 \times 10^1$
140	$1.13 \times 10^2$	$5.65 \times 10^1$
150	$7.71 \times 10^1$	
160	$5.23 \times 10^1$	

Table A-7

Beryllium (Solid) -- Thermal-Neutron Flux

z, Distance from Source (cm)	Thermal-Neutron Flux (neutrons/cm <sup>2</sup> /sec)			
	1/2 FC	3FC	BF <sub>3</sub> (SB)	BF <sub>3</sub> (DB)
11.6	5.255 x 10 <sup>7</sup>			
11.8	5.168 x 10 <sup>7</sup>			
15	3.324 x 10 <sup>7</sup>			
20	1.054 x 10 <sup>7</sup>			
25	2.989 x 10 <sup>6</sup>			
30	9.583 x 10 <sup>5</sup>	8.385 x 10 <sup>5</sup>		
40	1.158 x 10 <sup>5</sup>	1.056 x 10 <sup>5</sup>		
50		1.817 x 10 <sup>4</sup>		
60		3.716 x 10 <sup>3</sup>		
70		8.998 x 10 <sup>2</sup>	8.753 x 10 <sup>2</sup>	7.935 x 10 <sup>2</sup>
80		2.468 x 10 <sup>2</sup>	2.444 x 10 <sup>2</sup>	2.351 x 10 <sup>2</sup>
90			6.872 x 10 <sup>1</sup>	6.681 x 10 <sup>1</sup>
100			2.086 x 10 <sup>1</sup>	2.047 x 10 <sup>1</sup>
110			6.122 x 10 <sup>0</sup>	6.174 x 10 <sup>0</sup>
120			1.971 x 10 <sup>0</sup>	2.015 x 10 <sup>0</sup>
130			6.439 x 10 <sup>-1</sup>	7.052 x 10 <sup>-1</sup>
140			2.348 x 10 <sup>-1</sup>	2.344 x 10 <sup>-1</sup>
150			8.516 x 10 <sup>-2</sup>	9.450 x 10 <sup>-2</sup>
160			2.880 x 10 <sup>-2</sup>	4.363 x 10 <sup>-2</sup>

Table A-8

Beryllium (Solid) -- Fast-Neutron Dose Rate

z, Distance from Source (cm)	Fast-Neutron Dose Rate (mrep/hr), HD
70	$2.969 \times 10^0$
80	$7.284 \times 10^{-1}$
90	$2.436 \times 10^{-1}$

Table A-9

Beryllium (Solid) -- Gamma-Ray Dose Rate

z, Distance from Source (cm)	Gamma-Ray Dose Rate (mr/hr)
60	$3.030 \times 10^3$
70	$1.878 \times 10^3$
90	$7.456 \times 10^2$
100	$4.799 \times 10^2$
110	$3.143 \times 10^2$
120	$2.118 \times 10^2$
130	$1.435 \times 10^2$
140	$9.734 \times 10^1$
150	$6.766 \times 10^1$
160	$4.714 \times 10^1$

Table A-10

Bismuth -- Thermal-Neutron Flux

z, Distance from Source (cm)	Thermal-Neutron Flux (neutrons/cm <sup>2</sup> /sec)		
	Bismuth		Water, BF <sub>3</sub> (SB)
	3FC	BF <sub>3</sub> (SB)	
40	5.56 x 10 <sup>5</sup>		
50	5.83 x 10 <sup>4</sup>		
60	8.45 x 10 <sup>3</sup> 8.35 x 10 <sup>3</sup>		
70	1.68 x 10 <sup>3</sup>		9.87 x 10 <sup>2</sup>
80	4.13 x 10 <sup>2</sup>	4.13 x 10 <sup>2</sup>	3.44 x 10 <sup>2</sup> 3.21 x 10 <sup>2</sup>
90	1.08 x 10 <sup>2</sup>	1.08 x 10 <sup>2</sup>	9.18 x 10 <sup>1</sup> 9.33 x 10 <sup>1</sup>
100		3.03 x 10 <sup>1</sup>	2.73 x 10 <sup>1</sup> 2.73 x 10 <sup>1</sup>
110		8.99 x 10 <sup>0</sup>	8.39 x 10 <sup>0</sup> 8.22 x 10 <sup>0</sup>
120		2.77 x 10 <sup>0</sup>	2.62 x 10 <sup>0</sup> 2.71 x 10 <sup>0</sup>
130		8.81 x 10 <sup>-1</sup>	8.84 x 10 <sup>-1</sup>
140		2.84 x 10 <sup>-1</sup>	2.91 x 10 <sup>-1</sup>
150		8.90 x 10 <sup>-2</sup>	1.02 x 10 <sup>-1</sup>
160		3.56 x 10 <sup>-2</sup>	

Table A-11

Bismuth -- Gamma-Ray Dose Rate

z, Distance from Source (cm)	Gamma-Ray Dose Rate (mr/hr)	
	900 IC	ASC
40	$1.00 \times 10^3$	
50	$4.34 \times 10^2$	
60	$2.12 \times 10^2$	$2.18 \times 10^2$
70	$1.11 \times 10^2$	$1.10 \times 10^2$
80	$6.05 \times 10^1$	$5.93 \times 10^1$
90		$3.30 \times 10^1$
100		$1.87 \times 10^1$
110		$1.09 \times 10^1$
120		$6.51 \times 10^0$
130		$3.85 \times 10^0$
140		$2.38 \times 10^0$
150		$1.48 \times 10^0$
160		$9.09 \times 10^{-1}$

Table A-12

## Boric Oxide -- Thermal-Neutron Flux

z, Distance from Source (cm)	Thermal-Neutron Flux (neutrons/cm <sup>2</sup> /sec)						
	Boric Oxide					Water	
	1/2 FC	3FC	8BF <sub>3</sub>	BF <sub>3</sub> (SB)	BF <sub>3</sub> (DB)	BF <sub>3</sub> (SB)	BF <sub>3</sub> (DB)
40.8	1.808 x 10 <sup>6</sup>						
42	2.63 x 10 <sup>6</sup>						
44	2.65 x 10 <sup>6</sup>						
46	2.37 x 10 <sup>6</sup>						
48	1.803 x 10 <sup>6</sup>						
50	1.332 x 10 <sup>6</sup>	1.261 x 10 <sup>6</sup>					
60	2.02 x 10 <sup>5</sup>	1.922 x 10 <sup>5</sup>					
70	3.59 x 10 <sup>5</sup>	3.95 x 10 <sup>4</sup>					8.48 x 10 <sup>2</sup>
80		7.45 x 10 <sup>3</sup>	7.09 x 10 <sup>3</sup>			2.91 x 10 <sup>2</sup>	2.57 x 10 <sup>2</sup>
90		1.66 x 10 <sup>3</sup>	1.599 x 10 <sup>3</sup>			8.24 x 10 <sup>1</sup>	7.59 x 10 <sup>1</sup>
100		4.12 x 10 <sup>2</sup>	3.86 x 10 <sup>2</sup>	3.70 x 10 <sup>2</sup>		2.48 x 10 <sup>0</sup>	2.20 x 10 <sup>1</sup>
110			1.016 x 10 <sup>2</sup>	1.009 x 10 <sup>1</sup>	9.56 x 10 <sup>1</sup>	7.61 x 10 <sup>0</sup>	7.24 x 10 <sup>0</sup>
120			2.76 x 10 <sup>1</sup>	2.64 x 10 <sup>1</sup>	2.62 x 10 <sup>1</sup>	2.46 x 10 <sup>0</sup>	2.31 x 10 <sup>0</sup>
130			8.38 x 10 <sup>0</sup>	6.91 x 10 <sup>0</sup>	7.87 x 10 <sup>0</sup>	7.86 x 10 <sup>-1</sup>	7.61 x 10 <sup>-1</sup>
140			2.60 x 10 <sup>0</sup>	2.41 x 10 <sup>0</sup>	2.40 x 10 <sup>0</sup>	2.71 x 10 <sup>-1</sup>	2.68 x 10 <sup>-1</sup>
150				7.86 x 10 <sup>-1</sup>	7.80 x 10 <sup>-1</sup>	9.51 x 10 <sup>-2</sup>	9.60 x 10 <sup>-2</sup>
160				2.42 x 10 <sup>-1</sup>		3.75 x 10 <sup>-2</sup>	3.20 x 10 <sup>-2</sup>
160.3					2.81 x 10 <sup>-1</sup>		

Table A-13

Boric Oxide -- Gamma-Ray Dose Rate

z, Distance from Source (cm)	Gamma-Ray Dose Rate (mr/hr)	
	900IC	ASC
60	$2.62 \times 10^3$	
70	$1.495 \times 10^3$	
73	$1.274 \times 10^3$	
80	$8.86 \times 10^2$	
90	$5.41 \times 10^2$	
100	$3.37 \times 10^2$	$3.06 \times 10^2$
110	$2.10 \times 10^2$	$1.911 \times 10^2$
120	$1.390 \times 10^2$	$1.294 \times 10^2$
130	$9.02 \times 10^1$	$8.15 \times 10^1$
140	$6.02 \times 10^1$	$5.45 \times 10^1$
150	$3.95 \times 10^1$	$3.66 \times 10^1$
160	$2.90 \times 10^1$	$2.40 \times 10^1$



Table A-14

Boron Carbide -- Thermal-Neutron Flux

z, Distance from Source (cm)	Thermal-Neutron Flux (neutrons/cm <sup>2</sup> /sec)		
	3FC	8BF <sub>3</sub>	BF <sub>3</sub> (SB)
58	7.945 x 10 <sup>3</sup>		
58.8		7.049 x 10 <sup>3</sup>	
60	8.459 x 10 <sup>3</sup>		
62	7.182 x 10 <sup>3</sup>	6.410 x 10 <sup>3</sup>	
65	4.782 x 10 <sup>3</sup>	4.380 x 10 <sup>3</sup>	
68		2.663 x 10 <sup>3</sup>	
70	2.104 x 10 <sup>3</sup>	1.931 x 10 <sup>3</sup>	
75	8.238 x 10 <sup>2</sup>		1.854 x 10 <sup>3</sup>
80		3.248 x 10 <sup>2</sup>	3.293 x 10 <sup>2</sup>
90		7.905 x 10 <sup>1</sup>	6.996 x 10 <sup>1</sup>
100		1.883 x 10 <sup>1</sup>	1.685 x 10 <sup>1</sup> 1.659 x 10 <sup>1</sup>
110			4.404 x 10 <sup>0</sup>
120			1.292 x 10 <sup>0</sup>
130			3.834 x 10 <sup>-1</sup>
140			1.182 x 10 <sup>-1</sup>
150			3.820 x 10 <sup>-2</sup>

Table A-15

Boron Carbide -- Fast-Neutron Dose Rate

z, Distance from Source (cm)	Fast-Neutron Dose Rate (mrep/hr), HD		
	Run 1	Run 2	Run 3
100			$3.369 \times 10^{-2}$
90	$1.449 \times 10^{-1}$	$1.337 \times 10^{-1}$	$1.303 \times 10^{-1}$
85	$2.721 \times 10^{-1}$		
80	$4.855 \times 10^{-1}$	$4.883 \times 10^{-1}$	
70	$2.267 \times 10^0$	$2.061 \times 10^0$	$9.878 \times 10^0$
60	$1.004 \times 10^1$	$9.531 \times 10^0$	$2.008 \times 10^0$
55.3	$2.662 \times 10^1$	$2.335 \times 10^1$	$2.565 \times 10^1$
	$2.555 \times 10^1$		

Table A-16

Boron Carbide -- Gamma-Ray Dose Rate

z, Distance from Source (cm)	Gamma-Ray Dose Rate (mr/hr), 900IC
60.3	$3.684 \times 10^2$
70	$2.420 \times 10^2$
80	$1.571 \times 10^2$
90	$1.008 \times 10^2$
100	$6.739 \times 10^1$
110	$4.500 \times 10^1$
120	$3.011 \times 10^1$
130	$2.075 \times 10^1$
140	$1.478 \times 10^1$
150	$1.106 \times 10^1$
160	$8.352 \times 10^0$

Table A-17

Carbon -- Thermal-Neutron Flux

z, Distance from Source (cm)	Thermal-Neutron Flux (neutrons/cm <sup>2</sup> /sec)		
	1/2 FC	3FC	BF <sub>3</sub> (SB)
38.2	$5.493 \times 10^6$		
40	$3.552 \times 10^6$		
45	$8.748 \times 10^5$		
50	$2.470 \times 10^5$	$3.335 \times 10^5$	
60	$3.084 \times 10^4$	$3.365 \times 10^4$	
70		$5.842 \times 10^3$	
80		$1.358 \times 10^3$	$1.245 \times 10^3$
90		$3.396 \times 10^2$	$3.397 \times 10^2$
100			$9.151 \times 10^1$
110			$2.594 \times 10^1$
120			$7.630 \times 10^0$
130			$2.333 \times 10^0$
140			$7.226 \times 10^{-1}$
150			$2.504 \times 10^{-1}$
160			$8.313 \times 10^{-2}$

Table A-18

Carbon -- Fast-Neutron Dose Rate

z, Distance from Source (cm)	Fast-Neutron Dose Rate (mrep/hr), HD
39.2	$4.188 \times 10^2$
45	$2.135 \times 10^2$
50	$1.146 \times 10^2$
60	$3.563 \times 10^1$
	$3.535 \times 10^1$
70	$7.791 \times 10^0$
	$8.805 \times 10^0$
80	$2.536 \times 10^0$
90	$7.232 \times 10^{-1}$
100	$2.145 \times 10^{-1}$
110	$6.974 \times 10^{-2}$

Table A-19

Carbon -- Gamma-Ray Dose Rate

z, Distance from Source (cm)	Gamma-Ray Dose Rate (mr/hr)	
	900IC	ASC
60	$3.207 \times 10^3$	$3.059 \times 10^3$
70	$1.868 \times 10^3$	$1.755 \times 10^3$
80	$1.154 \times 10^3$	$1.054 \times 10^3$
90	$7.149 \times 10^2$	$6.643 \times 10^2$
100	$4.542 \times 10^2$	$4.214 \times 10^2$
110	$2.970 \times 10^2$	$2.710 \times 10^2$
120	$1.931 \times 10^2$	$1.828 \times 10^2$
130	$1.309 \times 10^2$	$1.187 \times 10^2$
140	$8.881 \times 10^1$	$8.183 \times 10^1$
150	$6.121 \times 10^1$	$5.651 \times 10^1$
160	$4.267 \times 10^1$	$3.891 \times 10^1$

Table A-20

## Copper -- Thermal-Neutron Flux

z, Distance from Source (cm)	Thermal-Neutron Flux (neutrons/cm <sup>2</sup> /sec)				
	Copper				Water,
	1/2FC	3FC	BF <sub>3</sub> (SB)	BF <sub>3</sub> (DB)	3FC
21	4.43 x 10 <sup>6</sup>				
23	5.54 x 10 <sup>6</sup>				
26	3.56 x 10 <sup>6</sup>				
28	2.75 x 10 <sup>6</sup>				
30	1.681 x 10 <sup>6</sup>	1.623 x 10 <sup>6</sup>			5.31 x 10 <sup>5</sup>
40	1.328 x 10 <sup>5</sup>	1.433 x 10 <sup>5</sup>			9.53 x 10 <sup>4</sup>
50		1.327 x 10 <sup>4</sup>			2.05 x 10 <sup>4</sup>
60		2.03 x 10 <sup>3</sup>	1.475 x 10 <sup>3</sup>		4.66 x 10 <sup>3</sup>
70		4.35 x 10 <sup>2</sup>	3.45 x 10 <sup>2</sup>	4.18 x 10 <sup>2</sup>	1.174 x 10 <sup>3</sup>
80			8.49 x 10 <sup>1</sup>	1.081 x 10 <sup>2</sup>	3.20 x 10 <sup>2</sup>
90			2.24 x 10 <sup>1</sup>	3.01 x 10 <sup>1</sup>	
100			6.59 x 10 <sup>0</sup>	8.91 x 10 <sup>0</sup>	
110			2.04 x 10 <sup>0</sup>	2.67 x 10 <sup>0</sup>	
120			7.33 x 10 <sup>-1</sup>	8.72 x 10 <sup>-1</sup>	
			6.47 x 10 <sup>-1</sup>		
130			2.03 x 10 <sup>-1</sup>	2.94 x 10 <sup>-1</sup>	
140			7.40 x 10 <sup>-2</sup>		

Table A-21

Copper -- Fast-Neutron Dose Rate

z, Distance from Source (cm)	Fast-Neutron Dose Rate (mrep/hr)	
	Copper	Water
30	$4.18 \times 10^2$	$5.23 \times 10^2$
40	$8.31 \times 10^1$	$5.28 \times 10^2$
50	$1.658 \times 10^1$	$1.41 \times 10^2$
60	$3.76 \times 10^0$	$1.46 \times 10^2$
70	$1.044 \times 10^0$	$4.88 \times 10^1$
80	$3.08 \times 10^{-1}$	$1.116 \times 10^1$
		$1.058 \times 10^0$
		$2.90 \times 10^{-1}$
		$8.61 \times 10^{-1}$

Table A-22

Copper -- Gamma-Ray Dose Rate

z, Distance from Source (cm)	Gamma-Ray Dose Rate (mr/hr), 900 IC		
	Run 1	Run 2	Run 3
27.5	$3.86 \times 10^3$		
30	$3.41 \times 10^3$		
40	$1.711 \times 10^3$		
50	$9.06 \times 10^2$		
60		$5.14 \times 10^2$	
70		$3.02 \times 10^2$	
80	$1.831 \times 10^2$	$1.833 \times 10^2$	
90		$1.149 \times 10^1$	$1.140 \times 10^2$
100		$7.35 \times 10^1$	$7.39 \times 10^1$
110		$4.81 \times 10^1$	$4.82 \times 10^1$
120	$3.12 \times 10^1$	$3.16 \times 10^1$	$3.16 \times 10^1$
130	$2.11 \times 10^1$	$2.14 \times 10^1$	$2.14 \times 10^1$
140	$1.483 \times 10^1$	$1.483 \times 10^1$	$1.49 \times 10^1$
	$1.194 \times 10^1$		

Table A-23

Fluorothene -- Thermal-Neutron Flux

z, Distance from Source (cm)	Thermal-Neutron Flux (neutrons/cm <sup>2</sup> /sec)		
	1/2 FC	3 FC	BF <sub>3</sub> (SB)
17.7	1.432 x 10 <sup>7</sup>		
20	1.750 x 10 <sup>7</sup>		
22	1.430 x 10 <sup>7</sup>		
24	1.028 x 10 <sup>7</sup>		
30	2.969 x 10 <sup>6</sup>		
40	3.846 x 10 <sup>5</sup>	3.251 x 10 <sup>5</sup>	
50	6.173 x 10 <sup>4</sup>	5.194 x 10 <sup>4</sup>	
60		1.014 x 10 <sup>4</sup>	
70		2.048 x 10 <sup>3</sup>	
80		5.067 x 10 <sup>2</sup>	5.097 x 10 <sup>2</sup>
90		1.43 x 10 <sup>2</sup>	1.410 x 10 <sup>2</sup>
100			3.975 x 10 <sup>1</sup>
110			1.155 x 10 <sup>1</sup>
120			3.478 x 10 <sup>0</sup>
130			1.124 x 10 <sup>0</sup>
140			3.424 x 10 <sup>-1</sup>
150			1.226 x 10 <sup>-1</sup>
160			4.722 x 10 <sup>-2</sup>

Table A-24

Fluorothene -- Fast-Neutron Dose Rate

z, Distance from Source (cm)	Fast-Neutron Dose Rate (mrep/hr), HD
60	$2.608 \times 10^1$
70	$6.925 \times 10^0$
80	$2.108 \times 10^0$
90	$6.088 \times 10^{-1}$

Table A-25

Fluorothene -- Gamma-Ray Dose Rate

z, Distance from Source (cm)	Gamma-Ray Dose Rate (mr/hr)	
	900 IC	ASC
70	$2.437 \times 10^3$	
80	$1.524 \times 10^3$	
90	$9.583 \times 10^2$	
100	$6.182 \times 10^2$	
110	$4.010 \times 10^2$	$4.142 \times 10^2$
120	$2.651 \times 10^2$	$2.737 \times 10^2$
130	$1.795 \times 10^2$	$1.831 \times 10^2$
140	$1.205 \times 10^1$	$1.244 \times 10^1$
150	$8.353 \times 10^1$	$8.509 \times 10^1$
160	$5.854 \times 10^1$	$5.815 \times 10^1$



Table A-26

## Heavy Water -- Thermal-Neutron Flux

z, Distance from Source (cm)	Thermal-Neutron Flux (neutrons/cm <sup>2</sup> /sec)					
	Heavy Water			Plain Water		
	3FC	BF <sub>3</sub> (SB)	BF <sub>3</sub> (DB)	BF <sub>3</sub> (DB)		BF <sub>3</sub> (DB), In 26-in. Tank <sup>a</sup>
				Run 1	Run 2	
30						5.11 x 10 <sup>5</sup>
40						9.12 x 10 <sup>4</sup>
50						1.908 x 10 <sup>4</sup>
60						4.45 x 10 <sup>3</sup>
70	3.72 x 10 <sup>6</sup>					
75	5.67 x 10 <sup>5</sup>					
	9.40 x 10 <sup>5</sup>					
71.8						6.46 x 10 <sup>2</sup>
76						4.64 x 10 <sup>2</sup>
80	1.564 x 10 <sup>5</sup>			3.06 x 10 <sup>2</sup>	3.17 x 10 <sup>2</sup>	2.96 x 10 <sup>2</sup>
90	3.85 x 10 <sup>3</sup>		1.947 x 10 <sup>3</sup>			8.71 x 10 <sup>1</sup>
95		8.13 x 10 <sup>2</sup>				
100	1.572 x 10 <sup>2</sup>	1.650 x 10 <sup>2</sup>	1.093 x 10 <sup>2</sup>		2.78 x 10 <sup>1</sup>	2.60 x 10 <sup>1</sup>
		1.249 x 10 <sup>2</sup>				
105			3.54 x 10 <sup>1</sup>			
110		1.650 x 10 <sup>1</sup>	1.566 x 10 <sup>1</sup>			8.12 x 10 <sup>0</sup>
		1.679 x 10 <sup>1</sup>				
115			7.79 x 10 <sup>0</sup>			
120		3.96 x 10 <sup>0</sup>	4.14 x 10 <sup>0</sup>	1.88 x 10 <sup>0</sup>	2.74 x 10 <sup>0</sup>	2.64 x 10 <sup>0</sup>
130		1.235 x 10 <sup>0</sup>	1.364 x 10 <sup>0</sup>			
140		3.93 x 10 <sup>-1</sup>	4.74 x 10 <sup>-1</sup>	3.34 x 10 <sup>-1</sup>		
150			1.90 x 10 <sup>-1</sup>			
160			8.78 x 10 <sup>-2</sup>			

<sup>a</sup> See Table 1, p. 7.

Table A-27

Heavy Water -- Fast-Neutron Dose Rate

z, Distance from Source (cm)	Fast-Neutron Dose Rate (mrep/hr), HD		
	Heavy Water		Plain Water
	Run 1	Run 2	
70	$1.791 \times 10^1$	$1.452 \times 10^1$ $6.63 \times 10^0$ $2.28 \times 10^0$ $9.95 \times 10^{-1}$	$3.44 \times 10^0$
71			
72			
75			
80	$2.28 \times 10^0$		
85	$4.49 \times 10^{-1}$		
90	$1.329 \times 10^{-1}$		
100			

Table A-28

Heavy Water -- Gamma-Ray Dose Rate

z, Distance from Source (cm)	Gamma-Ray Dose Rate (mr/hr), 900IC		
	Heavy Water	Plain Water	
		In 26-in. Tank <sup>a</sup>	Without Tank <sup>a</sup>
70			$1.496 \times 10^3$ $1.467 \times 10^3$
76.6		$1.172 \times 10^3$	
80	$3.07 \times 10^3$	$1.010 \times 10^3$	
90	$1.729 \times 10^3$	$6.42 \times 10^2$	$5.57 \times 10^2$
100	$1.055 \times 10^3$	$4.06 \times 10^2$	
110	$6.61 \times 10^2$	$2.70 \times 10^2$	$2.17 \times 10^2$
120	$4.31 \times 10^2$	$1.741 \times 10^2$	
130	$2.82 \times 10^2$	$1.180 \times 10^1$	$9.07 \times 10^1$
140	$1.912 \times 10^2$	$7.87 \times 10^1$	
150	$1.288 \times 10^1$	$5.42 \times 10^1$	$4.16 \times 10^1$
160	$8.95 \times 10^1$		
170	$6.44 \times 10^1$		

<sup>a</sup> See Table 1, p. 7.

Table A-29

Iron -- Thermal-Neutron Flux

z, Distance from Source (cm)	Thermal-Neutron Flux (neutrons/cm <sup>2</sup> /sec)	
	BF <sub>3</sub> (SB)	3FC
37.3		7.575 x 10 <sup>5</sup>
40		1.086 x 10 <sup>6</sup>
42		9.351 x 10 <sup>5</sup>
45		5.596 x 10 <sup>5</sup>
50		1.577 x 10 <sup>5</sup>
60		8.092 x 10 <sup>3</sup>
70	1.726 x 10 <sup>3</sup>	5.520 x 10 <sup>2</sup>
80	1.451 x 10 <sup>2</sup>	7.392 x 10 <sup>1</sup>
90	2.282 x 10 <sup>1</sup>	
100	5.137 x 10 <sup>0</sup>	
110	1.432 x 10 <sup>0</sup>	
120	4.449 x 10 <sup>-1</sup>	
130	1.526 x 10 <sup>-1</sup>	
140	4.920 x 10 <sup>-2</sup>	
150	1.616 x 10 <sup>-2</sup>	

Table A-30

Iron -- Fast-Neutron Dose Rate

z, Distance from Source (cm)	Fast-Neutron Dose Rate (mrep/hr), HD	
	Run 1	Run 2
40	$2.982 \times 10^2$	$2.135 \times 10^2$
42	$1.704 \times 10^2$	
45	$9.601 \times 10^1$	
50	$2.249 \times 10^0$	$1.803 \times 10^1$
60	$2.883 \times 10^0$	$2.520 \times 10^0$
70	$5.841 \times 10^{-1}$	$5.351 \times 10^{-1}$
80	$1.453 \times 10^{-1}$	$1.374 \times 10^{-1}$

Table A-31

Iron -- Gamma-Ray Dose Rate

z, Distance from Source (cm)	Gamma-Ray Dose Rate (mr/hr)	
	900IC	ASC
41.9	$1.619 \times 10^3$	
50	$9.974 \times 10^2$	
60	$5.246 \times 10^2$	$5.193 \times 10^2$
70	$2.899 \times 10^2$	$2.877 \times 10^2$
80		$1.689 \times 10^2$
90		$1.025 \times 10^1$
100		$6.392 \times 10^1$
110		$4.049 \times 10^1$
120		$2.615 \times 10^1$

Table A-32

Lead -- Thermal-Neutron Flux

z, Distance from Source (cm)	Thermal-Neutron Flux (neutrons/cm <sup>2</sup> /sec)			
	Lead			Water, BF <sub>3</sub> (SB)
	1/2FC	3FC	BF <sub>3</sub> (SB)	
32	2.29 x 10 <sup>6</sup>	1.52 x 10 <sup>6</sup>		
35	1.24 x 10 <sup>6</sup>			
40	5.15 x 10 <sup>5</sup>	4.37 x 10 <sup>5</sup>		
50		5.94 x 10 <sup>4</sup>		
60		7.47 x 10 <sup>3</sup>		
		7.99 x 10 <sup>3</sup>		
70		1.45 x 10 <sup>3</sup>	1.24 x 10 <sup>3</sup>	
80		3.34 x 10 <sup>2</sup>	3.45 x 10 <sup>2</sup>	
90			8.93 x 10 <sup>1</sup>	
100			2.55 x 10 <sup>0</sup>	2.72 x 10 <sup>1</sup>
110			7.46 x 10 <sup>0</sup>	8.54 x 10 <sup>0</sup>
120			2.19 x 10 <sup>-1</sup>	2.67 x 10 <sup>-1</sup>
130			6.86 x 10 <sup>-1</sup>	8.42 x 10 <sup>-1</sup>
140			2.05 x 10 <sup>-1</sup>	2.94 x 10 <sup>-1</sup>
150			7.84 x 10 <sup>-2</sup>	
160			2.51 x 10 <sup>-2</sup>	

Table A-33

Lead -- Gamma-Ray Dose Rate

z, Distance from Source (cm)	Gamma-Ray Dose Rate (mr/hr)			
	Lead		Water	
	900IC	ASC	900IC	ASC
40	$8.06 \times 10^2$			
50	$3.67 \times 10^2$	$4.33 \times 10^2$		
60	$1.81 \times 10^2$	$2.00 \times 10^2$	$2.41 \times 10^3$	
70	$9.50 \times 10^1$	$9.80 \times 10^1$		
		$1.02 \times 10^2$	$1.43 \times 10^3$	
80	$5.19 \times 10^1$	$5.44 \times 10^1$	$8.56 \times 10^2$	
90		$3.06 \times 10^1$	$5.24 \times 10^2$	
100		$1.76 \times 10^1$	$3.30 \times 10^2$	$3.53 \times 10^2$
110		$1.07 \times 10^0$	$2.11 \times 10^2$	$2.22 \times 10^2$
120		$6.30 \times 10^0$	$1.35 \times 10^1$	$1.38 \times 10^1$
130		$4.04 \times 10^0$	$8.62 \times 10^1$	$9.13 \times 10^1$
140		$2.24 \times 10^0$	$5.78 \times 10^1$	$5.91 \times 10^1$
150		$1.48 \times 10^0$	$3.81 \times 10^1$	$4.02 \times 10^1$
160			$2.48 \times 10^1$	$2.67 \times 10^1$

Table A-34

## Lithium -- Thermal-Neutron Flux

z, Distance from Source (cm)	Thermal-Neutron Flux (neutrons/cm <sup>2</sup> /sec)						
	Lithium in Oil					Oil Only	
	1/2FC	3FC	<sup>8</sup> BF <sub>3</sub>	BF <sub>3</sub> (DB)	BF <sub>3</sub> (SB)	BF <sub>3</sub> (DB)	BF <sub>3</sub> (SB)
40	$3.01 \times 10^6$ $3.08 \times 10^5$	$2.96 \times 10^5$ $2.97 \times 10^4$ $4.51 \times 10^3$ $9.32 \times 10^2$ $2.39 \times 10^2$	$4.96 \times 10^3$ $9.61 \times 10^2$ $2.31 \times 10^2$ $6.40 \times 10^1$ $1.81 \times 10^0$ $5.45 \times 10^0$ $1.77 \times 10^0$				
50							
60							
70							
80							
90							
100							
110							
120							
130							
140							
150							
159							

Table A-35

Lithium -- Gamma-Ray Dose Rate

z, Distance from Source (cm)	Gamma-Ray Dose Rate (mr/hr)		
	Lithium in Oil, ASC	Oil Only	
		ASC	900IC
80			$1.34 \times 10^3$
90			$8.87 \times 10^2$
100			$5.91 \times 10^2$
110			$4.01 \times 10^2$
120	$2.98 \times 10^2$		$2.74 \times 10^2$
130	$2.10 \times 10^2$	$1.82 \times 10^2$	$1.89 \times 10^2$
140	$1.45 \times 10^2$	$1.30 \times 10^1$	$1.34 \times 10^1$
150	$1.04 \times 10^2$	$9.09 \times 10^1$	$9.48 \times 10^1$
158			$7.15 \times 10^1$
160	$7.37 \times 10^1$	$6.66 \times 10^1$	



Table A-36

Lithium Fluoride -- Thermal-Neutron Flux

z, Distance from Source (cm)	Thermal-Neutron Flux (neutrons/cm <sup>2</sup> /sec)			
	Lithium Fluoride			Water,
	1/2FC	3FC	BF <sub>3</sub> (SB)	BF <sub>3</sub> (SB)
40.3	5.40 x 10 <sup>6</sup>			
50	2.40 x 10 <sup>6</sup>	2.48 x 10 <sup>6</sup>		
60	2.40 x 10 <sup>5</sup>	2.80 x 10 <sup>5</sup>		
70		3.62 x 10 <sup>4</sup>		
80		6.35 x 10 <sup>3</sup>		
90		1.40 x 10 <sup>3</sup>	1.34 x 10 <sup>3</sup>	8.63 x 10 <sup>1</sup>
100			3.47 x 10 <sup>2</sup>	2.62 x 10 <sup>1</sup>
110			9.43 x 10 <sup>1</sup>	7.92 x 10 <sup>0</sup>
120			2.69 x 10 <sup>1</sup>	2.56 x 10 <sup>0</sup>
130			8.15 x 10 <sup>0</sup>	8.44 x 10 <sup>-1</sup>
140			2.55 x 10 <sup>0</sup>	3.01 x 10 <sup>-1</sup>
150			8.44 x 10 <sup>-1</sup>	1.00 x 10 <sup>-1</sup>
160			2.92 x 10 <sup>-1</sup>	

Table A-37

Lithium Fluoride -- Fast-Neutron Dose Rate

z, Distance from Source (cm)	Fast-Neutron Dose Rate (mrep/hr), HD	
	Lithium Fluoride	Water
41.7	$1.51 \times 10^3$	$7.50 \times 10^2$
45	$9.51 \times 10^2$	$5.04 \times 10^2$
50	$5.08 \times 10^2$	$2.74 \times 10^2$
60	$1.34 \times 10^2$	$7.55 \times 10^1$
70	$4.02 \times 10^1$	$2.19 \times 10^1$
80	$8.96 \times 10^0$	$7.00 \times 10^0$
90	$2.55 \times 10^0$	$2.26 \times 10^0$
100	$7.69 \times 10^{-1}$	$7.33 \times 10^{-1}$

Table A-38

Lithium Fluoride -- Gamma-Ray Dose Rate

z, Distance from Source (cm)	Gamma-Ray Dose Rate (mr/hr), 900IC	
	Lithium Fluoride	Water
70	$2.10 \times 10^3$	$1.35 \times 10^3$
80	$1.24 \times 10^3$	$8.20 \times 10^2$
90	$7.56 \times 10^2$	$5.10 \times 10^2$
100	$4.56 \times 10^2$	$3.15 \times 10^2$
110	$2.92 \times 10^2$	$2.05 \times 10^2$
120	$1.87 \times 10^2$	$1.25 \times 10^2$
130	$1.22 \times 10^2$	$8.30 \times 10^1$
140	$8.03 \times 10^1$	$5.30 \times 10^1$
150	$5.49 \times 10^1$	$3.55 \times 10^1$
160	$3.64 \times 10^1$	$2.35 \times 10^1$

Table A-39

Nickel -- Thermal-Neutron Flux

z, Distance from Source (cm)	Thermal-Neutron Flux (neutrons/cm <sup>2</sup> /sec)		
	3FC	BF <sub>3</sub> (SB)	BF <sub>3</sub> (DB)
30	1.601 x 10 <sup>6</sup>		
40	1.544 x 10 <sup>5</sup>		
50	1.506 x 10 <sup>4</sup>		
60	2.28 x 10 <sup>3</sup>		
70	4.78 x 10 <sup>2</sup>	5.08 x 10 <sup>2</sup>	4.43 x 10 <sup>2</sup>
80	1.099 x 10 <sup>2</sup>	1.214 x 10 <sup>2</sup>	1.103 x 10 <sup>2</sup>
90		3.14 x 10 <sup>1</sup>	3.02 x 10 <sup>1</sup>
100		8.95 x 10 <sup>0</sup>	8.75 x 10 <sup>0</sup>
110		2.72 x 10 <sup>0</sup>	2.73 x 10 <sup>0</sup>
120		8.70 x 10 <sup>-1</sup>	8.71 x 10 <sup>-1</sup>
130		2.92 x 10 <sup>-1</sup>	3.13 x 10 <sup>-1</sup>
140		1.002 x 10 <sup>-1</sup>	1.138 x 10 <sup>-1</sup>
150		3.70 x 10 <sup>-2</sup>	4.37 x 10 <sup>-2</sup>

Table A-40

Nickel -- Fast-Neutron Dose Rate

z, Distance from Source (cm)	Fast-Neutron Dose Rate (mrep/hr), HD
30	$5.34 \times 10^2$
40	$9.64 \times 10^1$
50	$2.14 \times 10^1$
60	$4.57 \times 10^0$
70	$1.213 \times 10^0$
80	$3.24 \times 10^{-1}$
90	$9.47 \times 10^{-2}$

Table A-41

Nickel -- Gamma-Ray Dose Rate

z, Distance from Source (cm)	Gamma-Ray Dose Rate (mr/hr)		
	90IC	900IC	ASC
23.2	$1.062 \times 10^4$		
30	$7.22 \times 10^3$		
40	$3.76 \times 10^3$	$3.78 \times 10^3$	
50	$2.09 \times 10^3$	$2.08 \times 10^3$	
60		$1.218 \times 10^3$	
70		$7.31 \times 10^2$	$7.42 \times 10^2$
80		$4.53 \times 10^2$	$4.61 \times 10^2$
90		$2.90 \times 10^2$	$2.95 \times 10^2$
100		$1.880 \times 10^2$	$1.908 \times 10^2$
110		$1.258 \times 10^2$	$1.262 \times 10^2$
120		$8.46 \times 10^1$	$8.58 \times 10^1$
130		$5.85 \times 10^1$	$5.78 \times 10^1$
140			$4.02 \times 10^1$
150			$2.83 \times 10^1$
160			$2.01 \times 10^1$

Table A-42

Oil -- Thermal-Neutron Flux

z, Distance from Source (cm)	Thermal-Neutron Flux (neutrons/cm <sup>2</sup> /sec)					
	Oil				Water	
	3FC		BF <sub>3</sub> (SB)			
	Run 1	Run 2	Run 1	Run 2	3FC	BF <sub>3</sub> (SB)
40					1.02 x 10 <sup>5</sup>	
40.6		4.04 x 10 <sup>4</sup>				
40.8	3.44 x 10 <sup>4</sup>					
44	2.54 x 10 <sup>4</sup>	2.86 x 10 <sup>4</sup>				
50	1.116 x 10 <sup>4</sup>	1.289 x 10 <sup>4</sup>			2.06 x 10 <sup>4</sup>	
60	2.91 x 10 <sup>3</sup>	3.35 x 10 <sup>3</sup>			4.68 x 10 <sup>3</sup>	
70	7.78 x 10 <sup>2</sup>	8.88 x 10 <sup>2</sup>	7.79 x 10 <sup>2</sup>	7.96 x 10 <sup>2</sup>	1.193 x 10 <sup>3</sup>	1.07 x 10 <sup>3</sup>
80	2.51 x 10 <sup>2</sup>		2.25 x 10 <sup>2</sup>	2.29 x 10 <sup>2</sup>	3.14 x 10 <sup>2</sup>	3.09 x 10 <sup>2</sup>
90			6.59 x 10 <sup>1</sup>	6.73 x 10 <sup>1</sup>	8.58 x 10 <sup>1</sup>	8.80 x 10 <sup>1</sup>
100			2.01 x 10 <sup>1</sup>	2.03 x 10 <sup>1</sup>	3.06 x 10 <sup>1</sup>	2.64 x 10 <sup>1</sup>
110			6.24 x 10 <sup>0</sup>	6.27 x 10 <sup>0</sup>		7.84 x 10 <sup>0</sup>
120			1.967 x 10 <sup>0</sup>	2.03 x 10 <sup>0</sup>		2.59 x 10 <sup>0</sup>
130			6.82 x 10 <sup>-1</sup>	6.57 x 10 <sup>-1</sup>		8.77 x 10 <sup>-1</sup>
140			2.28 x 10 <sup>-1</sup>			

Table A-43

Oil -- Fast-Neutron Dose Rate

z, Distance from Source (cm)	Fast-Neutron Dose Rate (mrep/hr), HD				
	Oil			Water	
	Run 1	Run 2	Run 3	Run 1	Run 2
30				$6.69 \times 10^2$	$6.51 \times 10^2$
40	$1.08 \times 10^2$		$1.038 \times 10^2$	$1.76 \times 10^2$	$1.722 \times 10^2$
40.2		$1.128 \times 10^2$			
50	$3.07 \times 10^1$	$3.84 \times 10^1$	$3.45 \times 10^1$	$5.53 \times 10^1$	$5.58 \times 10^1$
		$3.90 \times 10^1$			
60	$7.88 \times 10^0$	$8.60 \times 10^0$	$7.97 \times 10^0$	$9.31 \times 10^0$	$1.113 \times 10^1$
70	$2.29 \times 10^0$	$2.48 \times 10^0$	$2.27 \times 10^0$	$3.56 \times 10^0$	$3.12 \times 10^0$
80	$6.65 \times 10^{-1}$	$7.94 \times 10^{-1}$		$1.109 \times 10^1$	$9.14 \times 10^{-1}$
90		$2.94 \times 10^{-1}$			

Table A-44

Oil -- Gamma-Ray Dose Rate

z, Distance from Source (cm)	Gamma-Ray Dose Rate (mr/hr)				
	Oil			Water	
	900IC	ASC	900IC	ASC	900IC
60	$3.23 \times 10^3$				$2.43 \times 10^3$
70	$1.968 \times 10^3$				$1.440 \times 10^3$
80	$1.214 \times 10^2$		$1.158 \times 10^3$		$8.63 \times 10^2$
90	$7.72 \times 10^2$		$7.28 \times 10^2$		$5.24 \times 10^2$
100	$4.95 \times 10^2$	$4.57 \times 10^2$	$4.69 \times 10^2$	$3.36 \times 10^2$	$3.30 \times 10^2$
110	$3.18 \times 10^2$	$2.92 \times 10^2$	$3.01 \times 10^2$	$2.09 \times 10^2$	$2.06 \times 10^2$
120	$2.98 \times 10^2$	$1.880 \times 10^2$	$1.994 \times 10^2$	$1.344 \times 10^2$	$1.335 \times 10^2$
130	$1.388 \times 10^2$	$1.246 \times 10^2$	$1.319 \times 10^2$		$8.45 \times 10^1$
140	$9.46 \times 10^1$	$8.53 \times 10^1$	$8.96 \times 10^1$		
150	$6.30 \times 10^1$	$5.79 \times 10^1$	$6.07 \times 10^1$		
160	$4.55 \times 10^1$	$3.89 \times 10^1$	$4.16 \times 10^1$		

Table A-45

Paraffin -- Thermal-Neutron Flux

z, Distance from Source (cm)	Thermal-Neutron Flux (neutrons/cm <sup>2</sup> /sec)		
	Paraffin		Water, BF <sub>3</sub> (DB)
	3FC	BF <sub>3</sub> (DB)	
22.1	1.030 x 10 <sup>6</sup>		
26	5.57 x 10 <sup>5</sup>		
30	2.79 x 10 <sup>5</sup>		
40	5.43 x 10 <sup>4</sup>		
50	1.190 x 10 <sup>4</sup>		
60	2.92 x 10 <sup>3</sup>		
70	7.70 x 10 <sup>2</sup>	7.31 x 10 <sup>2</sup>	
80	2.16 x 10 <sup>2</sup>	2.19 x 10 <sup>2</sup>	3.14 x 10 <sup>2</sup>
90		6.49 x 10 <sup>1</sup>	9.23 x 10 <sup>1</sup>
100		2.00 x 10 <sup>1</sup>	2.79 x 10 <sup>1</sup>
110		6.46 x 10 <sup>0</sup>	8.77 x 10 <sup>0</sup>
120		2.17 x 10 <sup>0</sup>	2.88 x 10 <sup>0</sup>
130		7.21 x 10 <sup>-1</sup>	9.42 x 10 <sup>-1</sup>



Table A-46

Paraffin -- Fast-Neutron Dose Rate

z, Distance from Source (cm)	Fast-Neutron Dose Rate (mrep/hr), HD
21.7	$5.22 \times 10^2$
30	$2.16 \times 10^2$
40	$8.16 \times 10^1$
50	$2.26 \times 10^1$
60	$6.40 \times 10^0$
70	$2.03 \times 10^0$
80	$6.38 \times 10^{-1}$
90	$2.10 \times 10^{-1}$
100	$6.99 \times 10^{-2}$

Table A-47

Paraffin -- Gamma-Ray Dose Rate

z, Distance from Source (cm)	Gamma-Ray Dose Rate (mr/hr), 900IC	
	Paraffin	Water
60	$2.50 \times 10^3$	
70	$1.498 \times 10^3$	
80	$8.88 \times 10^2$	$9.01 \times 10^2$
90	$5.53 \times 10^2$	$5.59 \times 10^2$
100	$3.79 \times 10^2$	$3.56 \times 10^2$
	$3.52 \times 10^2$	
110	$2.20 \times 10^2$	$2.13 \times 10^2$
120	$1.409 \times 10^2$	$1.400 \times 10^2$
130	$9.07 \times 10^1$	$8.99 \times 10^1$
140	$6.05 \times 10^1$	$6.07 \times 10^1$
150	$3.94 \times 10^1$	$3.90 \times 10^1$
160	$2.80 \times 10^1$	$2.66 \times 10^1$

Table A-48

Perfluoroheptane -- Thermal-Neutron Flux

z, Distance from Source (cm)	Thermal-Neutron Flux (neutrons/cm <sup>2</sup> /sec)			
	Perfluoroheptane		Water	
	<sup>3</sup> FC	BF <sub>3</sub> (SB)	<sup>3</sup> FC	BF <sub>3</sub> (SB)
30			5.667 x 10 <sup>5</sup>	
40			1.041 x 10 <sup>5</sup>	
50	1.57 x 10 <sup>6</sup>		2.111 x 10 <sup>4</sup>	
55	4.74 x 10 <sup>5</sup>			
60	1.19 x 10 <sup>5</sup>		4.866 x 10 <sup>3</sup>	
65	3.64 x 10 <sup>4</sup>			
70	1.23 x 10 <sup>4</sup>		1.191 x 10 <sup>3</sup>	9.792 x 10 <sup>2</sup>
80	2.21 x 10 <sup>3</sup>		3.274 x 10 <sup>2</sup>	3.064 x 10 <sup>2</sup>
90	5.10 x 10 <sup>2</sup>	4.79 x 10 <sup>2</sup>		8.950 x 10 <sup>1</sup>
100	1.487 x 10 <sup>2</sup>	1.24 x 10 <sup>2</sup>		2.613 x 10 <sup>1</sup>
110		3.27 x 10 <sup>1</sup>		8.182 x 10 <sup>0</sup>
120		9.27 x 10 <sup>0</sup>		2.612 x 10 <sup>0</sup>
130		2.80 x 10 <sup>0</sup>		8.247 x 10 <sup>-1</sup>
140		9.13 x 10 <sup>-1</sup>		2.830 x 10 <sup>-1</sup>
150		2.77 x 10 <sup>-1</sup>		9.431 x 10 <sup>-2</sup>
160		9.48 x 10 <sup>-2</sup>		3.411 x 10 <sup>-2</sup>

Table A-49

Perfluoroheptane -- Fast-Neutron Dose Rate

z, Distance from Source (cm)	Fast-Neutron Dose Rate (mrep/hr), HD
70	$2.530 \times 10^1$
80	$5.73 \times 10^0$
90	$1.44 \times 10^0$
100	$4.13 \times 10^{-1}$
110	$1.228 \times 10^{-1}$

Table A-50

Perfluoroheptane -- Gamma-Ray Dose Rate

z, Distance from Source (cm)	Gamma-Ray Dose Rate (mr/hr)	
	Perfluoroheptane	Water
60	$4.14 \times 10^3$	$2.274 \times 10^3$
70	$2.36 \times 10^3$	$1.361 \times 10^3$
80	$1.42 \times 10^3$	$8.256 \times 10^2$
90	$8.81 \times 10^2$	$5.115 \times 10^2$
100	$5.55 \times 10^2$	$3.162 \times 10^2$
110	$3.60 \times 10^2$	$1.987 \times 10^2$
120	$2.38 \times 10^2$	$1.254 \times 10^2$
130	$1.581 \times 10^2$	$8.341 \times 10^1$
140	$1.08 \times 10^2$	$5.39 \times 10^1$
150	$7.42 \times 10^1$	$3.670 \times 10^1$
160	$5.16 \times 10^1$	$2.488 \times 10^1$

Table A-51

Tungsten -- Thermal-Neutron Flux

z, Distance from Source (cm)	Thermal-Neutron Flux (neutrons/cm <sup>2</sup> /sec)					
	Tungsten			Plastic <sup>a</sup>		
	1/2FC	3FC	BF <sub>3</sub> (SB)	1/2FC	3FC	BF <sub>3</sub> (SB)
10				1.40 x 10 <sup>7</sup>		
11.3	4.70 x 10 <sup>6</sup>					
12	6.61 x 10 <sup>6</sup>			1.09 x 10 <sup>7</sup>		
14	7.08 x 10 <sup>6</sup>					
16	6.97 x 10 <sup>6</sup>					
18	4.38 x 10 <sup>6</sup>					
20	3.16 x 10 <sup>5</sup>			2.67 x 10 <sup>6</sup>		
30	4.34 x 10 <sup>5</sup>	4.50 x 10 <sup>5</sup>		4.46 x 10 <sup>5</sup>	4.86 x 10 <sup>5</sup>	
40		7.96 x 10 <sup>4</sup>			9.11 x 10 <sup>4</sup>	
50		1.64 x 10 <sup>4</sup>			1.79 x 10 <sup>4</sup>	
60		3.68 x 10 <sup>3</sup>			4.22 x 10 <sup>3</sup>	
70		9.35 x 10 <sup>2</sup>	8.60 x 10 <sup>2</sup>		1.05 x 10 <sup>3</sup>	9.79 x 10 <sup>2</sup>
			8.68 x 10 <sup>2</sup>			
80		2.46 x 10 <sup>2</sup>	2.30 x 10 <sup>2</sup>			2.75 x 10 <sup>2</sup>
			2.34 x 10 <sup>2</sup>			
90			6.33 x 10 <sup>1</sup>			7.80 x 10 <sup>1</sup>
			6.53 x 10 <sup>1</sup>			
100			1.83 x 10 <sup>1</sup>			2.56 x 10 <sup>1</sup>
			1.88 x 10 <sup>1</sup>			
110			5.69 x 10 <sup>0</sup>			7.12 x 10 <sup>0</sup>
			5.81 x 10 <sup>0</sup>			
120			1.78 x 10 <sup>0</sup>			2.29 x 10 <sup>0</sup>
			1.82 x 10 <sup>0</sup>			
130			5.81 x 10 <sup>-1</sup>			7.68 x 10 <sup>-1</sup>
			6.17 x 10 <sup>-1</sup>			

a See Table 1, p. 7.

Table A-52

Tungsten -- Fast-Neutron Dose Rate

z, Distance from Source (cm)	Fast-Neutron Dose Rate (mrep/hr), HD	
	Tungsten	Water
20	$9.50 \times 10^2$	$6.37 \times 10^2$
30	$3.28 \times 10^2$	$2.34 \times 10^2$
40	$1.05 \times 10^2$	$8.84 \times 10^1$
50	$2.99 \times 10^1$	$2.72 \times 10^1$
60	$7.28 \times 10^0$	$7.20 \times 10^0$
70	$2.16 \times 10^0$	$2.32 \times 10^0$
80	$4.73 \times 10^{-1}$	$7.23 \times 10^{-1}$
90		$2.28 \times 10^{-1}$

Table A-53

Tungsten -- Gamma-Ray Dose Rate

z, Distance from Source (cm)	Gamma-Ray Dose Rate (mr/hr), 900 IC	
	Tungsten	Water
40	$3.49 \times 10^3$	
50	$2.09 \times 10^3$	
60	$1.25 \times 10^3$	$2.40 \times 10^3$
70	$7.73 \times 10^2$	$1.38 \times 10^3$
80	$4.85 \times 10^2$	$8.22 \times 10^2$
90	$3.10 \times 10^2$	$5.01 \times 10^2$
100	$2.01 \times 10^2$	$3.26 \times 10^2$
110	$1.30 \times 10^2$	$2.04 \times 10^2$
120	$8.84 \times 10^1$	$1.28 \times 10^2$
130		$8.39 \times 10^1$

Table A-54

Uranium -- Thermal-Neutron Flux

z, Distance from Source (cm)	Thermal-Neutron Flux (neutrons/cm <sup>2</sup> /sec)		
	Uranium		Water
	3FC	BF <sub>3</sub> (SB)	
46	2.13 x 10 <sup>4</sup>		
47	2.43 x 10 <sup>4</sup>		
48	2.47 x 10 <sup>4</sup>		
50	2.17 x 10 <sup>4</sup>		2.07 x 10 <sup>4</sup>
60	4.16 x 10 <sup>3</sup>		4.70 x 10 <sup>3</sup>
70	8.47 x 10 <sup>2</sup>	8.31 x 10 <sup>2</sup>	1.15 x 10 <sup>3</sup>
80	2.13 x 10 <sup>2</sup>	2.14 x 10 <sup>2</sup>	3.10 x 10 <sup>2</sup>
90		5.67 x 10 <sup>1</sup>	8.80 x 10 <sup>1</sup>
100		1.58 x 10 <sup>1</sup>	2.60 x 10 <sup>1</sup>
110		4.72 x 10 <sup>0</sup>	8.00 x 10 <sup>0</sup>
120		1.46 x 10 <sup>0</sup>	2.50 x 10 <sup>0</sup>
130		4.66 x 10 <sup>-1</sup>	8.00 x 10 <sup>-1</sup>
140		1.61 x 10 <sup>-1</sup>	2.60 x 10 <sup>-1</sup>

Table A-55

Uranium -- Gamma-Ray Dose Rate

z, Distance from Source (cm)	Gamma-Ray Dose Rate (mr/hr)	
	ASC	900IC
50		$5.53 \times 10^1$
60		$2.99 \times 10^1$
70		$1.69 \times 10^1$
80	$1.03 \times 10^1$	
90	$6.78 \times 10^0$	
100	$4.79 \times 10^0$	
110	$3.60 \times 10^0$	
120	$2.71 \times 10^0$	
130	$2.23 \times 10^0$	
140	$1.66 \times 10^0$	
150	$1.34 \times 10^0$	
160	$1.12 \times 10^0$	

## Appendix B

### VALUES OF THE SOURCE GEOMETRIC CORRECTION FACTOR F

As  $z$ , the distance from the source, becomes small it is necessary to rely more heavily on source geometric corrections. In order to facilitate the use of fast-neutron data close to the source, computations have been made of a correction factor  $F$ , which is defined as:

$$F = \frac{\left(\frac{z+t}{z}\right) \left\{ \left(\frac{z^2}{z^2 + a^2}\right) e^{(z/\lambda) \left[1 - \sqrt{1 + (a/z)^2}\right]} - 1 \right\}}{\left(\frac{z+t}{z + \lambda \Sigma t} - \frac{a^2}{(z+t)^2 + a^2}\right) e^{\left(\frac{z + \lambda \Sigma t}{\lambda}\right) \left[1 - \sqrt{1 + \left(\frac{a}{z+t}\right)^2}\right]} - \frac{z+t}{z + \lambda \Sigma t}}$$

where

$t$  = thickness of the sample,

$a$  = radius of the circular source,

$\lambda$  = relaxation length in water,

$\Sigma$  = macroscopic removal cross section.

$F$  has been computed for  $\lambda \Sigma = 0.7, 1.0$ , and  $1.3$  and for various values of  $t$ ,  $\lambda$ , and  $z + t$ . The results of these computations are presented in Figs. B-1 through B-15 and Tables B-1 through B-3.



-128-

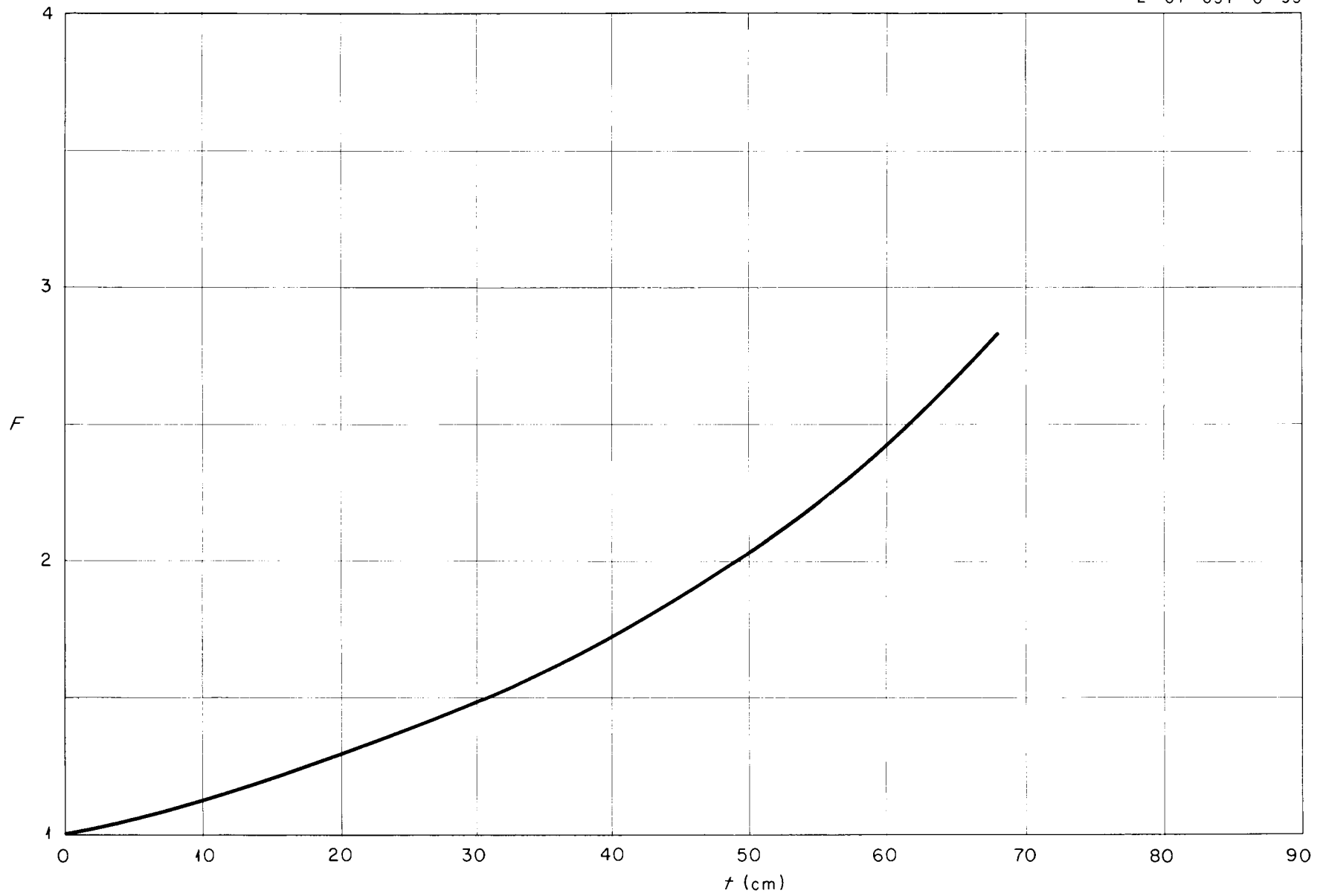


Fig.B-1. Geometric Correction Factor  $F$  vs.  $t$  for  $\lambda \Sigma = 0.7$ ,  $\lambda = 10$  cm, and  $z+t = 150$  cm

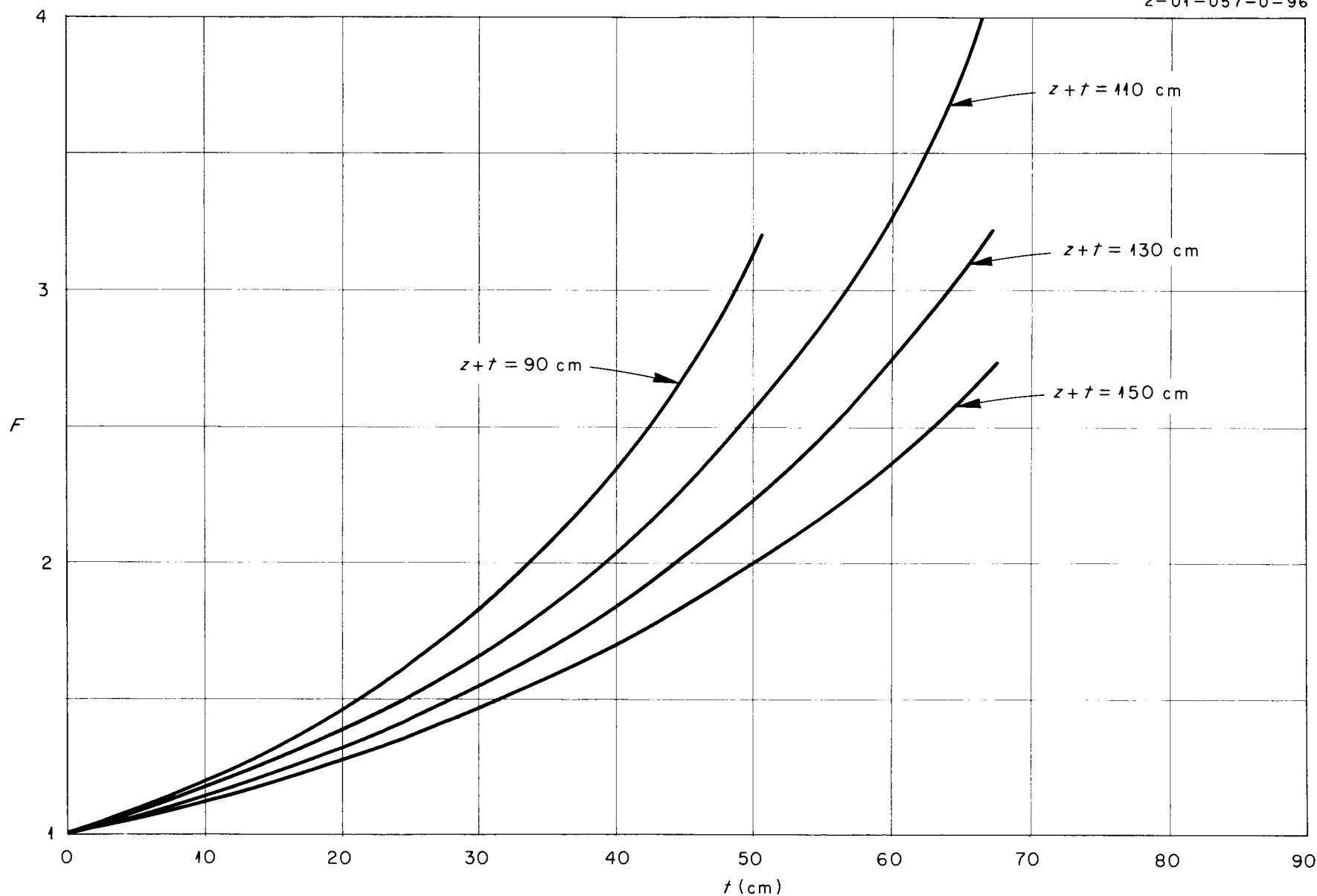


Fig. B-2. Geometric Correction Factor  $F$  vs.  $t$  for  $\lambda \Sigma = 0.7$ ,  $\lambda = 9$  cm, and  $z+t = 90, 110, 130$ , and  $150$  cm

-130-

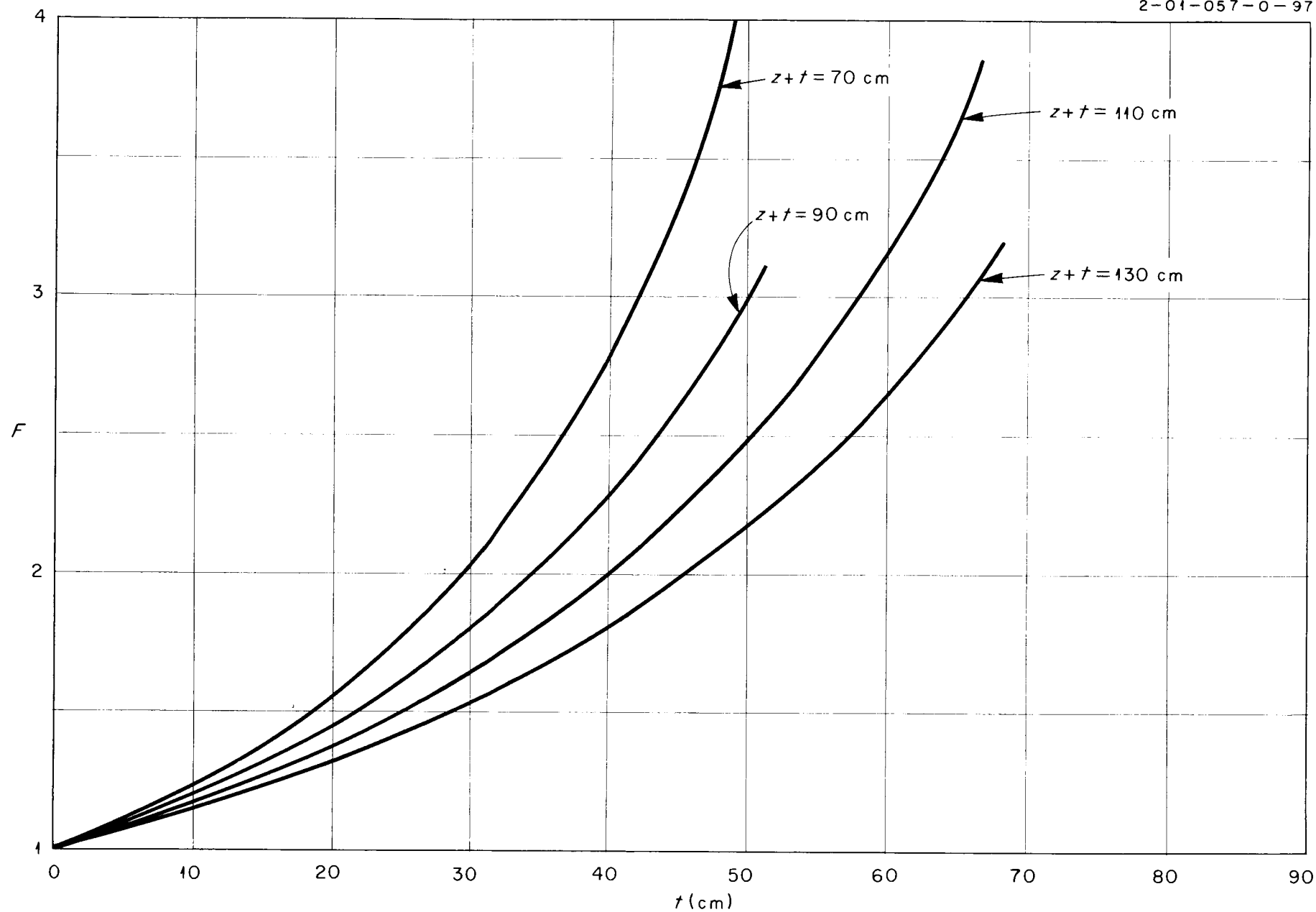


Fig. B-3. Geometric Correction Factor  $F$  vs.  $t$  for  $\lambda \Sigma = 0.7$ ,  $\lambda = 8$  cm, and  $z+t = 70, 90, 110$ , and  $130$  cm

-131-

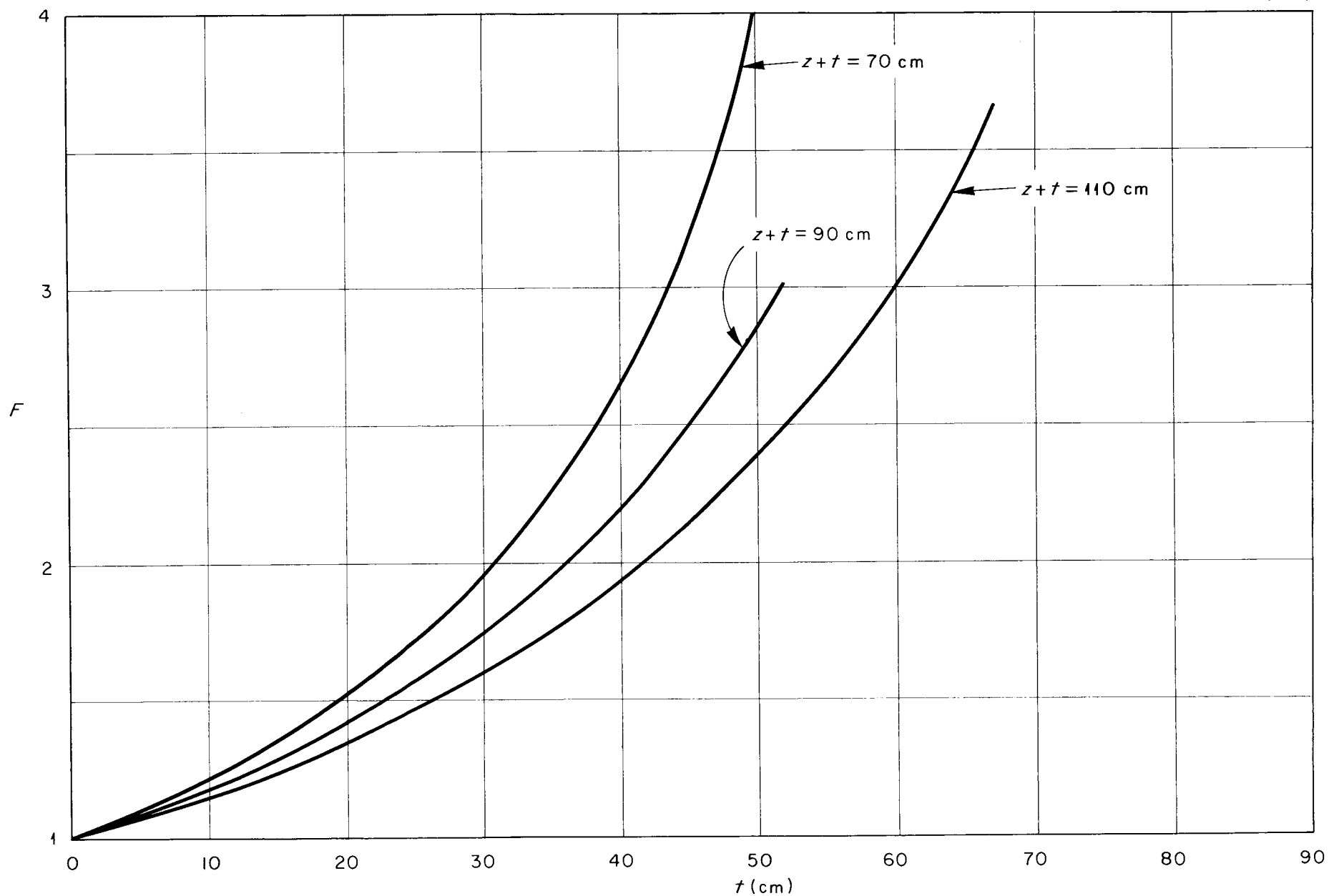


Fig. B-4. Geometric Correction Factor  $F$  vs.  $t$  for  $\lambda \Sigma = 0.7$ ,  $\lambda = 7$  cm, and  $z+t = 70, 90$ , and  $110$  cm

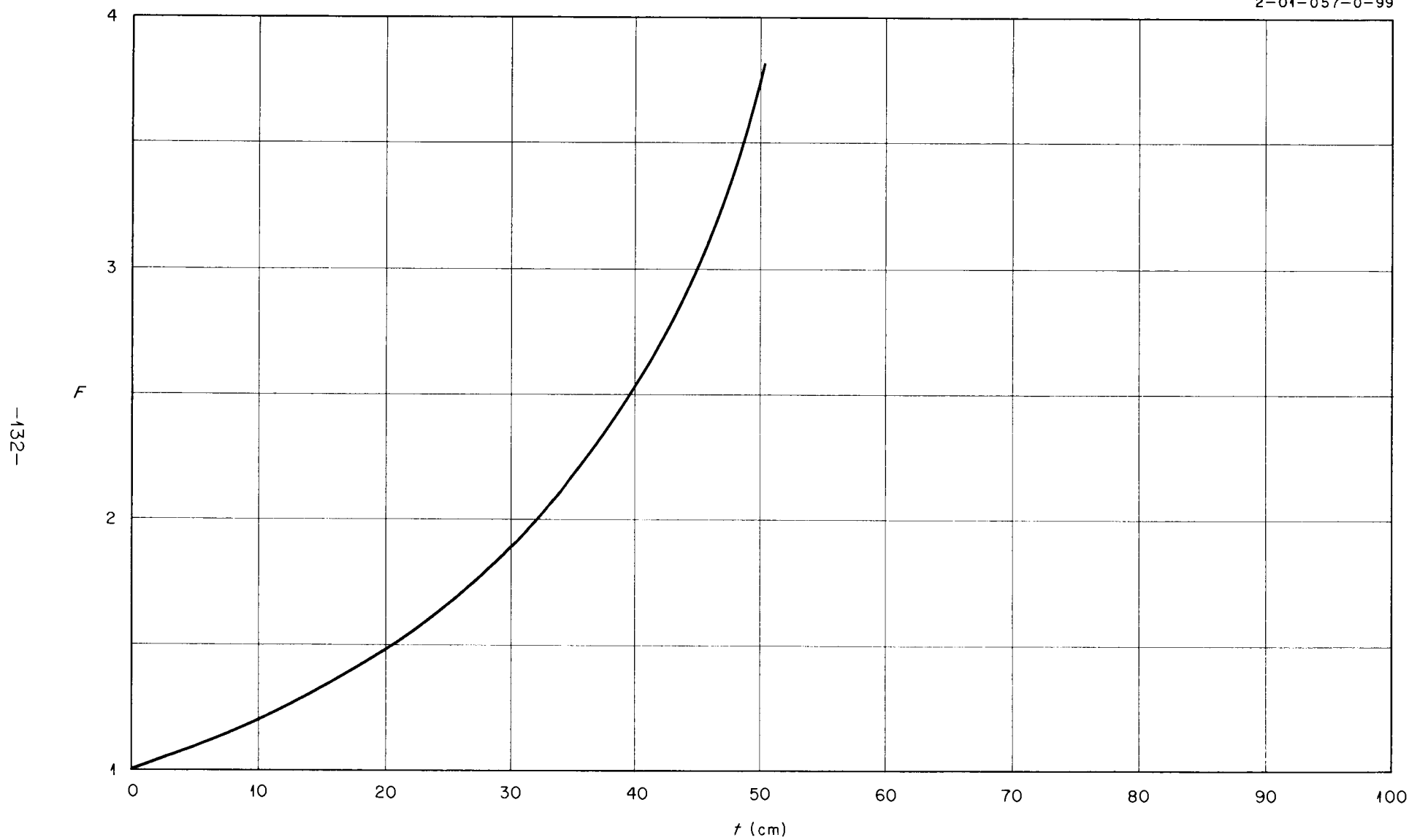


Fig. B-5. Geometric Correction Factor  $F$  vs  $t$  for  $\lambda \Sigma = 0.7$ ,  $\lambda = 6$  cm, and  $z + t = 70$  cm.

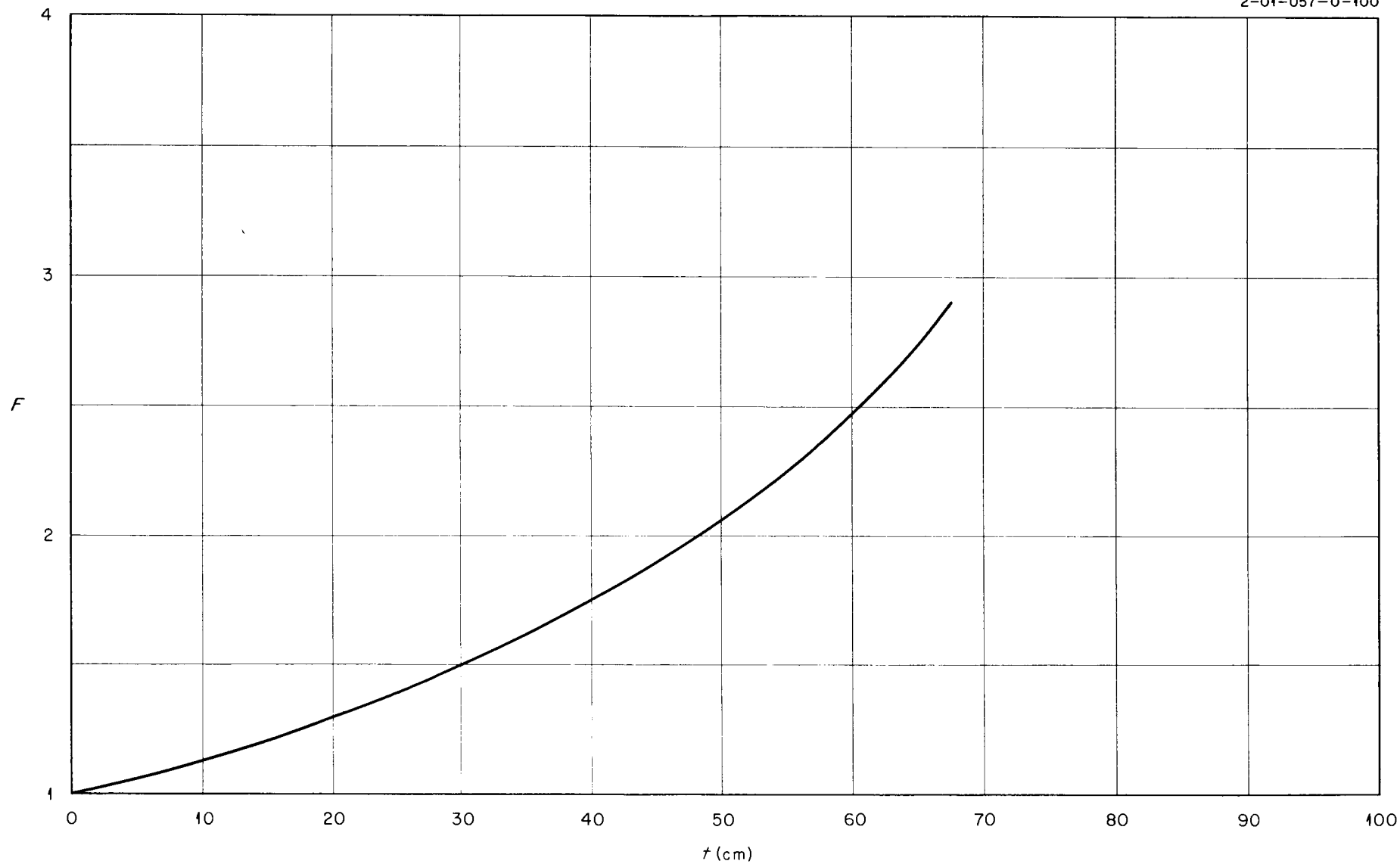


Fig. B-6. Geometric Correction Factor  $F$  vs  $t$  for  $\lambda \Sigma = 1$ ,  $\lambda = 10$  cm, and  $z + t = 150$  cm.

-134-

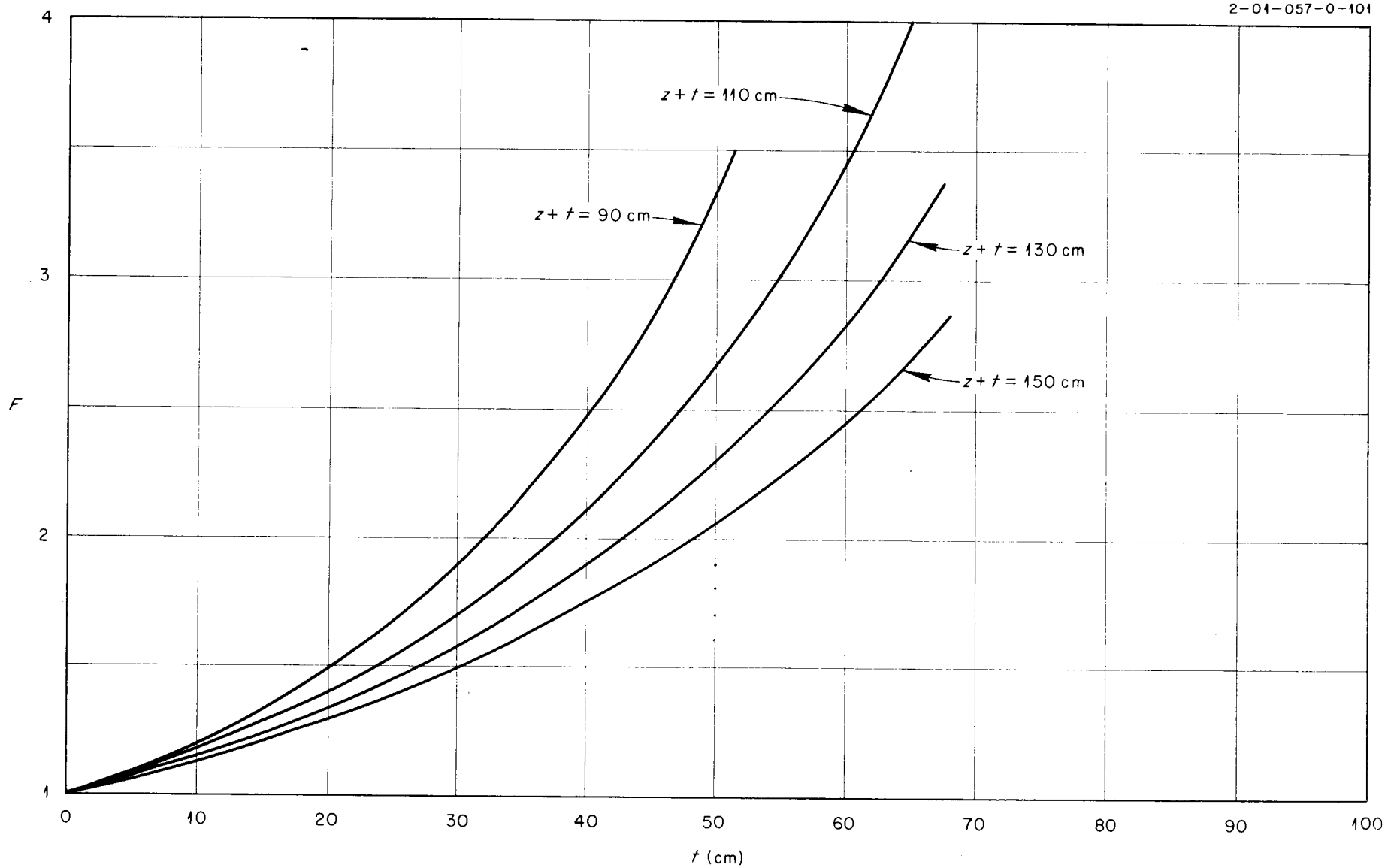


Fig. B-7. Geometric Correction Factor  $F$  vs  $t$  for  $\lambda \Sigma = 1$ ,  $\lambda = 9$  cm, and  $z+t = 90, 110, 130$ , and  $150$  cm.

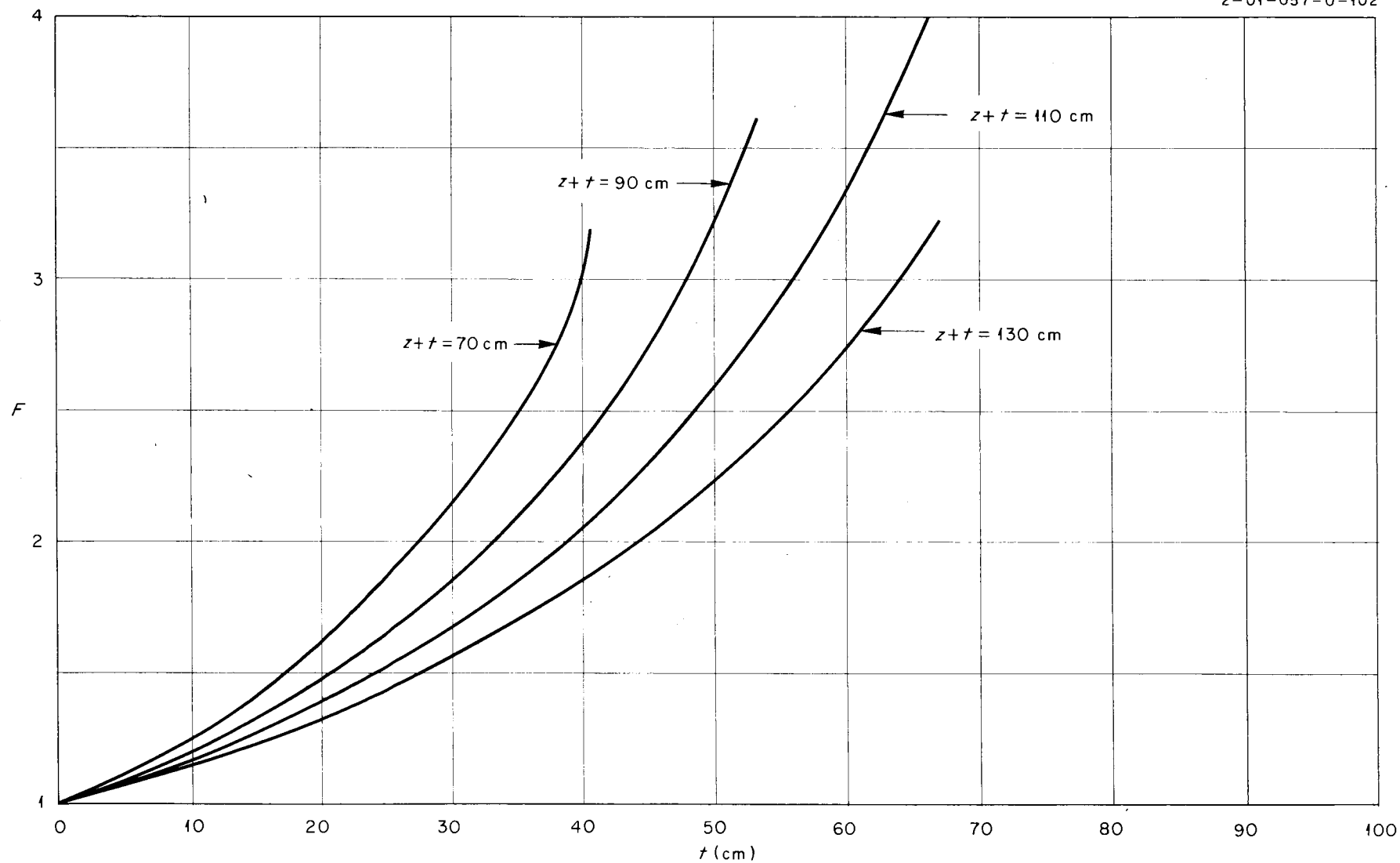


Fig. B-8. Geometric Correction Factor  $F$  vs.  $t$  for  $\lambda \Sigma = 1$ ,  $\lambda = 8$  cm, and  $z+t = 70, 90, 110$ , and  $130$  cm



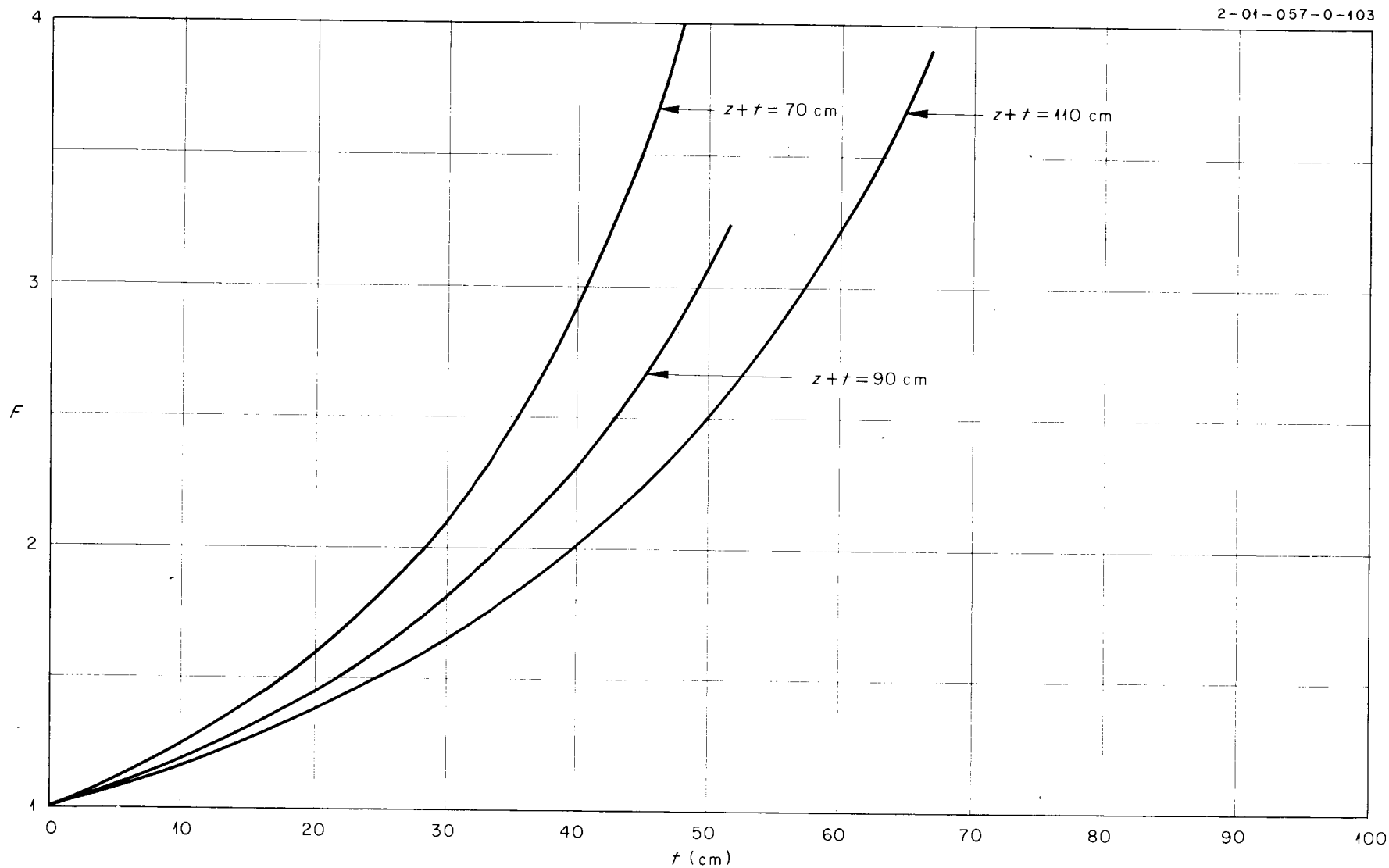


Fig. B-9. Geometric Correction Factor  $F$  vs.  $t$  for  $\lambda \Sigma = 1$ ,  $\lambda = 7$  cm, and  $z + t = 70, 90$ , and  $110$  cm

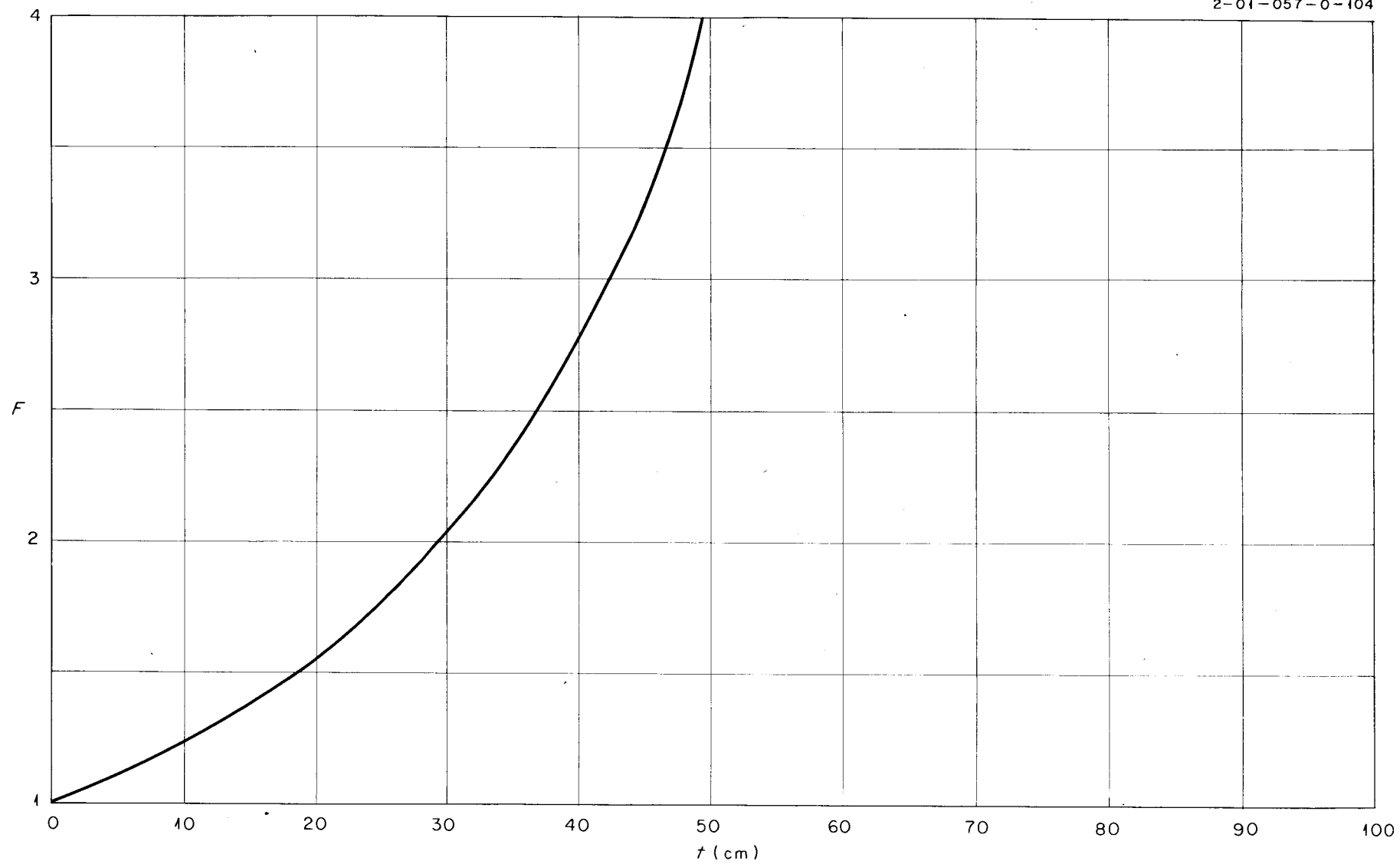


Fig. B-10. Geometric Correction Factor  $F$  vs.  $t$  for  $\lambda\Sigma=1$ ,  $\lambda=6$  cm, and  $z+t=70$  cm

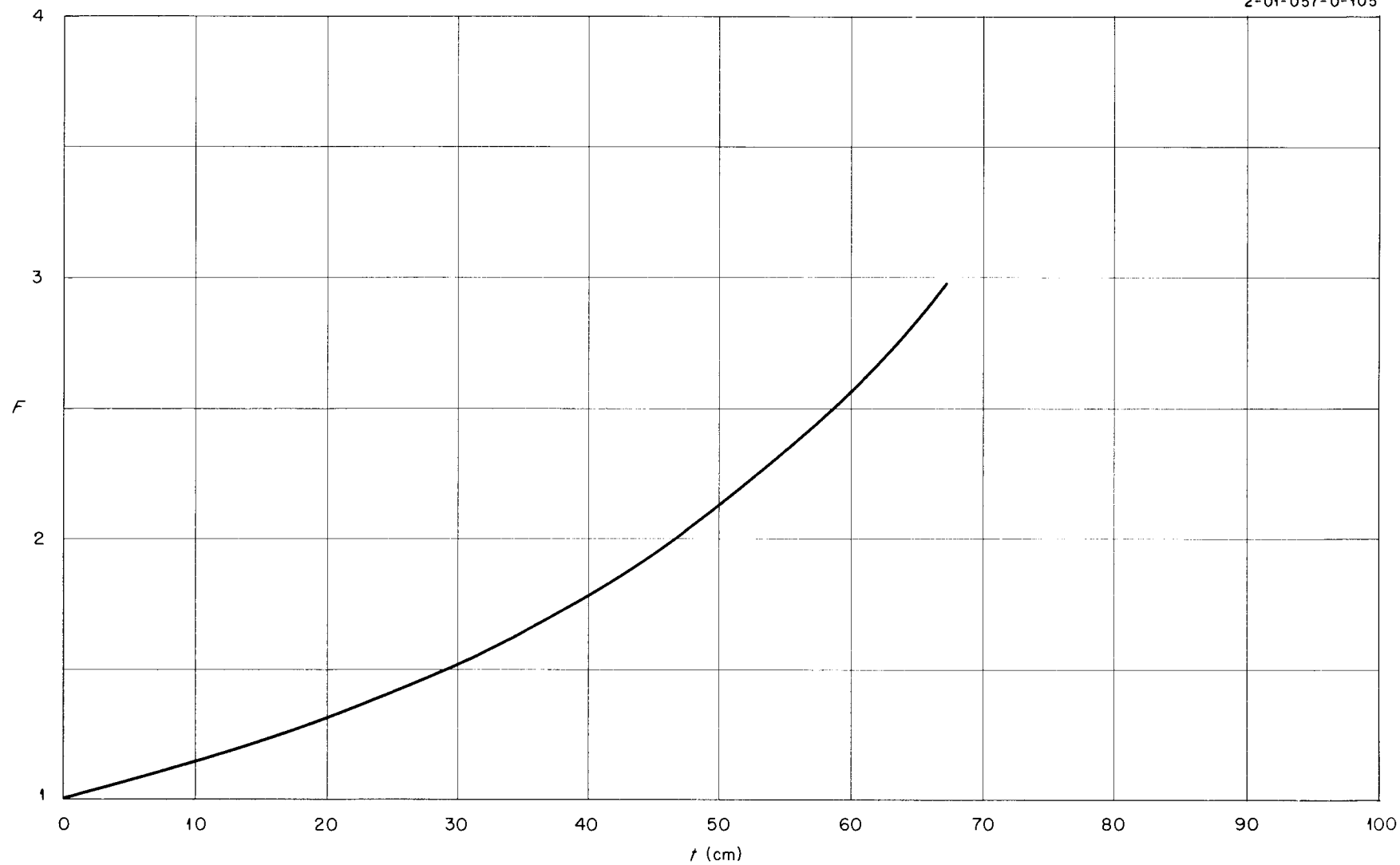


Fig. B-11. Geometric Correction Factor  $F$  vs.  $t$  for  $\lambda \Sigma = 1.3$ ,  $\lambda = 10$  cm and  $z + t = 150$  cm.

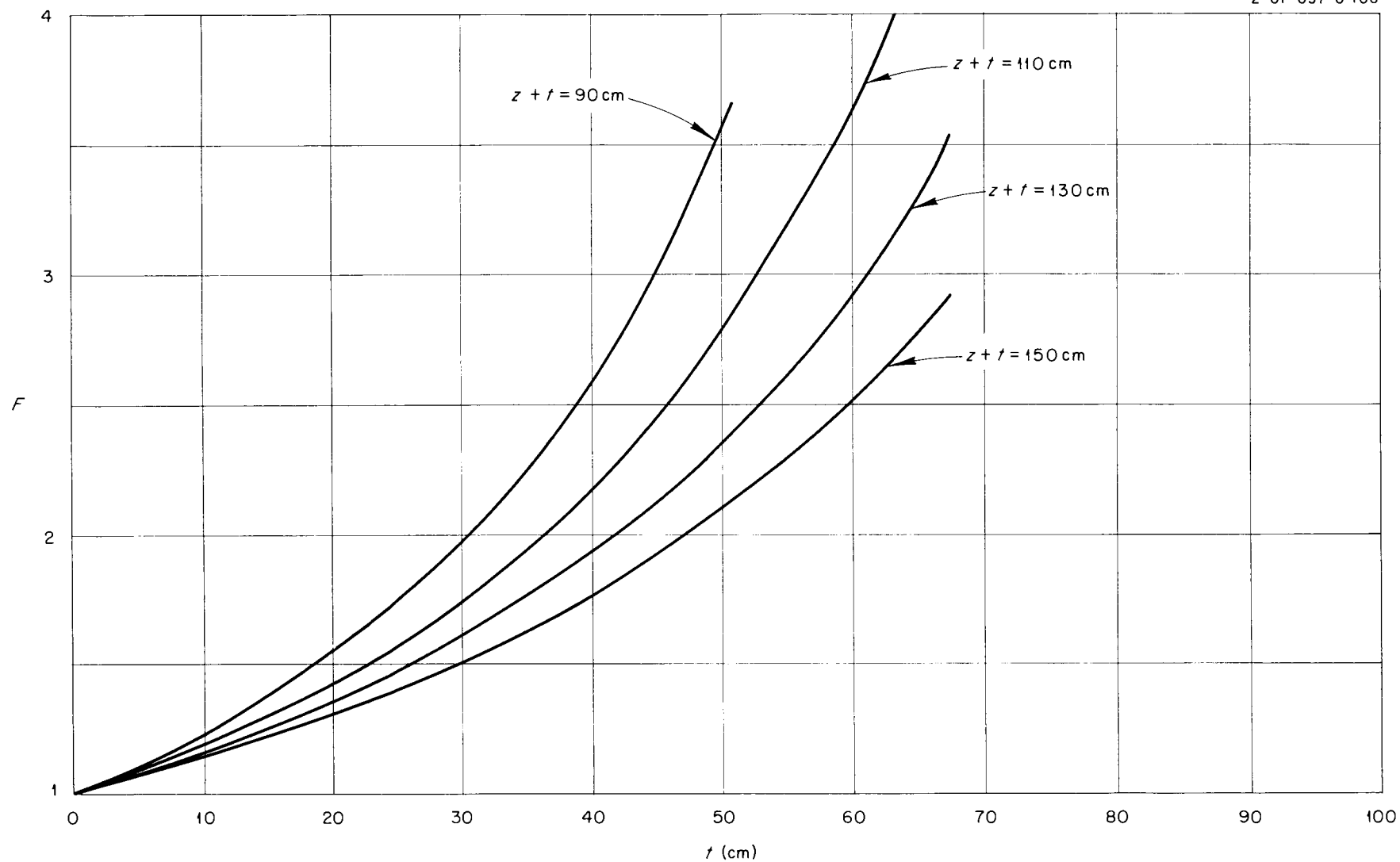


Fig. B-12. Geometric Correction Factor  $F$  vs.  $t$  for  $\lambda \Sigma = 1.3$ ,  $\lambda = 9$  cm, and  $z + t = 90, 110, 130$  and  $150$  cm.

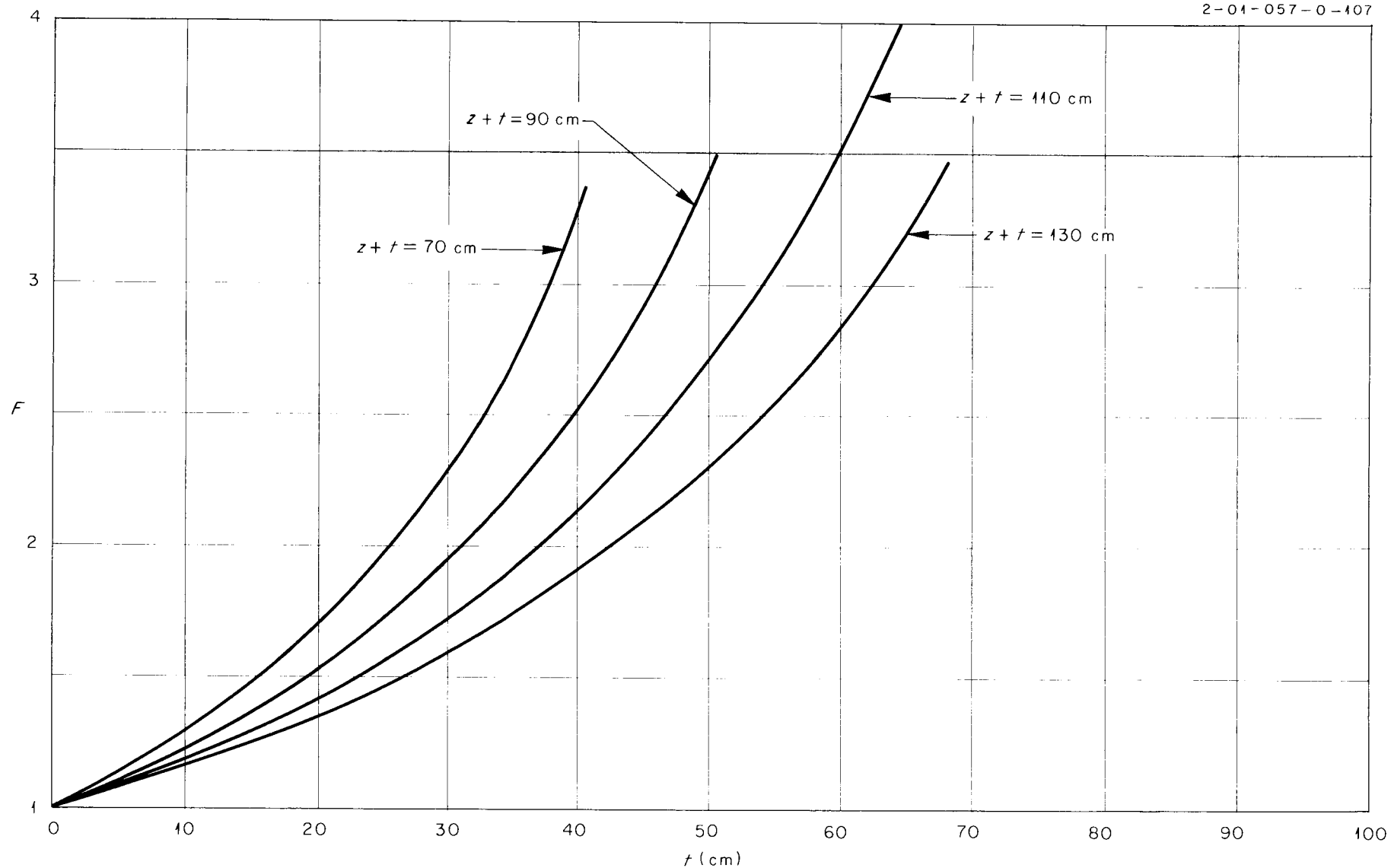


Fig. B-13. Geometric Correction Factor  $F$  vs.  $t$  for  $\lambda\Sigma=1.3$ ,  $\lambda=8$  cm, and  $z+t=70, 90, 110$ , and  $130$  cm

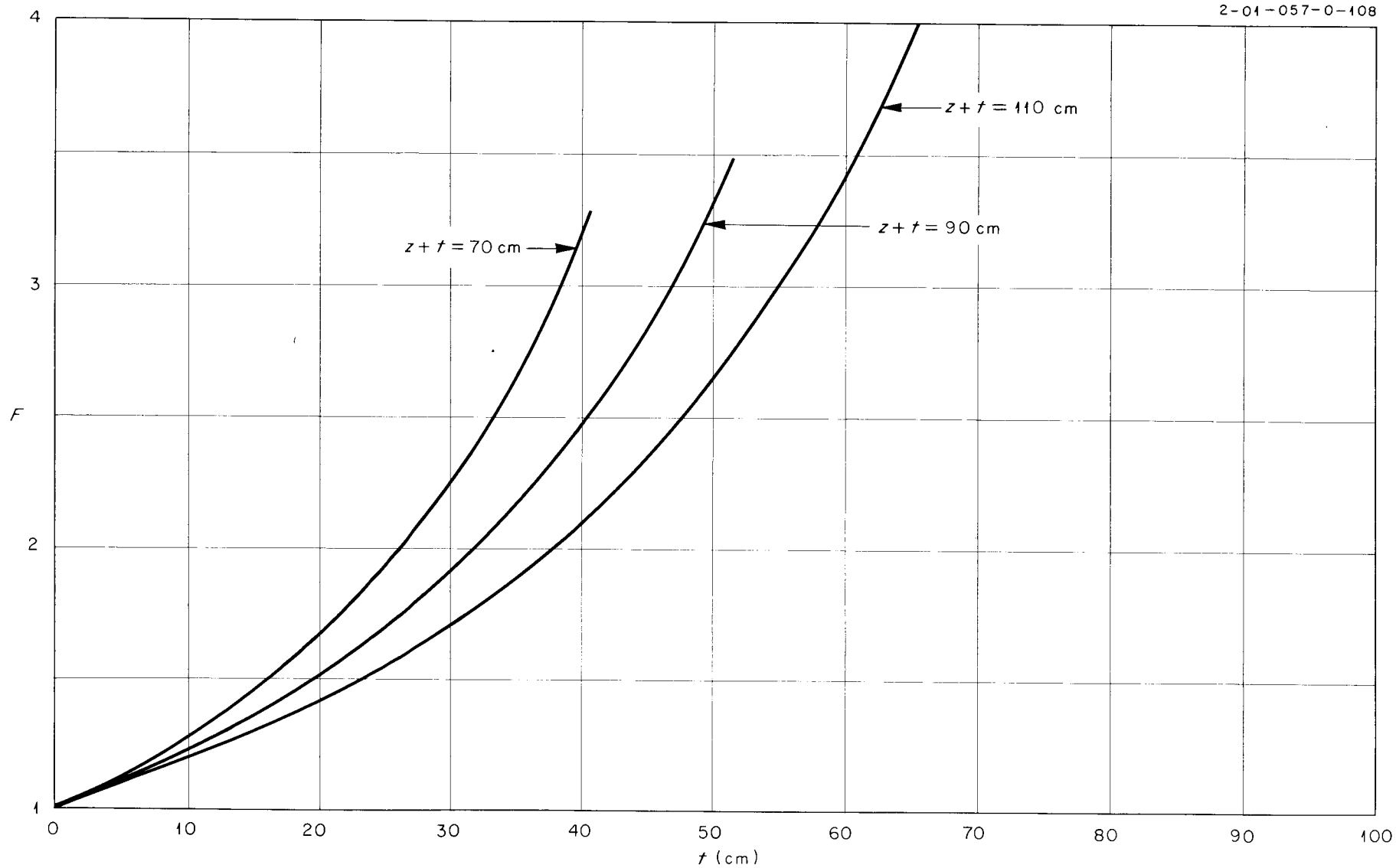


Fig. B-14. Geometric Correction Factor  $F$  vs.  $t$  for  $\lambda \Sigma = 1.3$ ,  $\lambda = 7$  cm, and  $z + t = 70, 90$ , and  $110$  cm

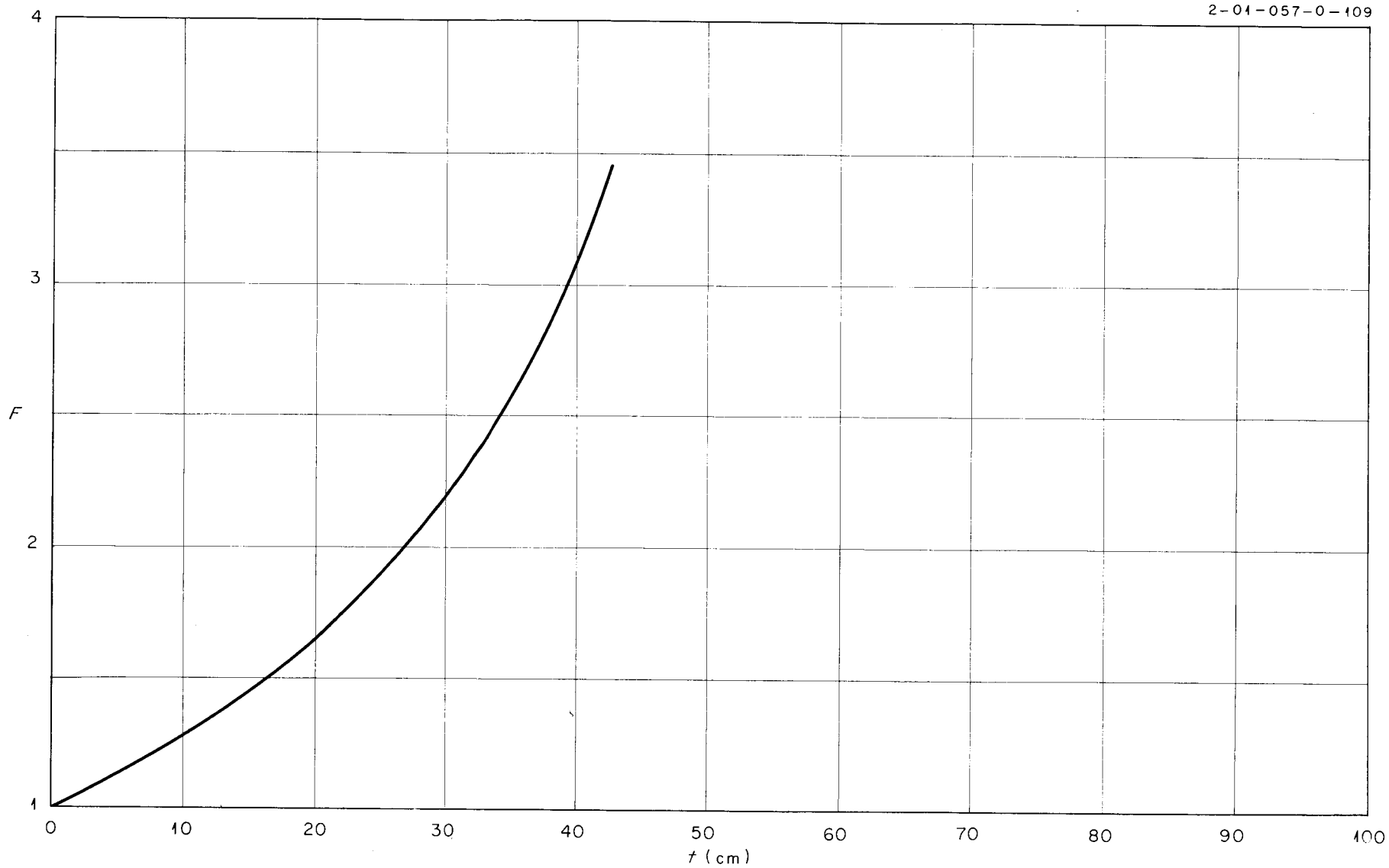


Fig. B-15. Geometric Correction Factor  $F$  vs.  $t$  for  $\lambda\Sigma=1.3$ ,  $\lambda=6$  cm, and  $z+t=70$  cm

Table B-1

Values of Geometric Correction Factor F for  $\lambda \Sigma = 0.7$

$\lambda$ (cm)	$z + t$ (cm)	$t$ (cm)	F	Fig. No.	$\lambda$ (cm)	$z + t$ (cm)	$t$ (cm)	F	Fig. No.
10	150	66	2.72	B-1	8	130	66	3.02	B-3
		50	2.03				50	2.17	
		40	1.72				40	1.81	
		30	1.48				30	1.53	
		20	1.29				20	1.32	
		10	1.13				10	1.14	
		5	1.06				5	1.07	
9	150	66	2.66	B-2		110	66	3.73	B-3
		50	2.00				50	2.48	
		40	1.70				40	1.99	
		30	1.47				30	1.64	
		20	1.28				20	1.37	
		10	1.13				10	1.16	
		5	1.06				5	1.08	
	130	66	3.12	B-2		90	50	2.99	B-3
		50	2.22				40	2.27	
		40	1.84				30	1.79	
		30	1.55				20	1.44	
		20	1.32				10	1.19	
		10	1.14				5	1.09	
		5	1.07						
	110	66	3.90	B-2		70	50	4.24	B-3
		50	2.56				40	2.79	
		40	2.04				30	2.03	
		30	1.66				20	1.55	
		20	1.38				10	1.23	
		10	1.17				5	1.10	
		5	1.08						
	90	50	3.12	B-2	7	110	66	3.53	B-4
		40	2.34				50	2.39	
		30	1.83				40	1.94	
		20	1.46				30	1.61	
		10	1.20				20	1.35	
		5	1.09				10	1.16	
							5	1.07	



Table B-1 (cont.)

$\lambda$ (cm)	$z + t$ (cm)	$t$ (cm)	F	Fig. No.	$\lambda$ (cm)	$z + t$ (cm)	$t$ (cm)	F	Fig. No.
7	90	50	2.85	B-4	6	70	50	3.76	B-5
		40	2.19				40	2.53	
		30	1.74				30	1.88	
		20	1.42				20	1.48	
		10	1.18				10	1.20	
		5	1.08				5	1.09	
	70	50	4.01	B-4					
		40	2.66						
		30	1.96						
		20	1.52						
		10	1.22						
		5	1.10						

Table B-2

Values of Geometric Correction Factor F for  $\lambda Z = 1$

$\lambda$ (cm)	$z + t$ (cm)	$t$ (cm)	F	Fig. No.	$\lambda$ (cm)	$z + t$ (cm)	$t$ (cm)	F	Fig. No.
10	150	66	2.80	B-6	8	130	66	3.16	B-8
		50	2.08				50	2.25	
		40	1.75				40	1.86	
		30	1.50				30	1.57	
		20	1.30				20	1.33	
		10	1.13				10	1.15	
		5	1.06				5	1.07	
9	150	66	2.74	B-7		110	66	3.97	B-8
		50	2.05				50	2.60	
		40	1.74				40	2.07	
		30	1.49				30	1.68	
		20	1.29				20	1.40	
		10	1.13				10	1.17	
		5	1.06				5	1.08	
	130	66	3.25	B-7		90	50	3.21	B-8
		50	2.29				40	2.40	
		40	1.89				30	1.86	
		30	1.58				20	1.48	
		20	1.34				10	1.21	
		10	1.15				5	1.10	
		5	1.07						
	110	66	4.13	B-7		70	40	3.04	B-8
		50	2.67				30	2.16	
		40	2.11				20	1.62	
		30	1.71				10	1.25	
		20	1.41				5	1.12	
		10	1.18						
		5	1.08						
	90	50	3.33	B-7	7	110	66	3.79	B-9
		40	2.47				50	2.52	
		30	1.90				40	2.02	
		20	1.50				30	1.66	
		10	1.21				20	1.38	
		5	1.10				10	1.17	
							5	1.08	

Table B-2 (cont.)

$\lambda$ (cm)	$z + t$ (cm)	$t$ (cm)	F	Fig. No.	$\lambda$ (cm)	$z + t$ (cm)	$t$ (cm)	F	Fig. No.
7	90	50	3.08	B-9	6	70	50	4.30	B-10
		40	2.33				40	2.81	
		30	1.82				30	2.04	
		20	1.46				20	1.56	
		10	1.20				10	1.23	
		5	1.09				5	1.11	
	70	50	4.52	B-9					
		40	2.93						
		30	2.10						
		20	1.59						
		10	1.24						
		5	1.11						

Table B-3

Values of Geometric Correction Factor F for  $\lambda \Sigma = 1.3$

$\lambda$ (cm)	$z + t$ (cm)	$t$ (cm)	F	Fig. No.	$\lambda$ (cm)	$z + t$ (cm)	$t$ (cm)	F	Fig. No.
10	150	66	2.88	B-11	8	130	66	3.30	B-13
		50	2.12				50	2.32	
		40	1.78				40	1.91	
		30	1.52				30	1.60	
		20	1.31				20	1.35	
		10	1.14				10	1.16	
		5	1.07				5	1.07	
9	150	66	2.83	B-12		110	66	4.22	B-13
		50	2.10				50	2.72	
		40	1.77				40	2.15	
		30	1.51				30	1.73	
		20	1.31				20	1.42	
		10	1.14				10	1.18	
		5	1.07				5	1.09	
	130	66	3.39	B-12		90	50	3.43	B-13
		50	2.36				40	2.53	
		40	1.94				30	1.94	
		30	1.61				20	1.52	
		20	1.36				10	1.22	
		10	1.16				5	1.10	
		5	1.08						
	110	66	4.37	B-12		70	40	3.31	B-13
		50	2.79				30	2.30	
		40	2.18				20	1.69	
		30	1.75				10	1.28	
		20	1.43				5	1.13	
		10	1.19						
		5	1.09						
90	50	3.54	B-12	7	110	66	4.05	B-14	
	40	2.59				50	2.65		
	30	1.97				40	2.11		
	20	1.54				30	1.71		
	10	1.23				20	1.41		
	5	1.11				10	1.18		
						5	1.08		

Table B-3 (cont.)

$\lambda$ (cm)	$z + t$ (cm)	$t$ (cm)	F	Fig. No.	$\lambda$ (cm)	$z + t$ (cm)	$t$ (cm)	F	Fig. No.
7	90	50	3.32	B-14	6	70	40	3.11	B-15
		40	2.47				30	2.20	
		30	1.91				20	1.64	
		20	1.51				10	1.27	
		10	1.22				5	1.12	
		5	1.10						
	70	40	3.21	B-14					
		30	2.25						
		20	1.67						
		10	1.27						
		5	1.12						